UNIVERSIDADE DO ALGARVE

Radio over fiber broadband access networks architectures based on wavelength division multiplexing techniques

(Arquiteturas de redes de acesso de banda larga para redes rádio sobre fibra baseadas em técnicas de multiplexagem de comprimento de onda)

Ricardo Pedro Custodinho da Avó

Tese

Doutoramento em Engenharia Eletrónica e Telecomunicações

Especialidade em Telecomunicações e Redes

Trabalho efetuado sob a orientação de:

Professora Doutora Maria do Carmo Raposo de Medeiros

2013

UNIVERSIDADE DO ALGARVE

Radio over fiber broadband access networks architectures based on wavelength division multiplexing techniques

(Arquiteturas de redes de acesso de banda larga para redes rádio sobre fibra baseadas em técnicas de multiplexagem de comprimento de onda)

Ricardo Pedro Custodinho da Avó

Tese

Doutoramento em Engenharia Eletrónica e Telecomunicações

Especialidade em Telecomunicações e Redes

Trabalho efetuado sob a orientação de:

Professora Doutora Maria do Carmo Raposo de Medeiros

2013

Declaração de autoria de trabalho

"Radio over fiber broadband access networks architectures based on wavelength division multiplexing techniques"

Declaro ser o autor deste trabalho, que é original e inédito. Autores e trabalhos consultados estão devidamente citados no texto e constam da listagem de referências incluída.

(Ricardo Pedro Custodinho da Avó)

Acknowledgments

I would like to express my sincere gratitude to my supervisor Professor Maria do Carmo Raposo de Medeiros, for accepting me as her student and for introducing me to the research area of radio over fiber networks. Professor Carmo has always been a very supportive supervisor, available for fruitful discussions and exchanges of ideas.

I want to thank my research center, CEOT, for the access to the laboratory and computing equipment. I am also grateful to FCT, the Portuguese Foundation for Science and Technology, for funding my work with the PhD grand (SFRH/BD/29138/2006) and research projects within CEOT.

I would like to give a special thanks to my former lab colleague, Mark Guerreiro for all his support, particularly with the laboratory work, especially on the test of devices and the never ending search for reflections on the optical connections.

I would also like to thank all my current and former research colleagues from CEOT, in particular José, Paulo, Hélio, Professor Álvaro Barradas and Professor Paula Laurêncio for their enthusiasm and fruitful discussions at CEOT.

Finally, my sincere gratitude to all my family, for all their support and their extreme patience.

Abstract

The recent remarkable growth in bandwidth of both wired optical and wireless access networks supports a burst of new high bandwidth Internet applications such as: peer-to-peer file sharing, cloud storage, on-line gaming, video streaming, etc. Within this scenario, the convergence of fixed and wireless access networks offers significant opportunities for network operators to satisfy user demands, and simultaneously reduce the cost of implementing and running separated wireless and wired networks.

The integration of wired and wireless network can be accomplished within several scenarios and at several levels. In this thesis we will focus on converged radio over fiber architectures, particularly on two application scenarios: converged optical 60 GHz wireless networks and wireless overlay backhauling over bidirectional colorless wavelength division multiplexing passive optical networks (WDM-PONs).

In the first application scenario, optical 60 GHz signal generation using external modulation of an optical carrier by means of lithium niobate ($LiNbO_3$) Mach- Zehnder modulators (MZM) is considered. The performance of different optical modulation techniques, robust against fiber dispersion is assessed and dispersion mitigation strategies are identified. The study is extended to 60 GHz carriers digitally modulated with data and to systems employing subcarrier multiplexed (SCM) mm-wave channels.

In the second application scenario, the performance of WDM-PONs employing reflective semiconductor optical amplifiers (RSOAs), transmitting an overlay orthogonal frequency-division multiplexing (OFDM) wireless signal is assessed analytically and experimentally, with the relevant system impairments being identified. It is demonstrated that the intermodulation due to the beating of the baseband signal and wireless signal at the receiver can seriously impair the wireless channel. Performance degradation of the wireless channel caused by the RSOA gain modulation owing to the downstream baseband data is also assessed, and system design guidelines are provided.

Keywords: (4 a 6)

Wavelength-division-multiplexed passive optical network (WDM-PON), Broadband access networks, Wireless backhauling, Radio-over-fiber, 60 GHz radio over fiber.

Resumo

As redes óticas estão-se a tornar muito populares como redes de acesso, isto é, o último troço que liga a rede do operador às instalações do cliente. Os operadores incumbentes que baseiam as suas redes de acesso em pares de cobre, as chamadas linhas telefónicas, estão ativamente a estudar a instalação em massa de redes óticas como novo método de acesso. A tendência, na Europa e Estados Unidos da América, tem sido a instalação de redes óticas passivas partilhadas por vários utilizadores, através da técnica de multiplexagem no tempo.

Tal como outras tecnologias, as redes óticas estão em constante evolução. Já existem novas versões em desenvolvimento e entre elas uma das hipóteses é converter o método de partilha do meio, de multiplexagem no tempo para multiplexagem de comprimento de onda. Caso sejam atribuídos comprimentos de onda dedicados por utilizador isto possibilitaria aumentos na largura de banda por utilizador de aproximadamente 32 vezes com tecnologia atual, rede ótica passiva *gigabit - gigabit passive optical network* (GPON), e de 128 vezes com o que se espera ser o sucessor, ainda baseado em multiplexagem no tempo, 10GPON.

Mas enquanto as redes de acesso óticas permitem levar grandes larguras de banda até casas e escritórios, os clientes finais ficam limitados a uma utilização fixa dentro das suas instalações, porque as tecnologias sem fios atuais têm dificuldade ou simplesmente não conseguem fornecer largura de banda suficiente para tirar partido completo do serviço. Para tal é necessário desenvolver novos padrões para redes sem fios que, em princípio, terão que utilizar partes do espectro radio elétrico ainda pouco utilizado. Uma banda que se encontra em estudo para responder a este desafio é a banda milimétrica, nomeadamente os 60 GHz. Esta banda tem disponível uma quantidade de espectro disponível considerável, por exemplo 9 GHz na Europa. Além de ser definida como livre de licenciamento em muitas regiões do mundo, por exemplo Europa, Estados Unidos da América, Japão e Coreia do Sul.

Esta tese estuda a transmissão de ondas milimétricas de forma transparente através de fibra ótica, propondo uma arquitetura utilizando um amplificador ótico semicondutor refletivo – *reflective semiconductor optical amplifier* (RSOA) como a fonte ótica nos nós remotos da rede. Este estudo está dividido em duas partes.

A primeira parte é o estudo por simulação da transmissão ótica de ondas milimétricas da estação central até ao nó remoto. O foco deste estudo é colocado na dispersão cromática da fibra e na intermodulação entre os vários canais de radio, utilizando-se quatro modulações óticas geradas através de um modelador do tipo Mach-Zehnder.

O problema da dispersão cromática é particularmente relevante na transmissão de sinais de elevada rádio frequência (RF). Ao modular um sinal deste tipo com a modulação tradicional de banda lateral dupla – *optical double side band* (ODSB) iremos ter, pelo menos três componentes óticos. A portadora ótica numa determinado comprimento de onda (λ), e as duas bandas laterais do sinal a enviar, centradas em λ + comprimento de onda do sinal RF (λ_{RF}) e em λ - λ_{RF}. O recetor ótico considerado nesta tese é um recetor de deteção direta. Ou seja, um sinal ODSB detetado no recetor como um batimento entre λ e o sinal em λ +λ_{RF}, resultando num sinal localizado em *RF*, o batimento entre λ e o sinal em λ - λ_{RF} resultando num sinal em *RF*, e o batimento entre as duas bandas laterais inferior e superior, resultando num sinal localizado no dobro da frequência original. Esta última componente é normalmente ignorada pois a largura de banda do recetor ótico é escolhida com base na frequência do sinal que interessa receber. Os outros dois sinais irão somar-se e gerar apenas um sinal elétrico. O conceito de dispersão cromática vem do facto que a velocidade de propagação de um sinal ótico depende do seu comprimento de onda. Ao trabalhar com sinais da ordem dos 60 GHz, a diferença na velocidade de propagação irá fazer que com suficiente comprimento de fibra, os dois sinais RF, irão chegar ao recetor com fases diferentes. O sinal resultante da soma das duas componentes irá fazer com que haja efeitos construtivos ou destrutivos conforme a distância percorrida. Uma das possíveis soluções para evitar o problema, será usar uma modulação que apenas gere uma componente RF, para que ao chegar ao recetor ótico, seja apenas detetado um sinal. Por exemplo a modulação ótica de banda lateral única - *optical single side band* (OSSB). As modulações estudadas nesta tese são a clássica modulação ODSB, a modulação OSSB e duas variantes desta última. As variantes são: banda lateral única com filtragem (F-OSSB) por forma a ter apenas a transmissão da portadora ótica e harmónica fundamental; a segunda variante consiste em utilizar apenas a harmónica fundamental e reintroduzir a portadora ótica antes da modulação do sinal elétrico, obtendo desta forma um sinal OSSB puro (P-OSSB). Estas duas modulações permitem identificar as causas da degradação do sinal OSSB gerado pelo MZM, quando aplicadas profundidades de modulação altas.

A segunda parte é a demonstração da transmissão bidirecional experimental de um sinal rádio, utilizando o padrão 802.11g nos 2.4 GHz, em conjunto com um sinal de banda base com 1 *gigabit* por segundo utilizando para tal um RSOA com uma largura de banda de 1.2 GHz sem recorrer a frequências intermédias. É estudado o impacto que a largura da banda do sinal banda base tem no sistema, assim como o nível de potência ótica que chega ao RSOA e a sua corrente de polarização.

O trabalho aqui apresentado tem como objetivo indicar um conjunto de regras sobre que modulações óticas utilizar, o seu comportamento em relação à profundidade de modulação para transmissão de sinais rádio na banda milimétrica. Também é demonstrado que o RSOA pode ser utilizado como fonte ótica nos nós remotos, utilizando para tal o dobro da largura de banda especificada pelo fabricante. Potenciando o seu uso com os sinais milimétricos quando os mesmos forem passados para frequências intermédias. Numa aplicação mais direta, a arquitetura apresentada nesta experiencia permite expandir o uso das redes óticas passivas. Já que poderão ser colocados sinais rádios gerados numa estação central utilizando os diversos padrões atuais, GSM, UMTS, LTE, e transmitindo-os de forma transparente para nós remotos. Nós remotos que poderão ser muito mais simples e de reduzida dimensão, pois apenas necessitarão de filtros, amplificadores e antenas. Dispensando todos os componentes de geração de sinal e gestão a nível lógico, que serão colocadas na estação central.

Palavras-chave: 4 a 6

Rede ótica passiva com multiplexagem de comprimentos de onda (WDM-PON), Redes de acesso de banda larga, Alimentação de estações-base sem fios, Radio sobre fibra, 60 GHz sobre fibra.

Table of contents

List of figures

List of tables

Acronyms

ADC	Analog-to-Digital Converter
ADSL	Asymmetric Digital Subscriber Line
AM	Amplitude Modulation
AP	Access Point (wireless)
APON	ATM Passive Optical Network
ASK	Amplitude Shift Keying
ATM	Asynchronous Transfer Mode
AWG	Arrayed Waveguide Gratings
BB	Band Base
BER	Bit Error Rate
BLS	Broadband Light Sources
BPON	Broadband Passive Optical Network
BPSK	Binary Phase Shift Keying
BS	Base Station
B-t-B	Back-to-Back
CAPEX	CAPital EXpenditures
CDWM	Coarse Wavelength Division Multiplexing
CMOS	Complementary Metal–Oxide–Semiconductor
CO	Central Office
CPRI	Common Public Radio Interface
CSMA/CA	Carrier Sense Multiple Access with Collision Avoidance
CTS	Clear To Send
CW	Continuous Wave
DAC	Digital-to-Analog Converter
DD	Direct Detection
DFB	Distributed FeedBack (laser)
DL	DownLink
DOCSIS	Data Over Cable Service Interface Specification
DSL	Digital Subscriber Line

DSSS	Direct-Sequence Spread Spectrum
DWDM	Dense Wavelength Division Multiplexing
EAM	Electro-Absorption Modulator
EDFA	Erbium Doped Fiber Amplifier
EPON	Ethernet Passive Optical Network
FDMA	Frequency Division Multiple Access
FEC	Forward Error Correction
FM	Frequency Modulation
F-OSSB	Filtered Optical Single Side Band
FHSS	Frequency Hopping Spread Spectrum
FTTB	Fiber-To-The-Building
FTTC	Fiber-To-The-Curb
FTTH	Fiber-To-The-Home
FTTx	Fiber-To-The-x
GEM	Gigabit-capable passive optical network Encapsulation Mode
GE-PON	Gigabit Ethernet Passive Optical Network
G-PON	Gigabit-capable Passive Optical Network
GPS	Global Positioning System
GSM	Global System for Mobile communications
GVD	Group Velocity Dispersion
HD	High Definition
HDMI	High-Definition Multimedia Interface
HDTV	High Definition TeleVision
Hi-Fi	High Fidelity (home stereo)
HS/DSSS	High Speed Direct-Sequence Spread Spectrum
HSPA	High Speed Packet Access
IEEE	Institute of Electrical and Electronics Engineers
IF	Intermediate Frequency
IM	Intensity Modulation
IMD_3	Third order InterModulation Distortion
IPTV	Internet Protocol TeleVision
IR	InfraRed
ITU	International Telecommunication Union

ITU-T	Telecommunication standardization sector for the International Telecommunication Union
LAN	Local Area Network
LDPC	Low-Density Parity-check Code
$LiNbO_3$	Lithium Niobate
LLC	Logical Link Control
LPF	Low Pass Filter
LTE	Long Term Evolution
LTE-A	Long Term Evolution Advanced
MAC	Media Access Control
MC	Multi Carrier
m_I	Modulation Index
MIMO	Multiple Input Multiple Output
MZM	Mach-Zehnder Modulator
NEXT	Near End **cross**Talk
NF	Noise Figure
NG-PON	Next Generation Passive Optical Network
NRZ	Non Return to Zero
OBSAI	Open Base Station Architecture Initiative
OCDMA	Optical Code-Division-Multiple-Access
OCS	Optical Carrier Suppression
ODN	Optical Distribution Network
ODSB	Optical Double Side Band
OFDM	Orthogonal Frequency Division Multiplexing
OLT	Optical Line Terminal
ONT	Optical Network Terminal
O-OFDM	Optical Orthogonal Frequency Division Multiplexing
OOK	On-Off Keying
OPEX	OPerational EXpenditures
OSSB	Optical Single Side Band
P2MP	Point-**to**-Multi-Point
P2P	Point-**to**-Point
PD	PhotoDetector

PM	Phase Modulator
PON	Passive Optical Network
P-OSSB	Pure Optical Single Side Band
POTS	Plain Old Telephone Service
QAM	Quadrature Amplitude Modulation
QPSK	Quadrature Phase Shift Keying
RF	Radio Frequency
RIN	Relative Intensity Noise
RN	Remote Node
RoF	Radio over Fiber
RSOA	Reflective Semiconductor Optical Amplifier
RTS	Request To Send
SC	Single Carrier
SCM	SubCarrier Multiplexing
SMF	Single Mode Fiber
SNR	Signal to Noise Ratio
SOA	Semiconductor Optical Amplifier
TDM	Time Division Multiplexing
TDMA	Time Division Multiple Access
UL	UpLink
VOA	Variable Optical Attenuator
VoD	Video on Demand
WDM	Wavelength Division Multiplexing
WDM-PON	Wavelength Division Multiplexed Passive Optical Network
WiMAX	Worldwide Interoperability for Microwave Access
WLAN	Wireless Local Area Network
WMAN	Wireless Metropolitan Area Network
WPAN	Wireless Personal Area Network
WWAN	Wireless Wide Area Network
x_c	modulation depth
XG-PON	10 Gigabit-capable Passive Optical Network

1

Introduction

1.1 Context

Telecommunication technologies are one of the most exciting markets to work in. It is impressive to analyze its remarkable growth and innovation, for example, the percentage of worldwide mobile-cellular telephone subscriptions has grown from around 18% to 85.7% in the last ten years [1.1], and extra grown is still forecasted for the near future.

Telecommunication technologies have come a long way before providing Gbit/s on wired connections or hundred of megabits on wireless connections. In the wired communications three main transmission medium technologies can be identified, namely: the copper twisted-pair, the coaxial cable and the optical fiber. The twisted-pair traditionally was deployed to support the plain old telephone (POTS) services using a mere 4 kHz of bandwidth, however nowadays it also supports well established digital

subscriber lines (DSL). Typically, DSL connections work by dividing the frequencies used in a single telephone line into two transmission bands, the data is transmitted over the high frequency band (25 kHz and above) whereas the voice is transmitted over the lower frequency band (4 kHz and below). The second transmission medium is the coaxial cable, initially used to connect one or more external antennas to TV receivers. Each cable transporting tens of analog television channels, each channel using 6 to 8 MHz of bandwidth. In some regions of the world, notably the US, local cable networks started to appear, mainly in areas where the broadcast signal were difficult to acquire in each individual home. A collective antenna was then installed in a privileged location with access to the signal, and a coaxial cable network used to distribute the signal to each individual home. It was the beginning of the cable companies. Nowadays, cable networks also provide cable modem-based services.

However, both the twisted-pair and coaxial cable are not able to provide the necessary bandwidth required to support the ever-increasing video-based applications. To overcome this limitation, it is essential to use single mode fiber (SMF) as the transmission media in future access networks. SMF provides essentially infinite bandwidth and very small attenuation when compared with copper pairs and coaxial cables. Due to the system cost, optical fiber cables were primarily deployed in the backbone network where high bandwidth was necessary.

On the wireless front no new means of transmission was developed, it always relies on air transmission[1]. However, the demand for higher bandwidth was accomplished mainly by the use of modulation schemes. Wireless communications started with the wireless telegraphy where virtually no bandwidth was necessary, a continuous waveform was switched on and off to represent the Morse code symbols. Shortly after, voice radio was developed, having in mind mainly military and marine applications. Commercial applications were initiated afterwards, among them radio broadcast technology that stills being used nowadays. Roughly, after 100 years of the amplitude modulated (AM) radio invention one can still find it on most high fidelity (Hi-Fi) equipment or car radios. AM radio uses less than 10 kHz of bandwidth with a frequency under 2 MHz (except for short wave, which can broadcast at up to 26 MHz). Audio communications continued to be the main focus, with the development of frequency modulated (FM) radio. Using a different modulation scheme, the system resistance to noise interference was improved; it also used

[1] Communications based on light transmission on free space, such as IR communications, were ignored for the sake of simplification.

higher bandwidths, improving the audio quality. Later came the television broadcast with 6 to 8 MHz bandwidth and transmitting in frequencies from 50 MHz to near 900 MHz. On the bidirectional wireless communications, the 80s saw the invention of the mobile phone. Up to that point several entities could use wireless communications, but were mainly used by military, public safety, amateur radio operators and very specific business users. The 90s saw the development of the digital mobile phone, wireless communications would never be the same. Several standards were developed, but only one could claim a worldwide success, the currently used global system for mobile communications (GSM) standard. The mobile phone benefited greatly from the developments in the semi-conductor industry, enabling smaller, cheaper devices, with more autonomy and more functionalities. This allowed the mobile phone to reach mass market. In recent years, the mobile phone has evolved from a voice calling machine to the currently multimedia device. From using 100 kHz bandwidth to, up to 20 MHz in the latest commercial technology, long term evolution (LTE).

The capacity increase of wireless networks also meant the need of higher capacity connections between base stations and the core network, thus the upgrade of the backhaul network. To cope with the need of high capacity connections wireless operators have even been forced to deploy fiber to connect their sites, but the technology used is not tailored for the transport of wireless signals. The present scenario is that optical fiber moved from strictly long haul and backbone connections to the backhaul of regional and local telephone exchanges and wireless base stations. In order to support hungry bandwidth applications, fiber has been deployed in the access network, closer to the end user and even entered the buildings and homes.

The interplay between wireless and optical technologies must be simplified. This simplification should lead to an overall cost reduction, particularly in long term operational expenditures (OPEX). Wireless optical convergence will also provide a reduction in terms of hardware footprint.

The overall objective of this thesis is to contribute to the study and development of efficient, low cost, network architectures able to support the convergence of wired optical access networks and high bandwidth wireless access/local networks.

1.2 Motivation and objectives

The remarkable growth in bandwidth, both in wired and wireless networks, supports a burst of new Internet applications, such as peer-to-peer file transfers, cloud storage, on-line gaming, multimedia content streaming, etc. Internet technologies are now considered as the universal communication platform. In parallel to the growth of the Internet, wireless and mobile network technologies have witnessed a great development.

The convergence of fixed and wireless/mobile access platforms offers significant opportunities for network operators to satisfy user demands, by simultaneously reducing the cost of operating separated wireless and wired networks. The integration of wireless and wired network can be accomplished with several scenarios and at several levels. In this thesis we will focus on two application scenarios: converged optical 60 GHz wireless networks and wireless overlay backhauling over bidirectional colorless wavelength division multiplexing passive optical networks (WDM-PONs).

Consumer demands for high speed wireless networking video based interactive and multimedia applications are an increasing reality. These applications, at the consumer level, are supported by devices that have emerged and quickly improved over the past few years such as: smartphones, tablets, gaming consoles, etc. These devices rely on their capability of being always connected to the Internet and on high transmission bandwidths. Users want to use their devices with the same perceived quality both indoors and outdoors. For outdoors environments new standards such as LTE-advanced systems [1.2], or mobile worldwide interoperability for microwave access (WiMAX) 2, targeting data rates up to 1 Gbit/s can support the needed transmission speeds, while for indoors applications new high bandwidth wireless personal area networks (WPANs) are being developed [1.3]. Cooperative outdoor and indoor environments, can lead to a more efficient usage of the radio spectrum. Bi-standard equipment can operate in mobile outdoor mode while the user is in the outdoor environment and automatically switch to Wi-Fi mode as soon as the user enters a building. Such a seamless handover as well as increasing the bit rate provided to the user has also an economical impact for the radio-mobile operator, since it is possible to deactivate costly functionalities such as paging, handover management, power control or charging functionalities for this user. Another approach is to deliver the mobile wireless service indoors, transparently, in overlay mode using the installed fiber infrastructure and in combination with other services.

The abundant unlicensed spectrum around 60 GHz offers the potential for multi-gigabit indoor WPANs. Recently it was demonstrated that it is possible to produce low cost complementary metal–oxide–semiconductor (CMOS) components and circuits operating at 60 GHz, it was also demonstrated the wireless transmission of uncompressed broadband high definition television (HDTV) channels at 60 GHz. These advances combined with the increasing consumer demands for high-speed multimedia data communications are driving intense research on this area. However, 60 GHz WPAN networks cover relatively short distances (10-30 meters) and, additionally, 60 GHz signals cannot cross walls. Therefore, radio over fiber (RoF) technology, with its potential huge bandwidth, provides the perfect backbone technology for 60 GHz wireless WPANs. Nevertheless, to implement 60 GHz radio over fiber networks a number of key technological trends have to achieved, ranging from wireless networks to fiber optics transmission systems and supporting opto-electronic components. The 60 GHz WPANs standards already approved, ECMA-387 [1.4], IEEE 802.15.3c [1.5] and WirelessHD™ [1.6], consider both single carrier (SC) and multi carrier (MC) modulations schemes, especially the ones belonging to the orthogonal frequency division multiplexing (OFDM). It has been demonstrated that advanced RoF techniques can efficiently generate and deliver mm-wave carriers to simplified antenna stations. This thesis focus on optical mm-wave signal generation using external modulation of an optical carrier by means of lithium niobate ($LiNbO_3$) Mach- Zehnder modulators (MZM). The objective is to evaluate the performance of different optical modulation techniques robustness against optical fiber dispersion, as well as to identify dispersion mitigation strategies. The study is extended to 60 GHz carriers digitally modulated with data and to systems employing subcarrier multiplexed (SCM) mm-wave channels.

The implementation of optical fiber backhauling links for wireless base stations is highly demanded by the industry and some commercial solutions are already available [1.7]. The emphasis is on low cost, low power consumption and technology integration. The widely deployed fiber-to-the-home (FTTH) infrastructure provides a cost-effective solution to provide backhaul to wireless base stations using the same optical infrastructure. This thesis focus on wireless base stations backhauling by WDM-PONs employing reflective semiconductor optical amplifiers (RSOAs). RSOAs are key components of next generation WDM-PON networks to be used at the customer premises equipment, enabling a colorless operation [1.8] and bidirectional transmission with only one fiber. In such networks the RSOA is seeded with either continuous wave (CW) light

from the optical line terminal (OLT) or with the downstream signal. Such wavelength reuse strategy improves both the cost-effectiveness and wavelength control functionalities of WDM-PONs. Although, recently RSOA based systems, potentially providing 10 Gbit/s transmissions, have been reported [1.9, 1.10], in this thesis we consider conventional commercially available RSOA devices with 3 dB bandwidth around 1.3 GHz. However, since the RSOA frequency transfer characteristics decreases smoothly it is possible to use more than 1 GHz bandwidth, with less than 20 dB attenuation, beyond the device 3 dB bandwidth. Therefore, the usable bandwidth is around 2.4 GHz, which can be used by either down converting the wireless signals or by direct modulation of the RSOA by the wireless signals. Fortunately all major cellular technologies and wireless LANs can operate within the 2 GHz window, e.g. GSM at 900 MHz, 1.8 or 1.9 GHz, high speed packet access (HSPA) family at 1.7, 1.9 or 2.1 GHz, LTE at 800, 900 MHz or 2.6 GHz and 802.11g, n at 2.4 GHz. In this thesis an overlay approach followed which considers joint transmission of a baseband signal plus a wireless signal.

1.3 Thesis outline

Following this introduction, chapter 2 will provide a brief review of the main landmarks of optical fiber optic access networks, as well as key possible evolution scenarios, which are the foundation for converged radio over optical access networks studies developed within this thesis. Particular attention is given to passive optical networks (PONs) employing WDM combined with RSOAs.

Chapter 3 provides the motivation for 60 GHz wireless networks with the state of the art and a brief overview of the relevant 60 GHz wireless standards available. RoF is introduced as a key enabling technology for 60 GHz wireless networks. The remainder of the chapter is dedicated to the generation and transmission of optical 60 GHz signals considering three optical modulation schemes using MZM, optical double side band (ODSB), optical single side band (OSSB), and optical carrier suppression (OCS). The mathematical analysis necessary for the understanding of the behavior of the different modulation schemes is presented. Transmission impairments owing to optical fiber chromatic dispersion are analyzed and discussed, as well as, the main dispersion mitigation strategies.

In chapter 4 the performance of RF carriers digitally modulated with data transmitted over fiber, operating in the 60 GHz range, is studied through simulation. Basically, two

scenarios are considered, a single radio frequency (RF) carrier modulated using binary phase shift keying (BPSK) and a SCM with four RF carriers also modulated using BPSK. The effect of several system operating parameters, such us: optical modulation configuration, optical modulation parameters and fiber length are considered with the relevant system impairments being identified.

Chapter 5 considers the wireless overlay backhauling over bidirectional colorless WDM-PONs employing RSOAs. The wireless signals are transparently transmitted over the WDM-PON, thus creating a virtual dedicated network without incurring into additional network installation and maintenance costs. In this thesis, the performance of a WDM-PON operating at 1 Gbit/s and transmitting an overlay OFDM wireless signal is assessed analytically and experimentally, with the relevant system impairments being identified. The intermodulation due to the beating of the baseband signal and wireless signal at the receiver show that it can seriously impair the wireless channel. Performance degradation of the wireless channel caused by the RSOA gain modulation owing to the downstream baseband data is also assessed, and system design guidelines are provided.

Chapter 6 concludes the thesis by summarizing the main achievements and identifying areas of further research.

1.4 Main contributions

The main contributions of this research program may be organized in three groups, as follows: converged radio over fiber architectures; generation and transmission impairments of 60 GHz signals; and wireless overlay backhauling over bidirectional colorless WDM-PONs.

The majority of the work developed during the course of this research work is reported in scientific publications, presented at conferences, published in journals and written in technical reports. In the following paragraphs, the main contributions of the thesis are listed, along with the correspondent publications produced.

Converged radio over fiber architectures:

- Identification of network architectures able to combine wired-wireless access networks, combining low complexity with flexibility and cost effectiveness.

- Identification of convergence scenarios of optical and 60 GHz broadband wireless access networks and assessment of their performance limitations.
- Identification of intermodulation effects that arise in a hybrid WDM-PON access network architecture supporting both wired and wireless users.

Publications:

- M. C. R. Medeiros, R. Avó, P. Laurêncio, N. S. Correia, A. Barradas, H. J. A. da Silva, I. Darwazeh, J. E. Mitchell, and P. M. N. Monteiro, "RoFnet-Reconfigurable Radio over Fiber Network Architecture Overview," *Journal of Telecommunications and Information Technology,* vol. 88, pp. 38-43, Nov 15 2009. (Journal Paper)
- M. C. R. Medeiros, R. Avó, P. Laurencio, I. Darwazeh, J. E. Mitchell, P. M. N. Monteiro, and H. J. A. da Silva, "Convergence of Optical and Millimeter-Wave Broadband Wireless Access Networks," *ICTON: 2009 11th International Conference on Transparent Optical Networks, Vols 1 and 2,* pp. 192-195, 2009. (Conference Paper)
- R. Avó, P. Laurêncio, and M.C.R. Medeiros, "mm-wave networks over optical access network architecture employing reflective semiconductor optical amplifiers: intermodulation effects," *14th European Conference on Networks and Optical Communications (NOC/OCI 2010) Proceedings, Valladolid,* pp. 249-256, Mar 2009. (Conference Paper)
- M. C. R. Medeiros, R. Avó, P. Laurencio, N. S. Correia, A. Barradas, H. J. A. da Silva, I. Darwazeh, J. E. Mitchell, and P. M. N. Monteiro, "Radio over fiber access network architecture employing reflective semiconductor optical amplifiers," *2007 Icton Mediterranean Winter Conference,* pp. 227-231, 2007. (Conference Paper)

Generation and transmission impairments of 60 GHz signals:

- Analysis of 60 GHz wireless networks state of the art and possible evolution scenarios.

- Comparative analysis of the optical dispersion robust modulation strategies OSSB and OCS.
- Demonstration that the fiber chromatic dispersion combined with intermodulation distortion introduced by the optical modulator are key system parameters, in single carrier and subcarrier multiplexed mm-wave radio over fiber system employing OSSB modulation.
- Assessment of the modulation depth employed in OSSB modulation as a key operational factor. For low modulation depth the system performance is dominated by the system noise, however, as the modulation depth increases higher order optical DSB harmonics become significant leading to power fading at the receiver. Additionally, by increasing the modulation depth the value of intermodulation products that fall near the optical carrier also increases, leading to system degradation.
- Comparative study between OSSB and OCS, considering the finite extinction ratio of MZMs and the optical amplifier noise.

Publications:

- R. Avó, P. Laurêncio, and M. C. R. Medeiros, "Comparative Study of Optical Up-Conversion Schemes," *ICTON 2011: Proceedings of the 13th International Conference on Transparent Optical Networks, Vol 3,* pp. 1-4, July 2011. (Conference paper)
- P. Laurencio, H. Vargues, I. Fortes, R. Avó and M. C. R. Medeiros "Dispersion Robustness of Millimeter Waves Generated by Up-Conversion Strategies," *Fiber and Integrated Optics,* vol. 29, pp. 441-452, 2010. (Journal paper)
- R. Avó, P. Laurencio, and M. C. R. Medeiros, "Generation and transmission of millimeter wave signals employing optical frequency quadrupling," *ICTON: 2010 12th International Conference on Transparent Optical Networks, Vols 1 and 2,* pp. 1-4, 2010. (Conference paper)
- R. Avó, P. Laurêncio, and M. C. R. Medeiros, "60 GHz radio-over-fiber transmission impairments for broadband wireless signals," *International*

Conference on Transparent Optical Networks (ICTON) Proceedings, pp. 1-4, 2010. (Conference paper)

- R. Avó, P. Laurencio, and M. C. R. Medeiros, "Transmission Performance of mm-Waves on Radio over Fiber Systems: Dispersion and Intermodulation Issues," *Emerging Trends in Technological Innovation,* vol. 314, pp. 289-296, 2010. (Conference paper)
- H. Vargues, R. Avó, P. Laurencio, and M. C. R. Medeiros, "Simulation of mm-Wave over Fiber Systems Employing Up-Conversion Using External Modulators," *Icton: 2009 11th International Conference on Transparent Optical Networks, Vols 1 and 2,* pp. 308-311, 2009. (Conference paper)
- R. Avó, P. Laurêncio, and M. C. R. Medeiros, "mm-wave networks over optical access network architecture employing reflective semiconductor optical amplifiers: intermodulation effects," *14th European Conference on Networks and Optical Communications (NOC/OCI 2010) Proceedings, Valladolid,* pp. 249-256, Mar 2009. (Conference paper)
- R. Avó, P. Laurencio, and M. C. R. Medeiros, "Simulation of mm-Wave over Fiber Employing Optical Single Sideband Modulation Combined with Subcarrier Multiplexing," *2008 2ª ICTON Mediterranean Winter (ICTON-MW),* pp. 50-54, 2008. (Conference paper)

Wireless overlay backhauling over bidirectional colorless WDM-PONs:

- Mathematical analysis and experimental validation of the intermodulation resulting from the beating of the baseband signal and wireless overlay signal transmitted over colorless WDM-PONs employing RSOA.
- Demonstration of bidirectional transmission of 802.11g signals over a colorless bidirectional WDM PONs employing RSOAs.
- Optimum design guidelines and analysis tools to assess the performance limits of single fiber bidirectional WDM-PON, employing RSOAs supporting both baseband and wireless OFDM signals.

Publications:

- R. Avó and M.C.R. Medeiros, " Wireless Overlay Backhauling over Bidirectional Colorless WDM-PONs: the Impact of the Baseband Channel," *JOCN*, 2012 (Journal paper, submitted).
- T. Ravach, R. Avó, and M.C.R. Medeiros, "Transmission Performance of Multiplexed OFDM Signals over Optical Access Network Architectures Employing RSOAs", WCNC 2012 Workshop on Hybrid Optical Wireless Access Networks, April 2012**.** (Conference paper)
- R. Avó, M. Guerreiro and M. C. R. Medeiros, "Bidirectional transmission of IEEE 802.11G over colorless WDM-PON employing a reflective semiconductor optical amplifier," *Microwave and Optical Technology Letters*, vol. 53, pp. 1464-1467, Jul 2011. (Journal paper)
- R. Avó, M. Guerreiro, and M. C. R. Medeiros, "Overlay services over WDM-PONs Employing Reflective Semiconductor Optical Amplifiers " *16th European Conference on Networks and Optical Communications (NOC/OCI 2011) Proceedings,* pp. 1-4, July 2011. (Conference paper)
- R. Avó, M. Guerreiro, and M. C. R. Medeiros, "Experimental transmission performance evaluation of IEEE 802.11g over a PON architecture using a RSOA," *15th European Conference on Networks and Optical Communications (NOC/OCI 2010) Proceedings,* pp. 227-232, June 2010. (Conference paper)

1.5 References

[1.1] ITU. (2012). *Measuring the Information Society 2012*. Available: http://www.itu.int/ITU-D/ict/publications/idi/material/2012/MIS2012_without_Annex_4.pdf

[1.2] S. Sesia*, et al.*, *LTE, The UMTS Long Term Evolution: From Theory to Practice*: Wiley, 2009.

[1.3] Z. Genc*, et al.*, "Home networking at 60 GHz: challenges and research issues," *Annals of Telecommunications,* vol. 63, pp. 501-509, 2008.

[1.4] ECMA, (December 2010). Standard ECMA-387: High Rate 60 GHz PHY, MAC and HDMI PALs - 2nd edition. Available: http://www.ecma-international.org/publications/files/ECMA-ST/ECMA-387.pdf, retrieved on October 20, 2011.

[1.5] "IEEE Standard for Information technology - Telecommunications and information exchange between systems - Local and metropolitan area networks - Specific requirements. Part 15.3: Wireless Medium Access Control (MAC) and Physical Layer

(PHY) Specifications for High Rate Wireless Personal Area Networks (WPANs) Amendment 2: Millimeter-wave-based Alternative Physical Layer Extension," *IEEE Std 802.15.3c-2009 (Amendment to IEEE Std 802.15.3-2003),* pp. c1-187, 2009.

[1.6] WirelessHD, (May, 2010). WirelessHD Specification Version 1.1 Overview. Available: http://www.wirelesshd.org/pdfs/WirelessHD-Specification-Overview-v1.1May2010.pdf, retrieved on October 20, 2011.

[1.7] Alcatel-Lucent, lightRadio: Evolve your wireless broadband network. *Website,* Available: http://www.alcatel-lucent.com/lightradio/, retrieved on December 12, 2012.

[1.8] P. Healey*, et al.*, "Spectral slicing WDM-PON using wavelength-seeded reflective SOAs," *Electronics Letters,* vol. 37, pp. 1181-1182, 2001.

[1.9] M. Omella*, et al.*, "Full-Duplex Bidirectional Transmission at 10 Gbps in WDM PONs with RSOA-Based ONU Using Offset Optical Filtering and Electronic Equalization," 2009, p. OThA7.

[1.10] S.-C. Lin*, et al.*, "Simple approach for bidirectional performance enhancement on WDM-PONs with direc tmodulation lasers and RSOAs," *Opt. Express,* vol. 16, pp. 3636-3643, 2008.

2

Optical access networks

2.1 Introduction

The recent and increasing demand for high bandwidth access networks have encouraged a shift towards optical fiber based access networks, which are widely accepted as the ultimate high bandwidth technology solution. Access networks based on optical technology, such as fiber to the home (FTTH) are rapidly and widely being deployed through the world [2.1], as well as, novel solutions are constantly being proposed within standardization bodies. This has been possible due to the cost reduction of optical components, optical fiber and in fiber deployment. The success of optical access networks relies on its capability to provide more bandwidth to more users at a lower cost per user.

The deployment of an optical fiber access network is particularly appellative to new telecommunication operators who do not have any legacy access network. However recently, incumbent telecommunication operators who rely on traditional copper to provide broadband Internet access, and high definition (HD) IPTV[2] are also upgrading their access networks with fiber optic technologies. Their main motivations are retaining current customers and attracting new ones. The sole business of fixed telephone is decreasing, and other services provided on top of copper suffer from bandwidth limitations, such as, Internet access and HD IPTV. The objective of this chapter is to provide a brief review of the main landmarks of optical fiber optic access networks, as well as, the key possible evolution scenarios, which are the foundation for converged radio over optical access networks studies developed within this thesis. Section 2.2 provides a brief review of access networks, focused on the limitations of non-optical access technologies. Section 2.3 presents actual passive optical networks (PONs) providing a comparison between the two most common types of PONs, point-to-point (P2P) and point-to-multi-point (P2MP). As the most common choice for deployment has been the P2MP, this network architecture is discussed as well as possible future evolution options in Section 2.4. Section 2.5 highlights relevant recent results of optical access technology and possible future network evolution, specifically PONs employing wavelength division multiplexing (WDM) combined with colorless devices such as reflective semiconductor optical amplifiers (RSOA). Finally, this chapter concludes with a brief summary.

2.2 PON evolution motivation

Traditionally telephone operators and cable operators only provided one service, telephone and TV respectively. Cable operators decided to upgrade their networks to provide bidirectional services, such as Internet access, which were being provided by telecoms using dialup. Telephone companies facing competition, decided to invest on their existing twisted pair access infrastructure to increase the available bandwidth. The most popular solution was the deployment of the asymmetric digital subscriber line (ADSL) and later ADSL2+ to provide broadband services. This technology is able to

[2] IPTV – A form of transmitting television programs or complete TV channels using IP packets. Usually with the usage of extra protocols to ensure a quality of service comparable to traditional broadcast TV channels.

provide up to 24 Mbit/s (downlink), for very short loops, and 1 Mbit/s in the uplink for each user. While cable companies main access technology was data over cable service interface specification (DOCSIS) 1.0 and 2.0, which is able to provide up to 50 Mbit/s in the downstream and 9 or 27 Mbit/s in the upstream, shared with all the users in the same neighborhood.

Eventually cable companies embraced voice over IP (VoIP) to provide a complete solution for their customers, the so called "triple-play" (TV, Internet and telephone service). Traditional operators fearing they could become irrelevant starting studying TV distribution schemes, choosing IPTV over various digital subscriber line (DSL) variants. However, novel services such as HDTV and 3D HDTV, or more traditional ones such as multi-room TV, multi channel recording, easily reach the DSL bandwidth limits. By their side cable companies were also facing new challenges; IPTV revolutionized the VoD service, especially for non-live programming, such as movie rentals. The movie playback can start at any time the customer demands it, while traditional VoD services where similar to movie theater sessions, with movies being transmitted on a loop on encrypted channels, and being unlock after a "ticket" was bought for a specific session.

Novel Internet applications were being limited by the available bandwidth in the access network, particularly in the upstream. These high bandwidth demanding applications include peer to peer file sharing (Bit Torrent), HD video conferencing (Skype), uploading of photos and videos (Flickr, YouTube) and cloud storage (Dropbox, Google Drive, Skydrive).

Cable companies approach has been to upgrade their cable infrastructure to DOCSIS 3.0 [2.2], capable of at least 200 Mbit/s (in the European version), and to reduce the number of clients served by each node. This strategy increased the pressure for traditional telecoms to upgrade their networks.

Some telecoms followed the cable operators philosophy, to re-use the deployed infrastructure, but with newer DSL technology. The technology chosen was VDSL, but due to the short range as shown in Figure 2.1, it implies the deployment of a large number of remote digital subscriber line access multiplexers (DSLAM) connected to the central office with optical fiber, an architecture known as fiber-to-the-curb (FTTC). Nevertheless, this option only gives a slighter higher bandwidth to the twisted cooper wires, and demands significant investment on DSLAMs and operational expenditure (OPEX), mainly on electric power since DSLAMs are active equipments.

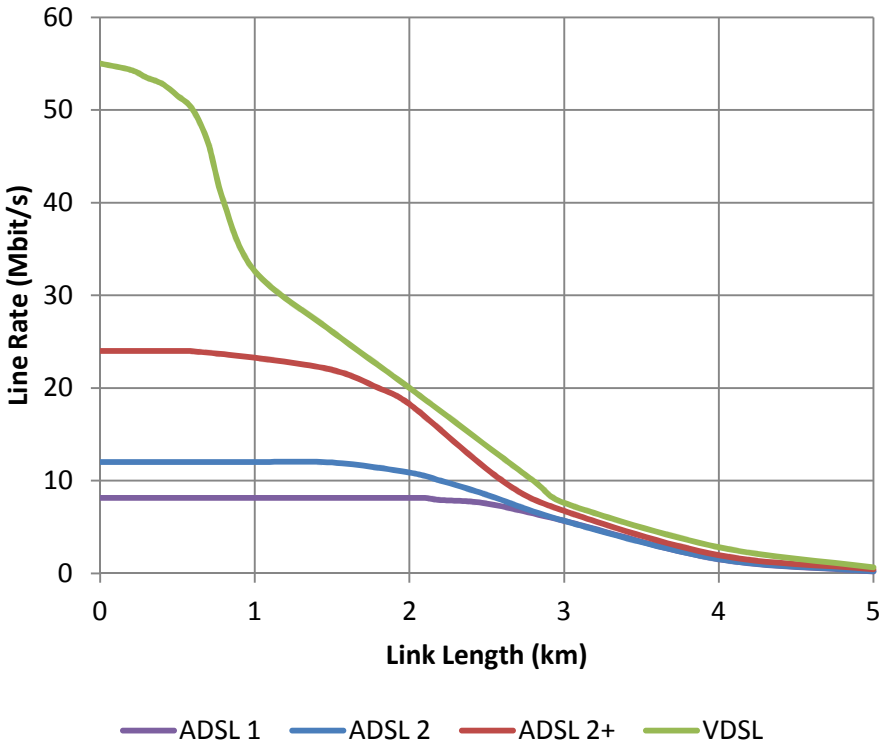

Figure 2.1 - Line rate performance as function of line length for ADSL, ADSL2, ADSL2+ and VDSL, based on [2.3, 2.4].

Due to the increased competition with cable operators some traditional telecommunication operators decided to invest in a future proof network, with very high bandwidth, a clear path for future upgrades, with low maintenance and operational costs. This network solution is the PON, an all fiber access network from the central office to the customer household, with no active equipment in between.

2.3 PON architectures

The most important aspects in PONs architectures are their simplicity and low power consumption [2.1]. In a PON, a shared optical fiber infrastructure connects a central office (CO), where an optical line terminal (OLT) is located, to fiber terminating nodes, Optical Network Terminals (ONTs). The feeder network comprises the part of the network that connects the OLT to a remote node (RN), where typically the ONTs served by the OLT are connected by a power splitter/combiner. All the network between the OLT and the ONT is also known as the optical distribution network (ODN).

Optical fiber links were traditionally used in core and metropolitan networks, such networks usually use two fibers, one for each direction. For the access network dual fiber solutions are not cost effective. Single fiber solutions reduce the infrastructure cost, but at the same time also reduce the available power budget, since 3 dB couplers must be used at the OLT and ONT to connect to each optical source and photoreceiver. Near end crosstalk (NEXT) interference might also be experienced.

P2P use a single star architecture, with dedicated links between the OLT and each ONT using Ethernet based technology, 100BASE-BX10 or 1000BASE-BX10 [2.5].

This architecture allows for gradual activation of OLTs and when new standards are deployed they can be set-up on a client by client basis. With dedicated fibers to each customer a higher level of privacy is provided as well as truly dedicated bandwidth, at least in the access network, this solution is also easier for the operation of several operators on the same deployed network. On the other hand, there is a higher cost in laying dedicated fibers, due to the cost of the fiber itself and also due to the space used in underground ducts. The high number of fibers can also increase the management burden at the central office leading to human errors.

Another option is to use P2MP architectures where the OLT to ONT connection is shared. The most common P2MP architecture is the passive tree with passive splitters between the OLT and ONT, as used on PON networks. Another possibility is an active star, instead of using passive splitters an active device is used, this last configuration is not very common. Figure 2.2 presents the P2P and the most common P2MP architecture.

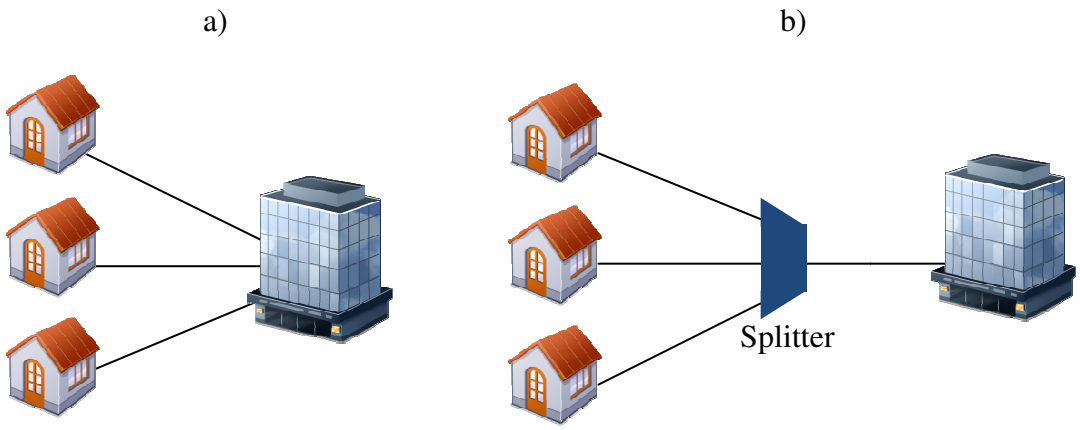

Figure 2.2 - a) Point-to-point architecture. b) Point-to-multipoint network architecture.

The major advantages of a P2MP architecture are the reduction of optical fibers and OLT cost sharing. The last feature allows for the use of cheaper components at the ONT, maintaining the same network requirements thanks to higher quality components at the OLT. Because the medium is shared by several ONTs, the media access control (MAC) layer is more complex than the MAC of P2P architectures. Also, as the bandwidth is shared by all ONTs connected to the same PON branch, higher aggregate bandwidths are needed to provide the same individual bandwidth, i.e. 100Mbit/s technology is enough to provide 100 Mbit/s in a P2P architecture, while 1 Gbit/s is needed if 10 clients are connected to the same OLT.

Current FTTH networks can be classified by, shared or dedicated, regarding the physical network topology and bandwidth offered. When the physical network is shared they can be classified by the medium access scheme employed such as: time division multiplexing (TDM) PONs, WDM PONs [2.6], optical code-division-multiple-access (OCDMA) [2.7], subcarrier multiplexing (SCM) [2.8] or orthogonal frequency division multiplexing (OFDM) [2.9].

In this thesis we will focus on WDM PONs, however, it should be noted that all PONs discussed here use some form of WDM, for example TDM PONs use independent wavelengths for downlink and uplink transmission, shared by all the users. While on a WDM-PON the physical medium is shared among users, the communication channels are logically separated by transmission wavelength, each user or group of users is assigned one or more wavelength channels.

Studies have been made to access the cost, benefit ratio for the different types of architectures [2.10]. For mass deployments operators have chosen P2MP architectures, which dominate in terms of deployments, particularly in the United States (Verizon) and Europe.

2.4 P2MP evolution

2.4.1 BPON

Broadband PON (BPON) was the first PON standard issued by ITU-T in 1998 as ‘ITU-T G.983 BPON’, with an aggregate of 622 Mbit/s in the downlink and 155 Mbit/s in the uplink [2.11], and later revised up to 1244 Mbit/s downlink and 622 Mbit/s uplink [2.12]. It uses a tree architecture, with an OLT feeding up to 32 ONTs. The maximum

distance between the OLT and the ONT is 20 km, due to the chosen power budget. It uses the asynchronous transfer mode (ATM) protocol as the layer 2 protocol, which makes it also known as APON or ATM PON. This PON version was only used in limited trials and a few initial deployments, notably Verizon's FiOS service [2.13]. BPON defined the use of two wavelengths, 1490 nm for the downlink, 1310 nm for the uplink and reserved several windows for future use, one of which is currently used in many deployments for the overlay RF video, 1550 nm [2.14].

2.4.2 EPON

Ethernet PON (EPON) or Gigabit EPON (GE-PON) is used to reference the Institute of Electrical and Electronics Engineers (IEEE) 802.3ah protocol. EPON was rectified in June 2004 and it competes with the International Telecommunication Union (ITU) standards. The available aggregated bandwidth is 1 Gbit/s, in downlink and uplink. The typical maximum number of ONTs is 16, but more can be used, typically 32, the only limitation is the optical power budget. The standard defines two variations in terms of maximum distance, 10 and 20 km, respectively 1000BASE-PX-10 and 1000BASE-PX-20 [2.5]. This standard is very popular in Japan and South Korea, where it was widely deployed.

2.4.3 10EPON

10G-EPON is designed as an upgrade for EPON and can coexist on the same ODN. 10G-EPON can be used with symmetrical or asymmetrical speeds, 10 Gbit/s downlink and uplink or 10 Gbit/s downlink and 1 Gbit/s uplink. 10 Gbit/s downlink uses a new wavelength at 1575-1580 nm, while the 10 Gbit/s uplink overlaps the 1Gbit/s uplink transmission window, so when the two are present in the same ODN, time division multiple access (TDMA) must be used to avoid interference. 10EPON, also known as 802.3av, was rectified on September 2009 [2.15].

2.4.4 G-PON

Gigabit-capable PON (G-PON) is the successor for BPON and it is defined within the G.984 standard family. The standardization process started in March 2003 with the

general characteristics [2.16] and physical layer [2.17], and continued in 2004 with the transmission convergence layer [2.18] and ONT management [2.19] specifications. The main new features are the bandwidth upgrade, 2.5 Gbit/s downlink and 1.25 Gbit/s uplink (2.5 Gbit/s uplink optional) and the creation of the G-PON encapsulation mode (GEM), which removes the mandatory use of the ATM protocol.

In G-PON the OLT and the ONT can be distanced up to 20 km, when using class B+ (28 dB budget) optical equipment, or 30 km if the split ratio is kept to 1:16. Class C+ (32 dB budget) gives an additional 10 km or the double split ratio.

More recently, tighter specifications regarding wavelength usage were developed to ensure a smoother transition to newer protocols [2.20]. Reach extension of G-PON has also been standardized [2.21]. The extra range is achieved using optical amplifiers, optical regenerators (optical to electrical to optical converter) or hybrid architectures. Introducing active elements in the architecture removes some of the OPEX advantages, but improves CAPEX when deploying G-PON in very sparse environments. Minor changes were made to allow more flexibility in distances between ONTs, increasing from 20 km to 40 km [2.22]. Currently this is the dominant PON standard in Europe and US (Verizon FiOS).

2.4.5 Portuguese PON landmarks

In Table 2.1 the main optical access networks landmarks are presented, with particular focus to the Portuguese market. The first operators to deploy and sell services based on PON in Portugal, were independent operators. TVTel, a small cable operator, explored an EPON on a town near Lisbon in 2007. This operator has then been bought by the main cable company, ZON. The second operator was Clix (Sonaecom), using G-PON technology and with a larger rollout, covering some areas of Lisbon and Oporto. Finally, in 2009 the incumbent operator, Portugal Telecom, started commercial exploration of their G-PON. Nowadays Portugal Telecom covers more than 1.600.000 households. To the date is the largest PON provider in Portugal.

Year	Landmark
1998	BPON standard rectified.
2004	EPON standard rectified.
2004	G-PON standard rectified.
2007	Independent operator TVTel starts commercial exploration of a small EPON network in Carnaxide, Lisbon.[3]
2008	Independent operator Clix / Sonaecom starts commercial exploration of the first G-PON network in Portugal [2.23], deployments in Lisbon and Oporto metropolitan areas.
May 2009	Incumbent operator, Portugal Telecom, starts G-PON network commercial exploration [2.24].
2010	XG-PON1 rectified.
October 2010	Portugal Telecom and Alcatel-Lucent agree to trial symmetric 10 Gbit/s solutions (future XG-PON2) [2.25].
October 2010	Portugal Telecom and Huawei complete trial with XG-PON1 equipment [2.26].
End of 2010	Portugal had 130,000 PON customers [2.27], and Portugal Telecom more than 1,000,000 homes capable of receiving G-PON services [2.28].
March 2011	Portugal had 152,000 PON customers and 1.55 million households covered [2.29].
June 2011	Portugal had 173,000 PON costumers [2.30].
End of 2011	Portugal Telecom plans to cover 1,600,000 households [2.31].

Table 2.1 - Optical access networks landmarks.

2.4.6 Next generation PON

Next generation access networks have to support an increased numbers of users, increased bandwidth demand and longer-range coverage [2.32]. It is interesting to note that the bandwidth demand at great extend, is due to the increase demand of wireless

[3] This company has been acquired by the major cable operator, all new optical access deployments have been canceled.

systems, since the bandwidth demands for backhauling cellular traffic are dramatically increasing. Future improvements to G-PON are being developed as part of next generation PON (NG-PON). They are divided in two groups, NG-PON1 and NG-PON2, but possibly more in future upgrades. The main difference between each initiative is the compatibility with G-PON. NG-PON1 proposals must be able to coexist with an operational G-PON, which might also have a video overlay service, while NG-PON2 proposals do not have to ensure this back compatibility [2.33].

To increase the PON's capacity there are three main options [2.34]:

- Line rate increase;
- Wavelength number increase;
- Other techniques such as optical coding, SCM or the use of coherent systems.

Each one has its own advantages and disadvantages, but traditionally the rule has been the increase of the line rate, while the system requirements allows it and it is economical viable. After reaching the system bandwidth limit, a new approach must be used. One idea is to reduce the number of users per wavelength, so that the average bandwidth per user increases. This, can be achieved by running multiple services at the same ODN using more wavelengths, i.e. two independent G-PON services would increase the average bandwidth by a factor of two. Instead of reusing standards not developed to run in parallel, dedicated wavelengths can be used to each ONT or shared dynamically. A third option includes increasing bit rate while maintaining or reducing the occupied bandwidth, by applying sophisticated modulation formats, instead of using on-off keying (OOK), for example optical OFDM (O-OFDM), a special form of SCM. But, the higher density of bits/Hz is usually accomplished at the expense of signal to noise ratio (SNR), newer hardware might be necessary.

The consensus for the NG-PON1 standard is the XG-PON family. The X in XG-PON comes from the Roman numeral that represents 10, in this case the 10 Gbit/s downlink.

The XG-PON family is divided in two groups, XG-PON1 and XG-PON2, both are defined by the recommendation group G.987 [2.35]. The objective is to have 10 Gbit/s in the downstream direction and 2.5 Gbit/s in the upstream in the XG-PON1 version, while in XG-PON2 the uplink is also at 10 Gbit/s. XG-PON2 is still in discussion phase, due to the upstream light source cost. XG-PON improves the available throughput with an increase in the line rate. While coexisting in the same PON, with an operational G-PON, thanks to the use of new dedicated wavelengths, as shown in Figure 2.3 where XG-PON

is represented in green, G-PON in blue and the RF overlay in red. Due to the improved cost/benefit for optical sources, the gain in bit rate experienced in XG-PON is accompanied by a reduction of optical spectrum usage.

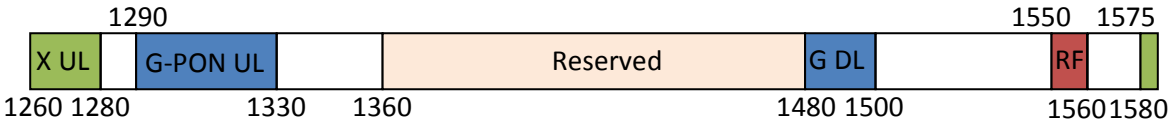

Figure 2.3 - Wavelength allocation in nm for G-PON and XG-PON1, based on [2.36].

10G-EPON and XG-PON are not compatible standards, but some convergence at the physical level has been subject to discussions between IEEE and ITU.

A NG-PON2 recommendation is expected in 2013 using WDM-PON technology. Ideally each ONT would have dedicated downstream and upstream wavelengths. Hybrid approaches can be employed [2.37], using several XG-PON wavelengths to achieve the same level of bandwidth per customer. A simpler version, with fixed wavelength ONTs can also maintain similar optical components costs, at the expense of an increase in ONTs stock management and deployment. This option will only be considered for deployment, if the cost of the pure WDM-PON solutions proves to be too high.

The future proof solution is one that is able to provide access to distances up to 100 km, 1000 users at 1 Gbit/s, also known as the 100x1000x1000 system [2.38].

2.5 WDM based PONs

WDM-PON networks have been considered for more than a decade [2.39], with several proposed approaches. The “holy grail” is a network where several wavelengths are transmitted by the ODN. Each wavelength can be shared by several ONTs, if the demand is low. However, an ONT can also use dedicated wavelengths if needed; any wavelength is available without any human intervention, i.e. without pre attributed wavelengths. However, all this features require very expensive equipment, such as: optical sources capable to work at any wavelength, tunable optical filters at the receivers, both the sources and filters must be very selective, to maximize the number of wavelengths.

The main advantage of WDM-PON is the ability to provide dedicated wavelengths to each client, as shown on Figure 2.4. Dedicated wavelengths reduce the pressure of aggregated data rates, allowing for simpler electronics and more relaxed requirements

when comparing with a possible 40 or 100G-PON. Another advantage of dedicated wavelengths is the possibility of virtual P2P connections on top of a P2MP physical network. P2P connections can improve the end-user privacy if each client only has access to their attributed wavelengths [2.38].

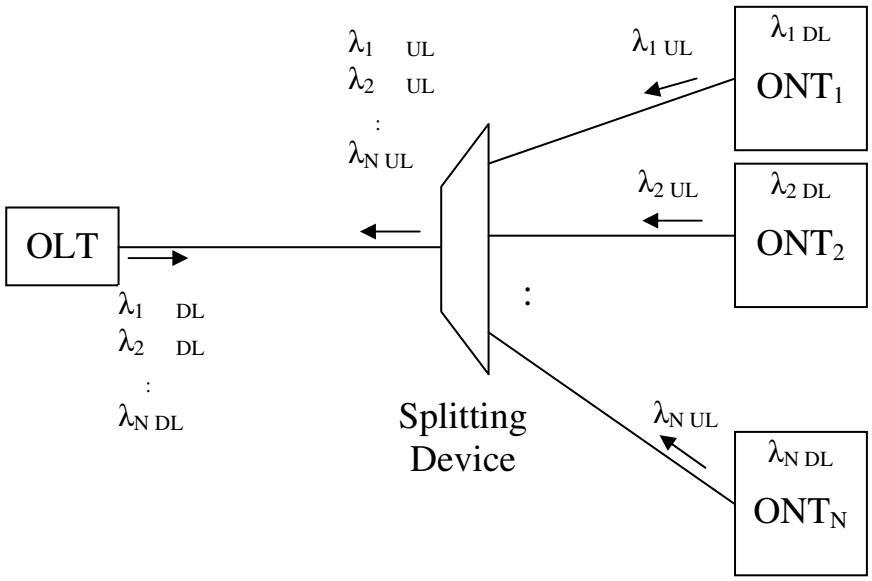

Figure 2.4 - Generic WDM-PON architecture. (OLT – optical line terminal; ONT – optical network terminal; DL – downlink; UL – uplink – λ wavelength)

A solution for WDM-PON is not yet established and several competing approaches are under research. Among them different architectures propose WDM for enhanced flexibility in resource management, for PON capacity scaling and for more convergence between different network segments (metro-access) and/or services (fixed-mobile). In future upgrades, dedicated wavelengths can allow for a gradual upgrade path, for example if a new standard proposes with a 10x increase in data rate, by replacing the laser source technology or by using a different data modulation technique. This technology can be applied, at least in theory, only to the customers which manifest interest.

The WDM-PON main challenges are [2.40]:

- Colorless sources
- Optical distribution network
- MAC protocol

Colorless sources

The main options are tunable lasers, several narrow band lasers in parallel or white sources followed by a wavelength splitter.

The solution should take into account the nature of P2MP PON networks, the laser source at the OLT should be a high performance device, reducing the cost of the ONT receiver.

Tunable lasers might not be the best solution for the OLT, since ideally if an OLT is designed to serve X clients, X wavelengths should be available, thus there is no need for optical tunable sources. The solution for the OLT colorless source should be a broadband light source with spectral splicing or several narrow band distributed feedback (DFB) lasers in parallel.

For the ONT the tunable laser is an efficient way of providing a tunable single wavelength channel. Nevertheless, such component is very expensive, especially for an end-user device. Another approach would be to generate the uplink wavelength in the OLT and modulated it in the ONT. In such approach some components are needed: a modulator to modulate the wavelength with the uplink data, a reflective component to transmit the wavelength back to the OLT, and an optical amplifier to boost the wavelength power before transmitting back to the OLT. All this tasks can be performed by a reflective semiconductor optical amplifier (RSOA), this device operates over a large optical spectrum range, typically around 40 nm, hence can be considered wavelength agnostic. Additionally, the optical signal can be modulated according to data by direct modulation of the device bias current. One of the main challenges is to develop a colorless transmitter that is able to operate over wide temperature range, ideally without a very elaborate temperature control system, and presenting a very stable wavelength response.

Optical distribution network

The ODN should be reusable without major changes, except at the split point. In here the passive splitters might be replaced with arrayed waveguide gratings (AWG), in order to simplify the ONT and, at the same time, to reduce the optical power loss, thus increasing the maximum reach of the network. Passive splitters share the entire optical spectrum with all ports; each receiver gets a fraction of the optical power. On the other

hand AWGs are wavelength selective this means that each wavelength channel will leave the AWG only through a single output port. If a large reach or active wavelength routing is needed, then active components such as optical amplifiers and optical-electrical-optical converters must be considered.

Another parameter to take into account is the number of wavelengths used, this is important to determine the grade of components used. If only 16 wavelengths are used, coarse WDM (CWDM) technology can be used, but if more wavelengths are needed then dense WDM (DWDM) components must be applied.

MAC protocol

The MAC layer complexity depends on the level of flexibly of the network. If each client has a dedicated wavelength, the ODN uses an AWG to split the optical signal and the ONT uses a RSOA as the uplink source, the MAC layer should be very similar to a P2P single fiber Ethernet link. On the other hand, if the wavelength distribution is dynamic or shared, the complexity of the MAC can be compared or be higher than G-PON family protocol.

2.5.1 WDM-PON employing RSOAs

Cost-efficient WDM technology is already well established in core network. However, its migration to access network segment relies on a large cost reduction of WDM transmitters especially for the customer terminal, ONT. A traditional tunable transceiver solution involves a wavelength management at each terminal and leads to prohibitive costs. This issue can be solved by new emerging architectures using "colorless" components (wavelength agnostic). In order to share high WDM costs, the general idea here is to put all wavelength management/generation/control complexity into CO and use wavelength agnostic remote modulation ONTs.

RSOAs have been, for several years identified as key components of next generation WDM-PON networks, at the customer premises allowing for colorless operation [2.41] and bidirectional transmission with only one single fiber. In such networks the RSOA is seeded with either continuous wave (CW) light from the OLT or with the downstream signal [2.42]. Such wavelength reuse strategy improves both the cost-effectiveness and wavelength control functionalities of WDM-PONs. The major limitation of RSOAs is

their electrical bandwidth, which is determined by the carrier lifetime in the active layer and typically limited to less than 3 GHz [2.43]. Although, RSOA based systems, with larger bandwidth have been reported, by using electronic equalization [2.44], or optical offset filtering together with electronic equalization [2.45]. Other approach that can be considered to overcome the bandwidth limitation of RSOAs is to use a reflective semiconductor amplifier integrated with an electro-absorption modulator, also known as reflective electro-absorption modulation (REAM) [2.46].

A network architecture employing a RSOA is depicted in Figure 2.5. The OLT will have at least a wavelength per client, a modulator and a photodetector. The several wavelengths sent and received will be multiplexed using an AWG. In the ODN, the traditional optical passive splitter would be replaced with an AWG, maintaining the existing fiber cabling. In this particular scenario, with only one wavelength per ONT, it would maximize the number of clients in the network and avoid the need of an optical filter at the ONT. However, it would mean that some form of sharing between the downlink and uplink occurs, for example, time division multiple access (TDMA) or frequency division multiple access (FDMA) using SCM. There is also the option to reuse the same wavelength for the uplink, without any sharing scheme. Using the RSOA characteristics, specifically the saturated state, this effectively removes the downstream signal, allowing to the upstream signal to be transmitted.

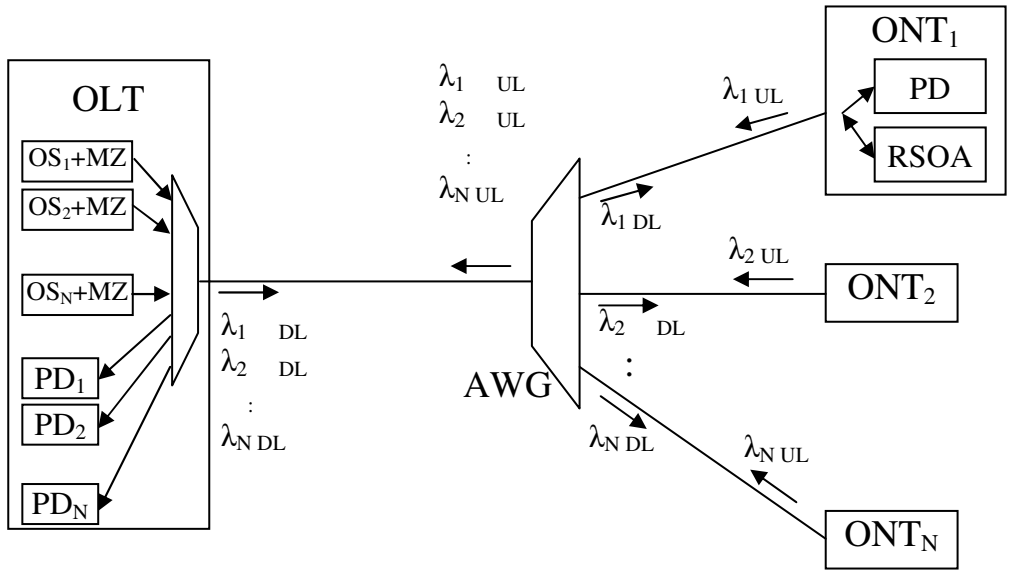

Figure 2.5 - Generic WDM-PON with RSOA architecture (OLT – optical line terminal; ONT – optical network terminal; DL – downlink; UL – uplink – λ wavelength, OS - optical source, MZ – Mach-Zehnder modulator, AWG - arrayed waveguide grating, PD – photodetector, RSOA – reflective semiconductor optical amplifier).

Other approaches to generate the wavelengths have been proposed, instead of using multiple DFB lasers [2.47, 2.48]. One approach consists on a broadband light source to generate all the channels simultaneously, followed by an AWG to distribute the individual channels. Next, each channel is fed to individual modulators where the different downlink signals are modulated. Because usually broadband light sources (BLSs) have limited power output, an erbium doped fiber amplifier (EDFA) might be necessary before the AWG, allowing the necessary power budget. If the RSOA electrical bandwidth is enough for the system requirements, the modulators and the EDFA might be replaced by one RSOA per downlink channel.

2.6 Summary

This chapter briefly introduced to broadband wired access networks, particularly PONs. We started the chapter with the motivation for investing in optical networks for access networks, which can be resumed in one word, bandwidth. Legacy technology cannot keep with consumer demands and expectations. Optical technology presents the best solution for this problem, as well as, providing network operators with a network asset to be sold or rented to other operators, such as backhaul for high speed cellular network.

The terminology for the basic components are presented, the OLT is the optical device at the operator premises, e.g. central office; ONT is the optical device at the client premises, and finally the third term is the ODN, which are all the components between the OLT and the ONT.

Two main architectures families were detailed, P2P and P2MP. P2P architectures are capable to provide the best performance and security per client, while P2MP presents the best economic results for operators since, less investment is required in the ODN, as well as less independent fibers which in turn means more reused ducts and poles. Additionally the OLT uses only one optical source and receiver per group of users (up to 32 or 64 depending on standard and power budget).

Taking in consideration that P2MP architectures are being chosen for most fiber access network deployments, the evolution for the two main standard families were presented. One of the standard families is supported by the IEEE which extends the Ethernet protocols to a P2MP optical architecture, the second institution is

Telecommunication Standardization Sector for the ITU (ITU-T). ITU-T work is closer to the telecommunication operators, thus the ATM protocol choice for BPON, while IEEE has a computer networks background. The two possible evolution paths are presented in Figure 2.6. Up to 10 EPON and XG-PON1 the standards are completed, the evolution from there is still undecided. There is some hope that some common ground can be achieved for a final 10G standard, at least for the symmetric approach. If at least the transmission windows and optical technology can be shared by the two standards, cost reduction in components should be experienced. The next evolution should be based on WDM techniques, due to the cost and complexity of increasing the transmission to 40 or 100 Gbit/s.

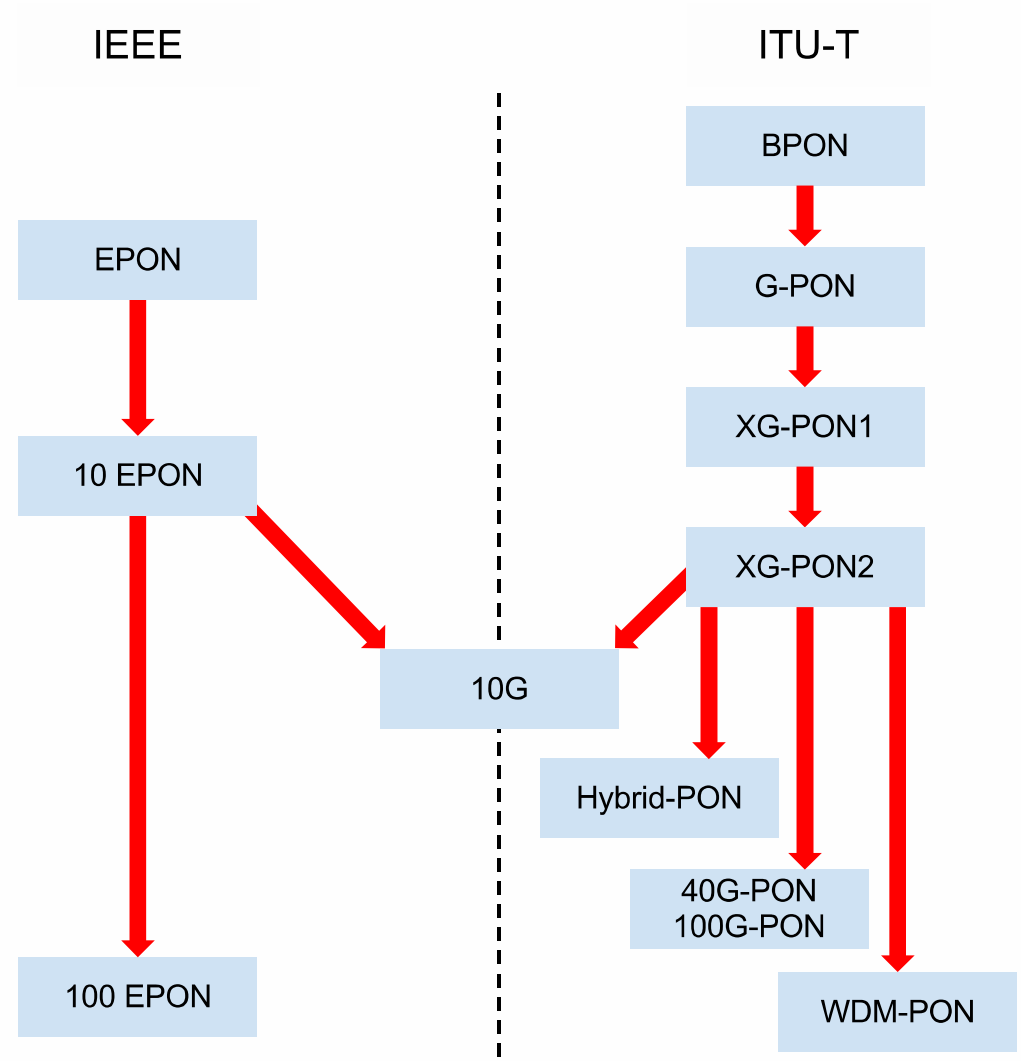

Figure 2.6 - Possible evolution paths for the two most used standards families.

WDM-PON challenges were introduced emphasizing, the need for colorless sources at the ONT. Although it is possible to use fixed wavelengths sources at the ONT,

it seems to be unviable to have 32, or more, equipment versions, one for each wavelength. And is even less viable to have tunable lasers, unless a major breakthrough occurs, lowering the component cost. The chapter ended with the overall overview of WDM-PON employing RSOAs, which is the architecture that will be referred in the remainder chapters of this thesis.

2.7 References

[2.1] L. G. Kazovsky, *et al.*, "Challenges in next-generation optical access networks: addressing reach extension and security weaknesses," *Optoelectronics, IET,* vol. 5, pp. 133-143, 2011.

[2.2] CableLabs, "Physical Layer Specification," *Data Over Cable Service Interface Specifications DOCSIS® 3.0,* November, 2011.

[2.3] T. Starr, *Dsl Advances*: Prentice Hall Professional, 2003.

[2.4] (2012). Internode ADSL Performance. *Website (Internode Systems Pty Ltd),* Available: http://www.internode.on.net/residential/adsl_broadband/easy_broadband/performance/, retrieved on April 21, 2012.

[2.5] IEEE-Computer_Society, "IEEE Standard for Information technology, Telecommunications and information exchange between systems, Local and metropolitan area networks, Specific requirements, Part 3: Carrier sense multiple access with Collision Detection (CSMA/CD) Access Method and Physical Layer Specifications (IEEE Std 802.3™-2008)," *Section 5, Clause 60,* 26 December 2008.

[2.6] S. S. Wagner, *et al.*, "Experimental demonstration of a passive optical subscriber loop architecture," *Electronics Letters,* vol. 24, pp. 344-346, 1988.

[2.7] J. A. Salehi and C. A. Brackett, "Code division multiple-access techniques in optical fiber networks. II. Systems performance analysis," *Communications, IEEE Transactions on,* vol. 37, pp. 834-842, 1989.

[2.8] R. Olshansky, *et al.*, "Subcarrier multiplexed lightwave systems for broad-band distribution," *Lightwave Technology, Journal of,* vol. 7, pp. 1329-1342, 1989.

[2.9] J. Armstrong, "OFDM for Optical Communications," *Lightwave Technology, Journal of,* vol. 27, pp. 189-204, 2009.

[2.10] R. Sananes, *et al.*, "Techno-economic comparison of optical access networks," in *Transparent Optical Networks, 2005, Proceedings of 2005 7th International Conference*, 2005, pp. 201-204 Vol. 2.

[2.11] ITU-T, "Broadband optical access systems based on Passive Optical Networks (PON)," *ITU-T Recommendation G.983.1, 1st Edition,* October 1998.

[2.12] ITU-T, "Broadband optical access systems based on Passive Optical Networks (PON)," *ITU-T Recommendation G.983.1, 2nd Edition,* January 2005.

[2.13] J. Finn, "PON Technology in the Verizon Network," *Globecom 2008 - 2008 Ieee Global Telecommunications Conference,* 2008.

[2.14] ITU-T, "A broadband optical access system with increased service capability by wavelength allocation," *ITU-T Recommendation G.983.3,* p. 20, March 2001.

[2.15] "IEEE Standard for Information technology - Telecommunications and information exchange between systems - Local and metropolitan area networks - Specific requirements Part 3: Carrier Sense Multiple Access with Collision Detection (CSMA/CD) Access Method and Physical Layer Specifications Amendment 1: Physical Layer Specifications and Management Parameters for 10 Gb/s Passive Optical Networks," *IEEE Std 802.3av-2009 (Amendment to IEEE Std 802.3-2008),* pp. c1-214, 2009.

[2.16] ITU-T, "Gigabit-capable passive optical networks (GPON): General characteristics," *ITU-T Recommendation ITU-T G.984.1,* March 2003.
[2.17] ITU-T, "Gigabit-capable Passive Optical Networks (GPON): Physical Media Dependent (PMD) layer specification," *ITU-T Recommendation G.984.2,* March, 2003.
[2.18] ITU-T, "Gigabit-capable Passive Optical Networks (G-PON): Transmission convergence layer specification," *ITU-T Recommendation G.984.3,* February 2004.
[2.19] ITU-T, "Gigabit-capable Passive Optical Networks (G-PON): ONT management and control interface specification," *ITU-T Recommendation G.984.4,* June 2004.
[2.20] ITU-T, "Gigabit-capable Passive Optical Networks (G-PON): Enhancement band," *ITU-T Recommendation G.984.5,* September 2007.
[2.21] ITU-T, "Gigabit-capable passive optical networks (GPON): Reach extension," *Recommendation ITU-T G.984.6,* March 2008.
[2.22] ITU-T, "Gigabit-capable passive optical networks (GPON): Long reach," *Recommendation ITU-T G.984.7,* July 2010.
[2.23] (2012). História Sonaecom. *Website (Portuguese) (Soneacom S.A.),* Available: http://www.sonae.com/sobre-a-sonaecom/historia/, retrieved on March 21, 2012.
[2.24] Portugal Telecom S.A., (2009). PT lança Rede para o Futuro. *Press Release (Portuguese),* Available: http://www.telecom.pt/InternetResource/PTSite/PT/Canais/Media/press_releases/PT+lan%C3%A7a+Rede+para+o+Futuro.htm, retrieved on May 12, 2011.
[2.25] Alcatel-Lucent, (2010). Portugal Telecom and Alcatel-Lucent perform Europe's first symmetrical 10G GPON trial. *Press Release,* Available: http://www.alcatel-lucent.com/wps/portal/!ut/p/kcxml/04_Sj9SPykssy0xPLMnMz0vM0Y_QjzKLd4x3tXDUL8h2VAQAURh_Yw!!?LMSG_CABINET=Docs_and_Resource_Ctr&LMSG_CONTENT_FILE=News_Releases_2010/News_Article_002245.xml, retrieved on May 24, 2011.
[2.26] Huawei, (2010). Portugal Telecom and Huawei Jointly Test IPTV Meo Service and 3DTV using 10G-GPON Technology for the First Time in Europe *Press Release,* Available: http://www.huawei.com/en/about-huawei/newsroom/press-release/hw-062663-10ggpon.htm, retrieved on May 24, 2011.
[2.27] ANACOM, "Informação Estatistica do Serviço de Acesso à Internet - 4.º Trimestre de 2010," 2011, Available: http://www.anacom.pt/streaming/SAI4trimestre2010.pdf?contentId=1072165&field=ATTACHED_FILE, retrieved on May 12, 2011.
[2.28] Portugal Telecom S.A., (2010). PT supera 1 milhão de clientes na Banda Larga Fixa. *Press Release (Portuguese),* Available: http://www.telecom.pt/InternetResource/PTSite/PT/Canais/Media/press_releases/PT+supera+1+milhao+de+clientes+na+Banda+Larga+Fixa.htm, retrieved on May 12, 2011.
[2.29] ANACOM, "Informação Estatistica do Serviço de Acesso à Internet - 1.º Trimestre de 2011," 2011, Available: http://www.anacom.pt/streaming/SAI_1trimestre2011.pdf?contentId=1090445&field=ATTACHED_FILE, retrieved on July 14, 2011.
[2.30] ANACOM, "Informação Estatistica do Serviço de Acesso à Internet - 2.º Trimestre de 2011," 2011, Available: http://www.anacom.pt/streaming/SAI_2trimestre2011.pdf?contentId=1097304&field=ATTACHED_FILE, retrieved on September 16, 2011.
[2.31] Portugal Telecom S.A., (2011). Portugal Telecom tem melhor rede de Fibra Óptica da Europa. *Press Release (Portuguese),* Available: http://www.telecom.pt/InternetResource/PTSite/PT/Canais/Media/press_releases/Portugal+Telecom+tem+melhor+rede+de+Fibra+Optica+da+Europa.htm, retrieved on May 12, 2011.
[2.32] R. P. Davey*, et al.*, "Long-Reach Passive Optical Networks," *Lightwave Technology, Journal of,* vol. 27, pp. 273-291, 2009.

[2.33] J. i. Kani, *et al.*, "Next-generation PON-part I: Technology roadmap and general requirements," *Communications Magazine, IEEE,* vol. 47, pp. 43-49, 2009.
[2.34] M. D. Andrade, *et al.*, "Evaluating strategies for evolution of passive optical networks," *Communications Magazine, IEEE,* vol. 49, pp. 176-184, 2011.
[2.35] ITU-T, "10-Gigabit-capable passive optical network (XG-PON) systems: Definitions, abbreviations, and acronyms," *ITU-T Recommendation G.987,* January 2010.
[2.36] ITU-T, "10-Gigabit-capable passive optical networks (XG-PON): General requirements," *ITU-T Recommendation G.987.1,* January 2010.
[2.37] F. Effenberger, *et al.*, "Next-generation PON-part II: Candidate systems for next-generation PON," *Communications Magazine, IEEE,* vol. 47, pp. 50-57, 2009.
[2.38] J. P. Elbers, "Optical access solutions beyond 10G-EPON/XG-PON," in *Optical Fiber Communication (OFC), collocated National Fiber Optic Engineers Conference, 2010 Conference on (OFC/NFOEC)*, 2010, pp. 1-3.
[2.39] R. D. Feldman, *et al.*, "An evaluation of architectures incorporating wavelength division multiplexing for broad-band fiber access," *Lightwave Technology, Journal of,* vol. 16, pp. 1546-1559, 1998.
[2.40] A. Mason, "Report for Ofcom: Fibre capacity limitations in access networks," XOF4G011V03, 13 January 2010 2010, Available, retrieved on
[2.41] P. Healey, *et al.*, "Spectral slicing WDM-PON using wavelength-seeded reflective SOAs," *Electronics Letters,* vol. 37, pp. 1181-1182, 2001.
[2.42] L. Wooram, *et al.*, "Bidirectional WDM-PON based on gain-saturated reflective semiconductor optical amplifiers," *Photonics Technology Letters, IEEE,* vol. 17, pp. 2460-2462, 2005.
[2.43] Y. Takushima, *et al.*, "Design Issues in RSOA-based WDM PON," in *PhotonicsGlobal@Singapore, 2008. IPGC 2008. IEEE*, 2008, pp. 1-4.
[2.44] K. Y. Cho, *et al.*, "Demonstration of 25.78-Gb/s, 20-km reach WDM PON using directly-modulated bandwidth-limited RSOA," in *Optical Fiber Communication Conference and Exposition (OFC/NFOEC), 2011 and the National Fiber Optic Engineers Conference*, 2011, pp. 1-3.
[2.45] I. Papagiannakis, *et al.*, "Investigation of 10-Gb/s RSOA-Based Upstream Transmission in WDM-PONs Utilizing Optical Filtering and Electronic Equalization," *Photonics Technology Letters, IEEE,* vol. 20, pp. 2168-2170, 2008.
[2.46] A. Garreau, *et al.*, "10Gbit/s Amplified Reflective Electroabsorption Modulator for Colourless Access Networks," in *Indium Phosphide and Related Materials Conference Proceedings, 2006 International Conference on*, 2006, pp. 168-170.
[2.47] T. T. Pham, *et al.*, "Colorless WDM-PON based on a Fabry-Pérot laser diode and reflective semiconductor optical amplifiers for simultaneous transmission of bidirectional gigabit baseband signals and broadcasting signal," *Opt. Express,* vol. 17, pp. 16571-16580, 2009.
[2.48] J. H. Lee, *et al.*, "First Commercial Deployment of a Colorless Gigabit WDM/TDM Hybrid PON System Using Remote Protocol Terminator," *J. Lightwave Technol.,* vol. 28, pp. 344-351, 2010.

3

Converged optical-60 GHz wireless networks

3.1 Introduction

Internet technologies are now considered as the universal communication platform. Traditional broadband access networks are widely available, e.g. asymmetric digital subscriber line (ADSL) is now available in almost all parts of Europe. However, this generation of access networks is not able to handle all the new emerging services, such as multi-room HDTV, digital distribution (videogames, movies, music), cloud storage (upload of pictures, videos, and documents). The solution is to take fiber access networks closer to the end-user with fiber-to-the-x (FTTx) architectures such as FTT-curb (FTTC), FTT-building (FTTB) or ideally FTT-home (FTTH).

In parallel to the growth of the Internet, wireless and mobile network technologies have witnessed a great development. Wireless/mobile network users want to be able to use their mobile terminals anywhere, inside and outside buildings, and enjoy the same user experience as they do while connected to their fixed broadband network. Consumer devices (laptops, smart phones, tablets, etc.) have interfaces enabling them to establish connection both wireless local area networks (WLANs) and to mobile networks. High speed WLANs hotspots based on IEEE 802.11x are a common reality, while 4G technologies such as long term evolution advanced (LTE-A) and worldwide interoperability for microwave access (WiMAX) 2 promise data up to 1 Gbit/s, are being developed. Present wireless technologies operate predominantly below the 10 GHz band, however, the abundant unlicensed spectrum around 60 GHz has been considered very attractive for multi-gigabit indoor wireless personal area network (WPAN), removing the bandwidth limitation of the present wireless networks [3.1]. Nevertheless, the transmission of 60 GHz wireless signals is limited to a few meters (~10 m), which implies the deployment of multiple radio access points to cover a single house or building. Besides the bandwidth limitations, the use of electrical lossy cables to drive the antennas has a significant impact on the energy consumption of the base station. Such high speed wireless networks require a broadband backbone network that can be provided by optical fiber links using radio over fiber (RoF) technology. However, the optical generation and distribution of radio signals at 60 GHz is susceptible of impairments that may degrade the overall system performance.

This chapter is devoted to the analysis of optical generation of 60 GHz radio RF carriers and their transmission impairments over optical fiber links. Section 3.2 provides the motivation for 60 GHz wireless networks with a brief overview of the relevant wireless standards available. Section 3.3 introduces RoF as key enabling technology for 60 GHz radio applications. The 60 GHz wireless-optical network scenarios are discussed in section 3.4. The generation and transportation of optical 60 GHz signals is considered in section 3.5, three optical modulation schemes using Mach-Zehnder modulators (MZMs), optical double side band (ODSB), optical single side band (OSSB) and optical carrier suppression (OCS) are considered. Section 3.6 is dedicated to the analysis of transmission impairments owing to the optical fiber chromatic dispersion, while section 3.7 discusses the main dispersion mitigation strategies and shows the robustness of OSSB and OCS modulation against optical fiber dispersion. The chapter concludes with a brief summary.

3.2 60 GHz wireless networks state of the art

A sample of the available unlicensed frequency bands within the world is: Japan, 59.0-66 GHz; USA and Canada, 57.05-64.0 GHz; Korea, 57.0-64.0 GHz; Europe, 57.0-66.0 GHz. It was demonstrated that it is possible to produce low cost complementary metal–oxide–semiconductor (CMOS) components and circuits operating at 60 GHz [3.2]. The IEEE has developed a standard for 60 GHz WPAN transmission systems, within the 802.15.3c working group [3.3, 3.4]. WPAN networks cover relatively short distances (usually up to 10 meters) and can support high data rate applications (up to several Gbit/s). IEEE 802.15.3c standard brings the 802.15.3 standard to the 60 GHz band with two types of modulation, single carrier (SC) modulation and orthogonal frequency division multiplexing (OFDM). Other standards using the 60 GHz band also include industry consortiums such as: WirelessHD™ [3.5] based on IEEE 802.15.3c. These standards are aimed to the video and audio transmission, providing a wireless replacement for high-definition multimedia interface (HDMI) cables. In the last specifications speeds up to 28 Gbit/s are envisaged. Another very similar standard is the ECMA-387 [3.6], a high-data-rate WPAN transport for both bulk data transfer and multimedia streaming; it specifies speeds up to 6.35 Gbit/s when using 1 channel or 25.4 Gbit/s with 4 channels.

It is too early in the standard life cycle to determine which of the three standards will prevail. IEEE 802.15.3c benefits from being an open standard with a focus on ad-hoc networks and P2P. Key players include Motorola, Intel, IBM, Panasonic, Qualcomm, Samsung and Philips. WirelessHD™ is based on IEEE 802.15.3c, but much more focused on a specific application, a wireless alternative to the HDMI cabling. This standard is based on an industry consortium, giving it more flexibility and shorter time-to-market solutions, some key players include Intel, Broadcom, LG and Panasonic. Already, products have been released with WirelessHD™ technology and with the help of marketing from the consortium players it should give it a head start. WirelessHD™ might win the battle in term of number of devices deployed if TV manufacturers include it in all their devices. This should give an incentive to telephone manufacturers to include the technology in future smart phones. Although it would benefit if at least a basic level of compatibly was created with IEEE 802.15.3c, making the WirelessHD™ an enhanced version, in terms of bit rate, antenna configuration and modulation schemes. ECMA-387

should have more difficulties to dominate due to the close nature of the standard. However, it does provide a simpler physical layer, with on-off- keying (OOK) being the mandatory modulation, niche applications should not be excluded.

Concerning WLANs standardization effort, the main objective is to provide a wireless service in the 60 GHz band with more than 10 meter of range. The two main standards are WiGig and IEEE 802.11ad.

WiGig [3.7] is an industry consortium, specifies up to 7 Gbit/s in the 60 GHz band. It is based on the 802.11 protocol and is compatible with the Wi-Fi standards in the 2.4 and 5 GHz bands. It also supports IP communication and transparent HDMI cable replacement like WirelessHD™. Its main feature is to increase the range with adaptive beam forming and multi directive antennas. The main supporters include AMD, Intel, Broadcom, Qualcomm, Cisco, Panasonic, and Samsung among others. WiGig specification was a contribution to the 802.11ad standardization process. It was proposed in May 2010 that it will be the basis of the IEEE 802.11ad protocol [3.7]. IEEE 802.11ad still on the definition stage [3.8], it is expected to be completed on December 2012.

Table 3.1 presents a brief summary of the main 60 GHz standardization efforts, dividing in network type (WPAN, WLAN), main applications and bandwidth.

Name	**Type**	**Application**	**Bit rate**
ECMA-387	WPAN	IP Data + A/V – HDMI replacement	6.35 Gbit/s per channel, up to 25.4 Gbit/s overall
802.15.3c	WPAN	Focus on P2P (IP Data and A/V)	Up to 5.7 Gbit/s
WirelessHD	WPAN	A/V – HDMI replacement, based on 802.15.3c	7.14 Gbit/s per channel, up to 28.6 Gbit/s overall
802.11ad	WLAN	IP Data, Back compatibility with 2.4 and 5 GHz Wi-Fi (based on WiGig)	Standard in discussion phase
WiGig	WLAN	IP Data + A/V – HDMI replacement + remote PCI Express / USB	Up to 7 Gbit/s

Table 3.1 - 60 GHz main standardization efforts [3.3-3.8].

WLAN solutions for the 60 GHz band are particularly attractive in terms of range, back compatibility, as well as technical challenges such as beam forming. At the same time this technical challenges will increase the cost of the system, as with the back compatibility, since radios and antennas operating in the 2.4 and 5 GHz bands will be

needed. It should not be a challenge for large devices, such as TV screens, but it will be for smaller devices such as smartphones, if several antennas are mandatory. Regarding the cost, back compatibility might be an issue for single purpose devices, such as audio/video (A/V) transmitters. However, other devices such as smartphones and even TV sets also have Wi-Fi access in their list of features. Ideally WirelessHD™ and IEEE 802.11ad would be compatible with each other, at least with a minimum set of features for interoperability, or in a worst case scenario with coordination to minimize interference issues. In theory IEEE 802.11ad has all to be the *de facto* standard for the 60 GHz, however, approving an IEEE 802.11 standard is known to be a long and slow process, which might compromise the standard success.

Other targeted applications operating in the 60 GHz frequency band is the provision of very-high-speed point-to-point radio links for future mobile network backhauling, or high speed WLAN bridging [3.9, 3.10].

Therefore, the application scenarios using the 60 GHz band are for medium-range outdoor wireless point-to-point (P2P) transmission offering speeds 10 Gbit/s as well as for high speed indoor short-reach WPANs.

3.3 Radio over fiber

A major limitation of 60 GHz wireless networks is their short range due to the high-atmospheric propagation attenuation, which can reach around 14 dB/km, as shown in Figure 3.1. Additionally, 60 GHz radio signals cannot cross the walls. Consequently, their indoor coverage is limited to a single room and to small areas, around 10 m radius [3.11-3.13].

As a consequence, a large number of remote antenna base stations (BSs) are necessary to cover an operational geographical area. Each BS will need high bandwidth connections to the rest of the network which can be provided by radio over fiber technology.

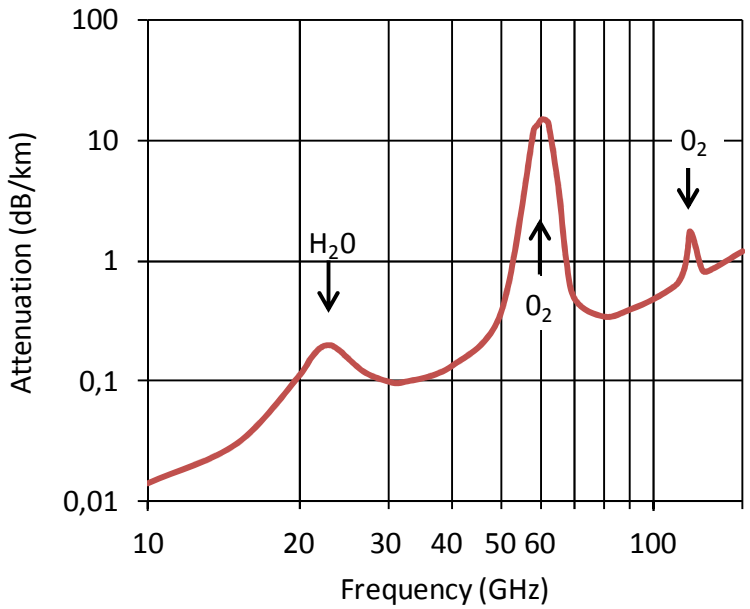

Figure 3.1 - Atmospheric attenuation at sea level with 20º C temperature, based on [3.14, 3.15].

RoF consists in transporting the radio signals by means of an optical carrier from the remote site to the head-end node of the cellular network where it is processed [3.16-3.18]. RoF links where an optical carrier is modulated by the wireless signals, known as analog RoF inherently suffer from inter modulation distortions arising from the nonlinearities of both RF and optical components [3.19]. Furthermore, it has been shown that the dynamic range of the analog optical link depend on the optical modulation that is used and optical fiber dispersion. Digitized RoF has been proposed during these last ten years thanks to the increasing speed of electronics. The main objective of digital RoF is to facilitate the usage of distributed antennas and to standardize the various interfaces of the radio equipment according to the common public radio interface (CPRI) or open base station architecture initiative (OBSAI). Such a modulation requires the usage of high-speed analog-to-digital converters (ADCs) at the source and Digital-to-Analog converters (DACs) at the destination. Similarly to analog RoF, it is possible to rebuild directly at destination the pre-modulated radio frequency (RF) signal without the usage of costly RF and intermediate frequency (IF) oscillators, in case of a low bandwidth and a low frequency signal. Meanwhile, in the case of broadband RF signals, the speed of electronics needed for the design of ADC/DAC may become restrictive. In that case, it is possible to digitize only the pre-modulated IF signal instead of the RF signal, an RF oscillator being needed at destination to up-convert the IF signal to the radio carrier frequency [3.20]. Contrary to what happens in analog systems, by employing digitalization of RF signals in optical

transport schemes it is possible to maintain its dynamic range irrespective of the optical fiber length, provided that the received signal amplitude is above the sensitivity of the link.

This thesis consider only analog RoF, therefore the acronym RoF will be used to refer to analog RoF being its main advantage, when compared with digital RoF, its capability of supporting multi-standard radio protocol and its transparency to the digital signal modulation format.

3.4 60 GHz wireless-optical network application scenarios

As discussed in section 3.2, mainly two application scenarios are envisaged for 60 GHz frequency band. Broadband WPANs, very-high-speed point-to-point radio links for future mobile network backhauling or high-speed WLAN bridging.

For WPANs, the role of optical fiber network is mainly to provide a transparent link to connect the different user and networking equipment. Today, most home/offices network schemes are based on gateways, which can be an IP router, typically placed at the premises entrance, where the external access network is terminated. User equipment is connected to this gateway through wired or wireless links. This solution is quite simple and efficient, as long as all services are digitalized and encapsulated into the same protocol. In such scenario, the optical fiber infrastructure can act only as distribution system. However, in a more advance architecture, using wavelength division multiplexing technology and exploiting its routing capabilities, it can enable the overall network with extra capabilities, such as dynamically bandwidth allocation in the optical domain [3.21, 3.22].

The application scenarios of very-high-speed point-to-point radio links for future mobile network backhauling or high-speed WLAN bridging, which are not limited to the operation in the 60 GHz band, and can be supported by the already widely deployed optical fiber access network. The simultaneous support of both wired and wireless technologies over the same physical access infrastructure is expected to result in both capital expenditures (CAPEX) and operational expenditures (OPEX) savings, by minimizing the total infrastructure that has to be installed and maintained. In the recent proposed solutions, the emphasis is on low cost, low power consumption and technology integration [3.23-3.27], other approaches [3.28, 3.29] are mainly focused on integrating

wireless access technologies with passive optical network (PON) standards (e.g. EPON, GPON).

In this chapter we focus on technology integration aspects, specifically how to generate and transport efficiently radio signals over optical fibers.

3.5 Techniques for generating and transporting radio signals over optical fiber

The generation and delivery of high-quality optical mm-wave signals, while maintaining the system simple and cost effective, is a key technical challenge in the implementation of RoF networks. Recently, several new approaches for the generation of optical mm-waves have been proposed [3.30]. Among them, optical mm-wave signal generation using external modulation of an optical carrier, by means of lithium niobate ($LiNbO_3$) MZM has proven to be a reliable approach due to the frequency range, excellent system stability, and high spectral purity of the generated signal. Hence this thesis focuses on mm-wave generation techniques using MZM.

ODSB, OSSB, and OCS modulation schemes have been widely investigated and demonstrated. Due to chromatic dispersion, ODSB is subject to dispersion-induced power fading [3.31]; this drawback can be overcome using OSSB and OCS [3.32-3.34]. OCS, besides providing robustness against chromatic dispersion, also acts as a frequency doubler. This last characteristic is particularly important since although commercially $LiNbO_3$ MZM with 60 GHz bandwidth are available, they are very expensive; using OCS modulation, only a drive RF signal of 30 GHz is required to generate 60 GHz. Other frequency up-conversion techniques that take advantage of the intrinsic non-linear characteristics of MZM have also been developed [3.34-3.40].

3.5.1 Optical Mach-Zehnder modulator model

The optical modulator considered in this thesis is the dual arm $LiNbO_3$ MZM. The basic principle of MZM is very simple: an input optical field coupled to two waveguide branches fabricated from the same material and with the same length. An electrical signal can be applied on each arm of the MZM separately. When the electrical signal that is

applied to MZM arms changes, the effective refractive index of the waveguide will change, this will change the phase of the optical field. Thus the phase delay of optical field, in each arm of MZM can be controlled by the external electrical signal field. The two optical fields at the output of each arm are then coherently added together by another coupler.

The optical field at the output of the dual arm MZM is given by:

$$E_{out}(t) = \frac{E_{in}(t)}{2}\left(e^{j\pi\frac{d_1(t)}{V_\pi}} + e^{j\pi\frac{d_2(t)}{V_\pi}}\right) \tag{3.1}$$

where $d_1(t)$ and $d_2(t)$ are the drive voltages applied to arms one and two, respectively, $E_{in}(t) = \sqrt{2P_o}e^{j\omega_c t}$ is the optical field at the input of MZM with angular frequency ω_c and average power and P_0, V_π is the switching voltage. Assuming that the drive voltage is a pure carrier at angular frequency ω_m, plus a DC component, $d_{1,2}(t) = V_m sen(\omega_m t + \theta_{1,2}) + V_{DC1,2}$, $\theta_{1,2}$ and $V_{DC1,2}$ can be adjusted to generate different optical modulation formats, being the modulation depth defined as: $x_c = \frac{V_m}{V_\pi}$.

3.5.2 Optical double side band modulation

An ODSB signal is obtained by applying to the electrodes of the dual arm MZM the following electrical signals:

$$\begin{aligned} d_1(t) &= x_c V_\pi m(t) - \frac{V_\pi}{4} \\ d_2(t) &= -x_c V_\pi m(t) + \frac{V_\pi}{4} \end{aligned} \tag{3.2}$$

where $m(t) = \sin(\omega_m t)$ is a sinusoidal signal of amplitude one and angular frequency ω_m.

Being the optical field at modulator output, $E_{ODSB}(t)$:

$$E_{ODSB}(t) = \frac{E_{in}(t)}{2}\left(e^{j\pi x_c m(t) - \frac{\pi}{4}} + e^{-j\pi x_c m(t) + \frac{\pi}{4}}\right) \tag{3.3}$$

$E_{ODSB}(t)$, can be written as a series of Bessel functions, as [3.41]:

$$E_{ODSB}(t) = \sqrt{2P_0}e^{j\omega_c t}\sum_{n=-\infty}^{\infty}\cos\left[\frac{\pi}{4}+n\frac{\pi}{2}\right]J_n(\pi x_c)e^{jn\left(\omega_m t+\frac{\pi}{2}\right)} \quad (3.4)$$

where $J_n(.)$ is the n_{th} order Bessel function of the first kind. In Figure 3.2a the MZM is presented with the necessary configuration for generating an ODSB signals, while Figure 3.2b illustrates a representative optical spectrum at the output of the MZM.

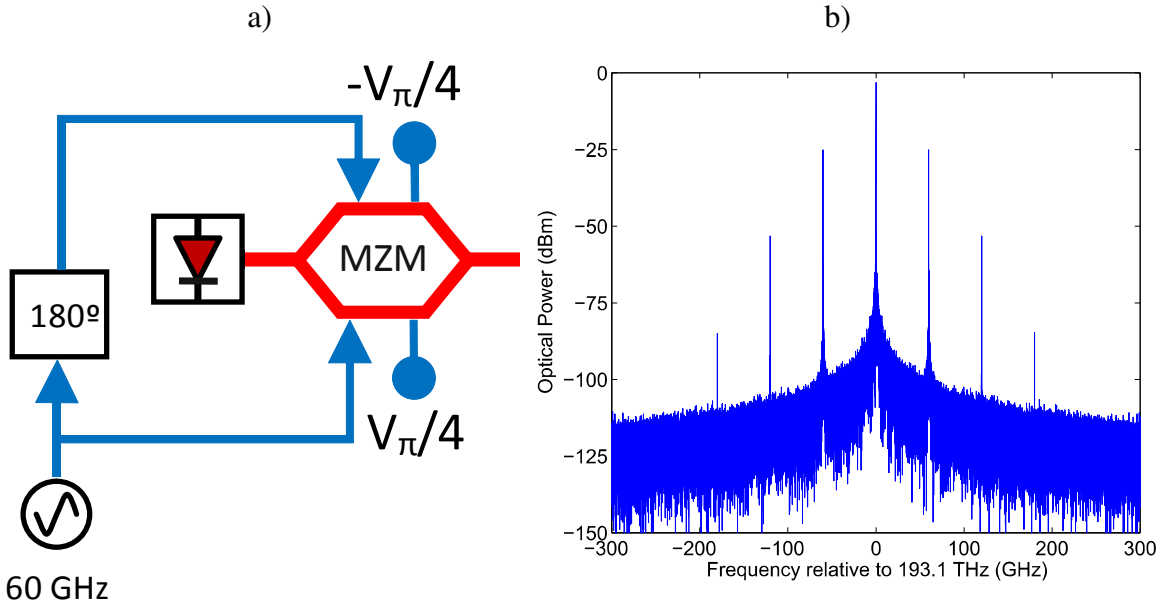

Figure 3.2 - a) MZM with ODSB configuration; b) ODSB spectrum at the MZM output.

3.5.3 Optical single side band modulation

Numerous techniques to suppress one sideband of the optical signal have been considered in the literature [3.42, 3.43]. The simplest technique consists in optical filtering using a narrow band notch fiber Bragg grating where the reflective band coincides with the unwanted sideband. Although this technique is simple to implement, it is not power efficient and since it is wavelength dependent it cannot be employed in frequency/wavelength agnostic networks.

Another well-known approach to achieve single sideband modulation is to use a dual-arm MZM in a configuration as shown in Figure 3.3a. An RF signal is applied to the two RF ports, with one being directly connected to the RF port and the other being phase shifted by 90º and then connected to the second RF port.

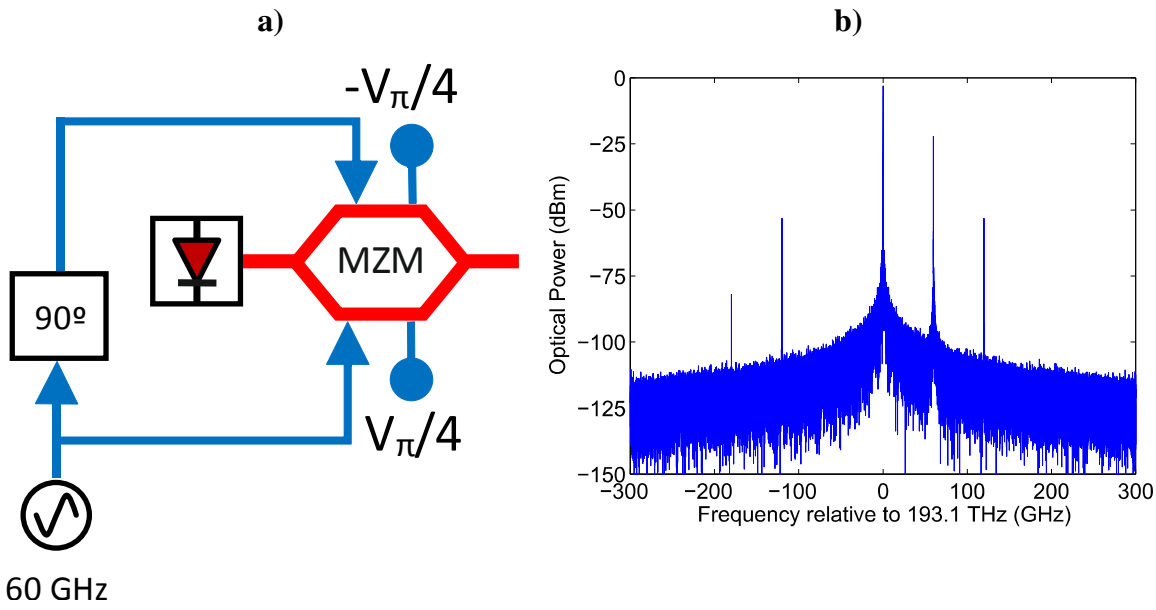

Figure 3.3 - a) MZM with OSSB configuration; b) OSSB signal at the MZM output.

The interaction between the RF modulation and the optical signals results in the suppression of one of the odd-harmonics modulation sidebands, as shown in Figure 3.3b.

An OSSB signal is obtained by applying to the electrodes of the dual arm MZM the following electrical signals:

$$d_1(t) = x_c V_\pi m(t) - \frac{V_\pi}{4}$$
$$d_2(t) = x_c V_\pi \hat{m}(t) + \frac{V_\pi}{4} \qquad (3.5)$$

where $\hat{m}(t)$ represents the signal m(t) with a 90º phase shift, replacing (3.5) in equation 3.1 can be expressed as:

$$E_{OSSB}(t) = \frac{E_{in}(t)}{2}\left(e^{j\pi x_c m(t) - \frac{\pi}{4}} + e^{j\pi x_c \hat{m}(t) + \frac{\pi}{4}}\right) \qquad (3.6)$$

A slightly different configuration has been proposed by [3.44]. It uses a combination of two optical modulators; a dual arm MZM cascaded with an optical phase modulator (PM). The electrical voltages applied on both electrodes of the dual arm MZM are given by $d_1(t)$ and $d_2(t)$, while the electrical signal that modulates the PM is $d_3(t)$. The system output is given by:

$$E_{out}(t) = \frac{E_{in}(t)}{2}\left(e^{j\pi\frac{d_1(t)}{V_\pi}} + e^{j\pi\frac{d_2(t)}{V_\pi}}\right)e^{j\pi\frac{d_3(t)}{V_\pi}} \tag{3.7}$$

To generate an OSSB signal with the equation 3.6 configuration, the following values should be applied to the d_1, d_2 and d_3:

$$\begin{aligned} d_1(t) &= x_c V_\pi m(t) - \frac{V_\pi}{4} \\ d_2(t) &= -x_c V_\pi m(t) + \frac{V_\pi}{4} \\ d_3(t) &= x_c V_\pi \hat{m}(t) \end{aligned} \tag{3.8}$$

replacing in equation 3.7:

$$E_{OSSB}(t) = \frac{E_{in}(t)}{2}\left(e^{j\pi x_c m(t)-\frac{\pi}{4}} + e^{j\pi x_c m(t)+\frac{\pi}{4}}\right)e^{j\pi x_c \hat{m}(t)} \tag{3.9}$$

This last configuration is more complex, but gives a greater level of flexibility when working in a laboratorial environment [3.45]. If we consider that a 90º phase shifter must used in the second arm with at least 3 dB attenuation, therefore an additional attenuator should be connected to the first arm driven by the *m(t)* signal to maintain identical power levels at both arms. With the use of the PM, the difference on the MZM arms must be 180º, which is the signal and the signal inverted. Usually signal generators provide these two signals right 'out-of-the-box'.

However, for a mass market perspective the first approach, should be cheaper and simpler, particularly if the electronic circuitry connected to the input arms are integrated in a single electronic package, or ideally integrated with the optical modulator. Depending on the signals introduced in the system, the two designs can be mathematical equivalent [3.46].

To ensure the two configurations are mathematically equivalent d_1 and d_2 signals for the first configuration should be:

$$\begin{aligned} d_1(t) &= x_c V_\pi\big(m(t) + \hat{m}(t)\big) - \frac{V_\pi}{4} \\ d_2(t) &= x_c V_\pi\big(-m(t) + \hat{m}(t)\big) + \frac{V_\pi}{4} \end{aligned} \tag{3.10}$$

The MZM optical field at the output of both configurations can be expressed as [3.41]:

$$E_{OSSB}(t) = E_{in}(t)\cos\left(x_c\pi m(t) - \frac{\pi}{4}\right)e^{jx_c\pi\hat{m}(t)} \qquad (3.11)$$

If we assume that *m(t)* is a pure normalized carrier, $m(t) = sin(\omega_m t)$, $E_{OSSB}(t)$ can be rewritten as a series of Bessel functions [3.41]:

$$E_{OSSB}(t) = E_{in}(t)\sum_{n=-\infty}^{\infty}\cos\left[(n-1)\frac{\pi}{4}\right]J_n\left(\sqrt{2}x_c\pi\right)e^{jn\left(w_m t-\frac{\pi}{2}\right)} \qquad (3.12)$$

Analyzing equation 3.12 we can see that each *n* corresponds to one optical sideband. The nth sideband is null whenever $\cos\left[(n-1)\frac{\pi}{4}\right]=0$; this occurs for $n=\cdots,-5,-1,+3,+7,\cdots$. Figure 3.3b shows an illustrative spectrum of an OSSB signal.

3.5.4 Optical carrier suppression modulation

The OCS modulation scheme, shown in Figure 3.4a, is another possible dispersion robust modulation scheme. OCS is generated by biasing a dual-arm MZM at the switching voltage V_π and applying RF signals with a π phase difference at each arm of the MZM. At the output of the MZM, the optical carrier will be suppressed and a double-sideband-suppressed carrier optical signal will be generated.

This is the same as using equation 3.1 and applying the electrodes the following signals:

$$\begin{aligned} d_1(t) &= x_c V_\pi m(t) - \frac{V_\pi}{2} \\ d_2(t) &= -x_c V_\pi m(t) + \frac{V_\pi}{2} \end{aligned} \qquad (3.13)$$

The optical field at the output of the MZM is given by:

$$E_{OCS}(t) = \frac{E_{in}(t)}{2}\left(e^{j\pi x_c m(t)-\frac{\pi}{2}} + e^{j\pi x_c m(t)+\frac{\pi}{2}}\right) \quad (3.14)$$

If we assume that $m(t)$ is a pure carrier, $m(t) = sin(\omega_m t)$, $E_{OCS}(t)$, can be written as a series of Bessel functions, as [3.41, 3.47]:

$$E_{OCS}(t) = \sqrt{2P_o}e^{j\omega_c t}\sum_{n=-\infty}^{\infty} J_{2n+1}(m_I/\sqrt{2})e^{j(n\omega_m t+\frac{\pi}{2})} \quad (3.15)$$

For clarity, some authors replace $\sqrt{2}x_c\pi$ with m_I, also known as modulation index [3.41].

The main advantage of such an implementation is to require only half the desired modulating frequency to drive the MZM. The mixing of the two optical carriers in a high-speed photodetector generates a single beat component at twice the drive frequency, which is not affected by dispersion-induced RF penalties if the MZM operates in the linear regime. Figure 3.4b shows the optical spectrum at the output of the MZM, the input RF signal used was 30 GHz. Note the absence of the optical carrier, which will allow the up-conversion of the 30 GHz signal to 60 GHz.

a) b)

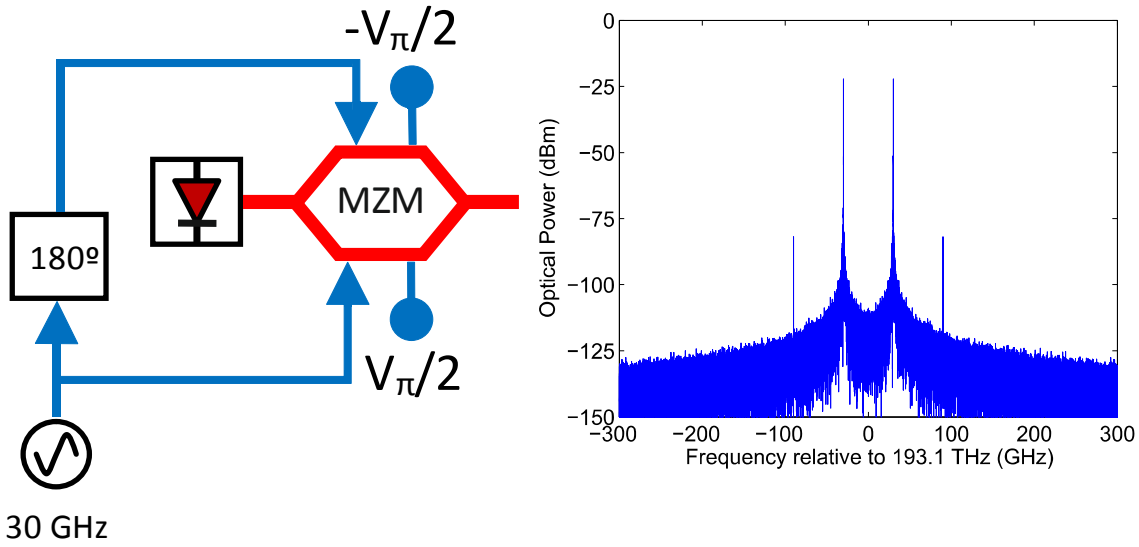

Figure 3.4 - a) MZM with OCS configuration; b) OCS signal at the MZM output.

3.5.5 60 GHz generation by up-conversion strategies

One solution to overcome the bandwidth limitation of commercially available MZM for high frequency operation is to use non-linearity induced optical frequency multiplication. In addition to complexity and power efficiency, a key important characteristic of any optical frequency multiplication technique is its robustness against fiber dispersion, which is offered by both OSSB and OCS modulation. Both strategies rely on the suppression of sidebands; in OSSB the positive or negative odd harmonic are suppressed while in OCS it is the optical carrier and the even harmonics.

The approach followed in this thesis [3.47] relies on the generation of high-order optical harmonics by setting the modulation index to an appropriate level, therefore taking advantage of the intrinsic non-linear characteristics of the MZM while using common ODSB, OSSB, and OCS modulation. By beating any two optical harmonics or/and beating any order optical harmonic with the optical carrier, upon photo-detection, mm-wave signals are generated with frequencies corresponding to the beatings fluctuations. Other frequency upconversion techniques that take advantage of the intrinsic nonlinear characteristics of MZMs have been developed [3.34-3.40]. However, some of these proposed upconversion schemes are complex, requiring two or more external modulators and/or narrow band optical filters to filter undesirable harmonics, which increases system complexity and cost.

3.6 Optical fiber dispersion effects on radio over fiber systems

The performance of RoF systems may be severely impaired by fiber chromatic dispersion [3.31]. The transfer function of a single-mode fiber around the optical carrier angular frequency ω_c, taking into account only the group velocity dispersion (GVD), can be modeled as:

$$H_{LINK}(z,\omega) = e^{\frac{-j\beta_2\omega^2 z}{2}} \tag{3.16}$$

where ω is the angular modulation frequency, z is the fiber longitudinal coordinate and β_2 is the first order dispersion, which can be calculated by expanding the mode-propagation constant β in a Taylor series around ω_c, the optical carrier frequency [3.48]:

$$\beta(\omega) = n(\omega)\frac{\omega}{c} = \beta_0 + \beta_1(\omega - \omega_c) + \frac{1}{2}\beta_2(\omega - \omega_c)^2 + \cdots \qquad (3.17)$$

where $n(\omega)$ is the refractive index, using the Sellmeier equation:

$$\beta_{\mathrm{m}} = \left.\frac{d^m\beta}{d\omega^m}\right|_{\omega=\omega_c} \qquad m = 0,1,2,\cdots \qquad (3.18)$$

$$\beta_2 = -\frac{\lambda^2}{2\pi c}D \qquad (3.19)$$

where D is the dispersion parameter, c is the vacuum velocity of light and λ is the operating wavelength.

The optical field after propagating through z meters of fiber, is given by equation 3.20, 3.21 and 3.22 for ODSB, OSSB and OCS respectively [3.47],

$$E_{F\_ODSB}(t) = \sqrt{2P_o}e^{j\omega_c t}\sum_{n=-\infty}^{\infty}\cos\left[\frac{\pi}{4} + n\frac{\pi}{2}\right]J_n(m_I/\sqrt{2})\exp\left\{j\left[n(\omega_m t + \frac{\pi}{2}) - \frac{\beta_2}{2}n^2\omega_m{}^2 z\right]\right\} \qquad (3.20)$$

$$E_{F\_OSSB}(t) = \sqrt{2P_o}e^{j\omega_c t}\sum_{n=-\infty}^{\infty}\cos\left[(n-1)\frac{\pi}{4}\right]J_n(m_I)\exp\left\{j\left[n(\omega_m t - \frac{\pi}{2}) - \frac{\beta_2}{2}n^2\omega_m{}^2 z\right]\right\} \qquad (3.21)$$

$$E_{F\_OCS}(t) = \sqrt{2P_o}e^{j\omega_c t}\sum_{n=-\infty}^{\infty}\left[0.5\left(1-(-1)^n\right)\right]J_{2n+1}(m_I/\sqrt{2})\exp\left\{j\left[n\omega_m t + \frac{\pi}{2} - \frac{\beta_2}{2}n^2\omega_m{}^2 z\right]\right\} \qquad (3.22)$$

Equation 3.20 to 3.22 shows that different optical field harmonics are affected by different phase changes due the fiber dispersion. Furthermore, as the optical signal is detected by a photodetector with responsivity, R_λ, the detected photocurrent, $i(t) = R_\lambda|E_F(t)|^2$, which is proportional to the envelope of optical field at the fiber output $E_F(t)$ consists of harmonic components result from a mixing product of the incoming optical field harmonics.

The corresponding optical power for a given harmonic p may be expressed equation 3.23, 3.24 and 3.25.

$$P_{out\_ODSB}(z,t) = 2P_o \cos(p\omega_m t + \frac{\pi}{2}) \sum_{n=\frac{p+1}{2}}^{\infty} (-1)^{n-(p-1)/2} J_n(m_I/\sqrt{2}) J_{n-p}(m_I/\sqrt{2}) \\ .\cos\left[p(2n-p)\frac{\beta_2}{2} z\omega_m{}^2 \right] \quad \text{for } p \text{ odd} \tag{3.23}$$

$$P_{out\_OSSB}(z,t) = \sum_{n=\frac{1-p}{2}}^{\infty} 4\sqrt{2}P_o \sin(p\frac{\pi}{4}) \cos\left[\frac{n+p-1}{2}\pi - (-1)^{\frac{p-1}{2}}\frac{\pi}{4} \right] J_n(m_I) J_{n+p}(m_I) \\ \sin\left\{ p\omega_m t - \cos\left[\frac{n+p-1}{2}\pi - (-1)^{\frac{p-1}{2}}\frac{\pi}{4} \right] .(p^2+2np)\frac{\sqrt{2}}{2}\beta_2 z\omega_m{}^2 \right\} \quad \text{for } p \text{ odd} \tag{3.24}$$

$$P_{out\_OCS}(t) = 2P_o \sum_{n=-\infty}^{\infty} \left[0.5\left(1-(-1)^n\right) \right] \left[0.5\left(1-(-1)^{p+n}\right) \right] J_n(m_I/\sqrt{2}) J_{n+p}(m_I/\sqrt{2}) \\ .\exp\left\{ j\left[p\omega_m t + \frac{\beta_2}{2}(p^2+2np)\omega_m{}^2 z \right] \right\} \tag{3.25}$$

For example, for ODSB modulation, for *p=1* the electrical current corresponding to the fundamental harmonic, considering the contribution from beating of all optical field components with an optical frequency separation of ω_m.

p=1, n=1

$$P_{ODSB}(z,t) = -2P_0 \cos\left(\omega_m t + \frac{\pi}{2}\right) J_1\left(\frac{m_I}{\sqrt{2}}\right) J_0\left(\frac{m_I}{\sqrt{2}}\right) cos\left(\frac{\beta_2}{2} z\omega_m{}^2\right)$$

p=1, n=2

$$P_{ODSB}(z,t) = 2P_0 \cos\left(\omega_m t + \frac{\pi}{2}\right) J_2\left(\frac{m_I}{\sqrt{2}}\right) J_1\left(\frac{m_I}{\sqrt{2}}\right) cos\left(3\frac{\beta_2}{2} z\omega_m{}^2\right)$$

p=1, n=3

$$P_{ODSB}(z,t) = -2P_0 \cos\left(\omega_m t + \frac{\pi}{2}\right) J_3\left(\frac{m_I}{\sqrt{2}}\right) J_2\left(\frac{m_I}{\sqrt{2}}\right) cos\left(5\frac{\beta_2}{2} z\omega_m{}^2\right)$$

Although the power received depends on a series of sums towards infinite, for small values of m_I it is a good approximation to use only *n=1* as is clearly shown in Figure 3.5. Where the first kind Bessel function is plotted versus m_I for the first 4 terms.

Equation 3.23 can be analyzed in three parts, the first one is the overall optical power of the optical field, which is spread over each harmonic; the second part accounts for the beating between two harmonic spaced by ω_m. The third factor takes into account optical dispersion and gives rise to the typical power fading characteristic of versus distance, of RoF systems employing ODSB modulation.

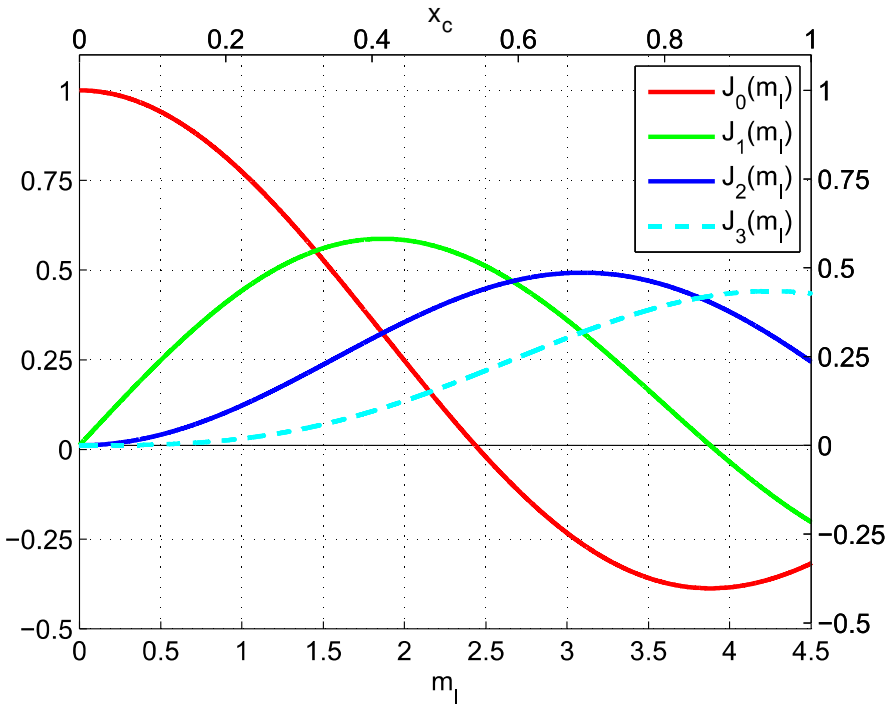

Figure 3.5 - First kind Bessel function for several orders in function of m_I and the corresponding x_c.

To quantify the power fading penalty, Figure 3.6 shows the calculated normalized received RF power in function of the link distance and the RF carrier, no fiber attenuation was considered. From the results it can be seen that the RF power varies in a periodic manner with complete power suppression occurring at certain modulating frequencies, for the 60 GHz RF carrier the first power null occurs around 1 km.

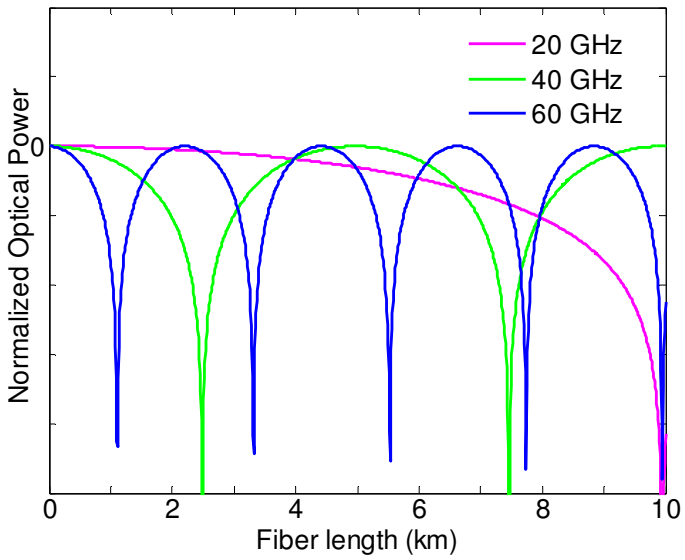

Figure 3.6 - Normalized received optical power for an ideal optical system employing ODSB. Three RF carrier frequencies are considered, 20 GHz, 40 GHz and 60 GHz.

3.7 Dispersion effects mitigation strategies

Since fiber dispersion penalties are so severe in direct-detection optically RoF systems, various techniques have been proposed to mitigate the dispersion effects in such systems. Among is the use of heterodyne receivers [3.49-3.52]. Another approach is to remove one of the optical signal side bands after the optical signal is modulated, thus converting an ODSB signal in an OSSB signal. This can achieved by applying an optical filter after the modulator, tuned in such a way that one of the side bands is removed. The simplest technique consists in optical filtering using a narrow band notch fiber Bragg grating where the reflective band coincides with the unwanted sideband, as shown in the literature [3.42, 3.43].

Another technique to generate OSSB is via cancellation of the unwanted optical sideband within an external optical modulator. This is the strategy used in this thesis. Although the filtering approach might seem the easiest approach, there are several drawbacks, especially in terms of flexibility. The filter will only work for one specific scenario, one particular wavelength and one particular RF band. Another drawback is the power efficiency, the energy used in the second side band is lost.

3.7.1 Dispersion robustness characteristics of OSSB modulation

The power fading characteristics of a 60 GHz system over 5 km of optical fiber is depicted in Figure 3.7, using equation 3.24 and 3.25. Both OSSB and OCS modulation schemes are considered as well as various modulation depths. Due to the inherent nonlinear characteristics of MZM, even when driven by low modulation depths both OSSB and OCS modulation schemes generate higher order harmonics. Upon photodetection the beating of any two optical harmonics or/and beating of any order optical harmonic with the optical carrier generates mm-wave signals with frequencies corresponding to the beatings. The beatings of the higher order harmonics give rise to received power fading effects as can be seen in Figure 3.7.

The received power strength varies periodically with the fiber length. The fundamental harmonic component of the photocurrent, at the 60 GHz frequency consists of the sum of the different optical field harmonics beats which are separated by 60 GHz in the optical domain. For OSSB, when small modulation depths are considered the

dominant term is the beating between the optical carrier and the first optical harmonic which is single sideband signal and therefore the received power fading is very small. When the modulation depth increases the higher harmonics become relevant which leads to higher power fading. These nonlinear distortions can be reduced by techniques such as pre-distortion of the analog signals and linearization of the MZM. Another approach is to use narrow band optical filter to filter undesirable harmonics. However, such linearization techniques are all devised at the system level and make the system more complex. When no linearization technique is employed it is useful to find the best operating region by adjusting the system operating parameters.

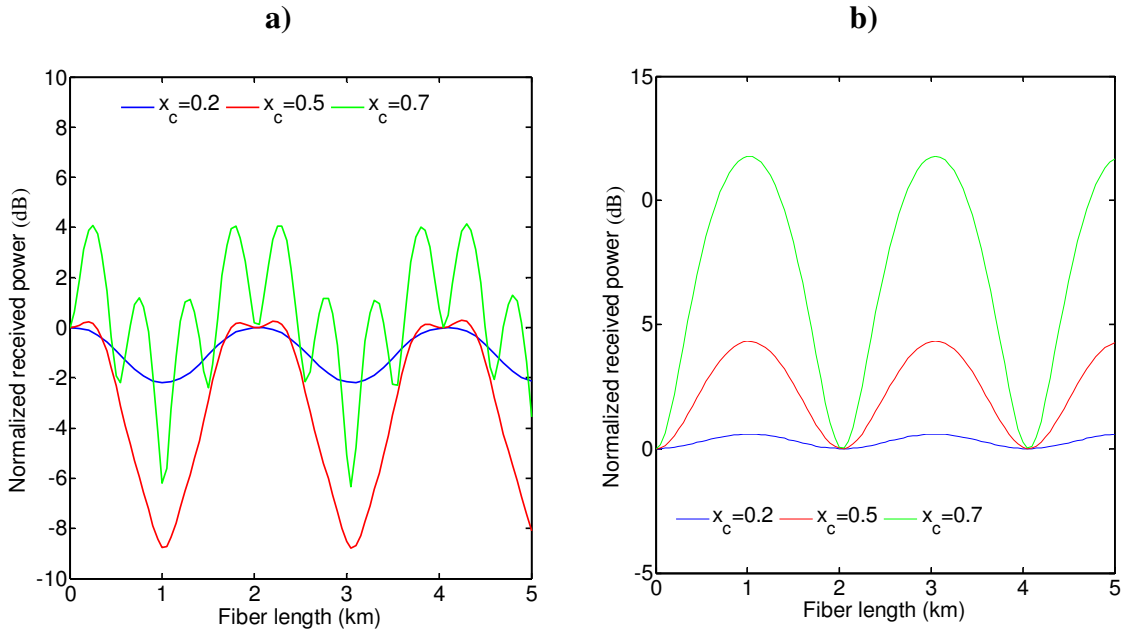

Figure 3.7 - Normalized received power for: a) OSSB modulation b) OCS modulation. (power normalized to the received power at a fiber length of 0 km)

3.8 Summary

This chapter described the main standards using 60 GHz in WPAN and WLAN networks, the motivation behind each proposal and their goals, as well as the limitations of using such high frequency bands, particularly the 60 GHz band, which is highly affected by attenuation induced by the atmosphere.

The concepts of digital radio over fiber and analog radio over fiber were presented.

Modulating and transmitting 60 GHz over fiber is very challenging. We decided to use the MZM for its unique capabilities, among them the capability of transmitting a 60 GHz signal with high performance and the possibility of using several modulation techniques. When transmitting signals with such high modulation frequencies, unwanted effects are experienced, one of the most important is the chromatic dispersion. Chromatic dispersion is responsible for the RF power swing upon photodetection.

The three modulation techniques studied in this chapter were ODSB, OSSB and OCS. ODSB is unviable for 60 GHz if distances of 500 meters or longer are to be used, due to the power fading effect. Ideally the photodetector should only receive two optical components with 60 GHz spacing to avoid the power fading. OSSB solves the problem by not generating one of the side bands, while the OCS uses a different approach it removes the optical carrier, leaving the two side bands, this will have some implications, the first is that the beating at the photodetector will be between two modulated signals, as opposed to an optical carrier and a modulated signal, the second is a very interesting one. Because the optical carrier is removed, the electrical signal at the photodetector will have double the frequency used in the MZM. It could be interesting to use in scenarios where the electrical generation components are very expensive.

3.9 References

[3.1] Z. Genc*, et al.*, "Home networking at 60 GHz: challenges and research issues," *Annals of Telecommunications,* vol. 63, pp. 501-509, 2008.

[3.2] B. Razavi, "A 60-GHz CMOS receiver front-end," *Solid-State Circuits, IEEE Journal of,* vol. 41, pp. 17-22, 2006.

[3.3] "IEEE Standard for Information technology - Telecommunications and information exchange between systems - Local and metropolitan area networks - Specific requirements. Part 15.3: Wireless Medium Access Control (MAC) and Physical Layer (PHY) Specifications for High Rate Wireless Personal Area Networks (WPANs) Amendment 2: Millimeter-wave-based Alternative Physical Layer Extension," *IEEE Std 802.15.3c-2009 (Amendment to IEEE Std 802.15.3-2003),* pp. c1-187, 2009.

[3.4] H. Singh*, et al.*, "Principles of IEEE 802.15.3c: Multi-Gigabit Millimeter-Wave Wireless PAN," in *Computer Communications and Networks, 2009. ICCCN 2009. Proceedings of 18th Internatonal Conference on*, 2009, pp. 1-6.

[3.5] WirelessHD, (May, 2010). WirelessHD Specification Version 1.1 Overview. Available: http://www.wirelesshd.org/pdfs/WirelessHD-Specification-Overview-v1.1May2010.pdf, retrieved on October 20, 2011.

[3.6] ECMA, (December 2010). Standard ECMA-387: High Rate 60 GHz PHY, MAC and HDMI PALs - 2nd edition. Available: http://www.ecma-international.org/publications/files/ECMA-ST/ECMA-387.pdf, retrieved on October 20, 2011.

[3.7] W. G. Alliance, (July, 2010). WiGig: Defining the Future of Multi-Gigabit Wireless Communications. Available: http://wirelessgigabitalliance.org/?getfile=1510, retrieved on October 20, 2011.

[3.8] E. Perahia, *et al.*, "IEEE 802.11ad: Defining the Next Generation Multi-Gbps Wi-Fi," in *Consumer Communications and Networking Conference (CCNC), 2010 7th IEEE*, 2010, pp. 1-5.

[3.9] A. Hirata, *et al.*, "120-GHz-band millimeter-wave photonic wireless link for 10-Gb/s data transmission," *Microwave Theory and Techniques, IEEE Transactions on,* vol. 54, pp. 1937-1944, 2006.

[3.10] M. Weiss, *et al.*, "60-GHz Photonic Millimeter-Wave Link for Short- to Medium-Range Wireless Transmission Up to 12.5 Gb/s," *Lightwave Technology, Journal of,* vol. 26, pp. 2424-2429, 2008.

[3.11] D. Bao Linh, *et al.*, "Toward a Seamless Communication Architecture for In-building Networks at the 60 GHz band," in *Local Computer Networks, Proceedings 2006 31st IEEE Conference on*, 2006, pp. 300-307.

[3.12] B. L. Dang, *et al.*, "Radio-over-Fiber based architecture for seamless wireless indoor communication in the 60 GHz band," *Computer Communications,* vol. 30, pp. 3598-3613, 2007.

[3.13] K. Hong Bong, *et al.*, "A radio over fiber network architecture for road vehicle communication systems," in *Vehicular Technology Conference, 2005. VTC 2005-Spring. 2005 IEEE 61st*, 2005, pp. 2920-2924 Vol. 5.

[3.14] ITU-R, "ITU-R Recommendations, Attenuation by atmospheric gases," *ITU-R P.676-5,* 2001.

[3.15] F.C.C., "Millimeter Wave Propagation: Spectrum Management Implications," in *Bulletin Number 70*, ed, July, 1997.

[3.16] C. Lim, *et al.*, "Fiber-Wireless Networks and Subsystem Technologies," *Lightwave Technology, Journal of,* vol. 28, pp. 390-405, 2010.

[3.17] C. Gee-Kung, *et al.*, "Architectures and technologies for very high throughput in-building wireless services using radio-over-fiber networks," in *Summer Topical Meeting, 2009. LEOSST '09. IEEE/LEOS*, 2009, pp. 37-38.

[3.18] K. Kitayama, *et al.*, "Fiber-wireless networks and radio-over-fibre technique," in *Lasers and Electro-Optics, 2008 and 2008 Conference on Quantum Electronics and Laser Science. CLEO/QELS 2008. Conference on*, 2008, pp. 1-2.

[3.19] T. Kurniawan, *et al.*, "Performance analysis of optimized millimeter-wave fiber radio links," *Microwave Theory and Techniques, IEEE Transactions on,* vol. 54, pp. 921-928, 2006.

[3.20] A. Nirmalathas, *et al.*, "Digitized Radio-Over-Fiber Technologies for Converged Optical Wireless Access Network," *Lightwave Technology, Journal of,* vol. 28, pp. 2366-2375, 2010.

[3.21] J. J. Vegas Olmos, *et al.*, "Dynamic Reconfigurable WDM 60-GHz Millimeter-Waveband Radio-Over-Fiber Access Network: Architectural Considerations and Experiment," *Lightwave Technology, Journal of,* vol. 25, pp. 3374-3380, 2007.

[3.22] M. C. R. Medeiros, *et al.*, "Convergence of optical and millimeter-wave broadband wireless access networks," in *Transparent Optical Networks, 2009. ICTON '09. 11th International Conference on*, 2009, pp. 1-4.

[3.23] C. Gee-Kung, *et al.*, "Key Technologies of WDM-PON for Future Converged Optical Broadband Access Networks [Invited]," *Optical Communications and Networking, IEEE/OSA Journal of,* vol. 1, pp. C35-C50, 2009.

[3.24] S. Dahlfort and K. Laraqui, "Exploring the Antenna Lambda Connection," 2012, p. NTh4E.5.

[3.25] T. Quinlan, *et al.*, "First Demonstration of Cooler-less, Bi-Directional, Format-Agnostic, Wireless and Gigabit Ethernet Network Provision using Off-The-Shelf VCSELs," 2012, p. OTh3G.1.

[3.26] K. Ohata, *et al.*, "1.25Gbps wireless Gigabit Ethernet link at 60GHz-band," in *Microwave Symposium Digest, 2003 IEEE MTT-S International*, 2003, pp. 373-376 vol.1.

[3.27] H.-C. Chien, *et al.*, "60 GHz millimeter-wave gigabit wireless services over long-reach passive optical network using remote signal regeneration and upconversion," *Opt. Express,* vol. 17, pp. 3016-3024, 2009.

[3.28] W. Kellerer, *et al.*, "Novel cellular optical access network and convergence with FTTH," in *Optical Fiber Communication Conference and Exposition (OFC/NFOEC), 2012 and the National Fiber Optic Engineers Conference*, 2012, pp. 1-3.

[3.29] S. Gangxiang, *et al.*, "Fixed Mobile Convergence Architectures for Broadband Access: Integration of EPON and WiMAX [Topics in Optical Communications]," *Communications Magazine, IEEE,* vol. 45, pp. 44-50, 2007.

[3.30] Y. Jianping, "Microwave Photonics," *Lightwave Technology, Journal of,* vol. 27, pp. 314-335, 2009.

[3.31] H. Schmuck, "Comparison of optical millimetre-wave system concepts with regard to chromatic dispersion," *Electronics Letters,* vol. 31, pp. 1848-1849, 1995.

[3.32] J. Zhensheng, *et al.*, "Simultaneous Generation of Independent Wired and Wireless Services Using a Single Modulator in Millimeter-Wave-Band Radio-Over-Fiber Systems," *Photonics Technology Letters, IEEE,* vol. 19, pp. 1691-1693, 2007.

[3.33] G. H. Smith, *et al.*, "Technique for optical SSB generation to overcome dispersion penalties in fibre-radio systems," *Electronics Letters,* vol. 33, pp. 74-75, 1997.

[3.34] Y. Jianjun, *et al.*, "Optical millimeter-wave generation or up-conversion using external modulators," *Photonics Technology Letters, IEEE,* vol. 18, pp. 265-267, 2006.

[3.35] W. Kai, *et al.*, "A Radio-Over-Fiber Downstream Link Employing Carrier-Suppressed Modulation Scheme to Regenerate and Transmit Vector Signals," *Photonics Technology Letters, IEEE,* vol. 19, pp. 1365-1367, 2007.

[3.36] M. Mohamed, *et al.*, "Frequency sixupler for millimeter-wave over fiber systems," *Opt. Express,* vol. 16, pp. 10141-10151, 2008.

[3.37] M. Mohamed, *et al.*, "Analysis of frequency quadrupling using a single Mach-Zehnder modulator for millimeter-wave generation and distribution over fiber systems," *Opt. Express,* vol. 16, pp. 10786-10802, 2008.

[3.38] C.-T. Lin, *et al.*, "A continuously tunable and filterless optical millimeter-wave generation via frequency octupling," *Opt. Express,* vol. 17, pp. 19749-19756, 2009.

[3.39] P.-T. Shih, *et al.*, "WDM up-conversion employing frequency quadrupling in optical modulator," *Opt. Express,* vol. 17, pp. 1726-1733, 2009.

[3.40] J. Ma, *et al.*, "Optical millimeter wave generated by octupling the frequency of the local oscillator," *J. Opt. Netw.,* vol. 7, pp. 837-845, 2008.

[3.41] P. Laurencio and M. C. R. Medeiros, "Dynamic range of optical links employing optical single side-band modulation," *Photonics Technology Letters, IEEE,* vol. 15, pp. 748-750, 2003.

[3.42] J. Park, *et al.*, "Elimination of the fibre chromatic dispersion penalty on 1550 nm millimetre-wave optical transmission," *Electronics Letters,* vol. 33, pp. 512-513, 1997.

[3.43] M. Attygalle, *et al.*, "Transmission improvement in fiber wireless links using fiber Bragg gratings," *Photonics Technology Letters, IEEE,* vol. 17, pp. 190-192, 2005.

[3.44] B. Davies and J. Conradi, "Hybrid modulator structures for subcarrier and harmonic subcarrier optical single sideband," *Photonics Technology Letters, IEEE,* vol. 10, pp. 600-602, 1998.

[3.45] M. P. Thakur, *et al.*, "Optical frequency tripling with improved suppression and sideband selection," in *Optical Communication (ECOC), 2011 37th European Conference and Exhibition on*, 2011, pp. 1-3.

[3.46] M. Sieben, *et al.*, "Optical single sideband transmission at 10 Gb/s using only electrical dispersion compensation," *Lightwave Technology, Journal of,* vol. 17, pp. 1742-1749, 1999.

[3.47] P. Laurencio*, et al.*, "Dispersion Robustness of Millimeter Waves Generated by Up-Conversion Strategies," *Fiber and Integrated Optics,* vol. 29, pp. 441-452, 2010.
[3.48] G. P. Agrawal, *Nonlinear fiber optics*. San Diego [u.a.]: Academic Press, 2001.
[3.49] A. H. Gnauck*, et al.*, "Linear microwave-domain dispersion compensation of 10-Gb/s signals using heterodyne detection," in *Optical Fiber Communication Conference, 2005. Technical Digest. OFC/NFOEC*, 2005, p. 3 pp. Vol. 5.
[3.50] K. Iwashita and N. Takachio, "Chromatic dispersion compensation in coherent optical communications," *Lightwave Technology, Journal of,* vol. 8, pp. 367-375, 1990.
[3.51] N. Takachio and K. Iwashita, "Compensation of fibre chromatic dispersion in optical heterodyne detection," *Electronics Letters,* vol. 24, pp. 108-109, 1988.
[3.52] U. Gliese*, et al.*, "Chromatic dispersion in fiber-optic microwave and millimeter-wave links," *Microwave Theory and Techniques, IEEE Transactions on,* vol. 44, pp. 1716-1724, 1996.

4

Transmission performance assessment of 60 GHz RoF systems

4.1 Introduction

To implement 60 GHz radio over fiber networks a number of key technological trends still have to be achieved, ranging from wireless networks to fiber optics transmission systems and supporting opto-electronic components. A specific aspect that is still under consideration is the digital modulation format that is more appropriated. Multi carrier (MC) modulations schemes combined with frequency-domain receivers implementations, especially the ones belonging to the orthogonal frequency division multiplexing (OFDM) [4.1] class are widely used, in several broadband wireless communication systems which have to deal with strongly frequency-selective fading channels, and are considered a good

candidate for this application. However, conventional single carrier (SC) [4.2] modulations have also been shown to be suitable for block transmission schemes, additionally providing low-implementation complexity.

In the previous chapter we have analyzed the performance of an unmodulated radio frequency (RF) carrier using optical single side band (OSSB) and optical carrier suppression (OCS). It was shown that these modulation schemes are robust to fiber dispersion. In this chapter the performance transmission over fiber of digitally modulated with data of RF carriers, operating in the 60 GHz range, is studied through simulation. Basically two scenarios are considered, a single RF carrier modulated using binary phase shift keying (BPSK) and a subcarrier multiplexed system (SCM) with four RF carriers also modulated using BPSK. The effect of several system operating parameters, such us: optical modulation configuration, optical modulation parameters and fiber length are considered with the relevant system impairments being identified. Section 4.2 presents the simulation model and discusses the simulation environment. In section 4.3, in order to identify transmission limitations, besides the optical double side band (ODSB) and OSSB modulation using Mach-Zehnder modulators (MZMs) with the configuration presented in the previous chapter, two modified signals: filtered OSSB (F-OSSB) and pure OSSB (P-OSSB) are considered and analyzed. Performance comparison analysis of OSSB and OCS is presented in section 4.4, with the effects of the finite extinction of the MZM and the optical amplifier noise being taken into consideration. Section 4.5 analyses the transmission of subcarrier multiplexed RF signals using OSSB, emphasizing the intermodulation effects arising from the nonlinear behavior of the MZM and fiber dispersion. The chapter concludes with a brief summary.

4.1.1 Simulation model description

A macro view of the system schematic is illustrated in Figure 4.1. A distributed feedback (DFB) laser emitting at 1552.5 nm with 100 kHz linewidth and 0 dBm output power is used as optical source. The modulator is a dual arm MZM biased and modulated according to the desired optical modulation scheme. The electrical drive signal can be a single RF carrier or several SCM RF carriers. The RF carriers are digitally modulated by data using simple modulation formats such amplitude shift keying (ASK) modulation or BPSK. Data is filtered by a square root raised cosine filter before modulation. In practical

systems, a most common approach is have a DFB laser, followed by a broadband MZM modulated with the RF carrier.

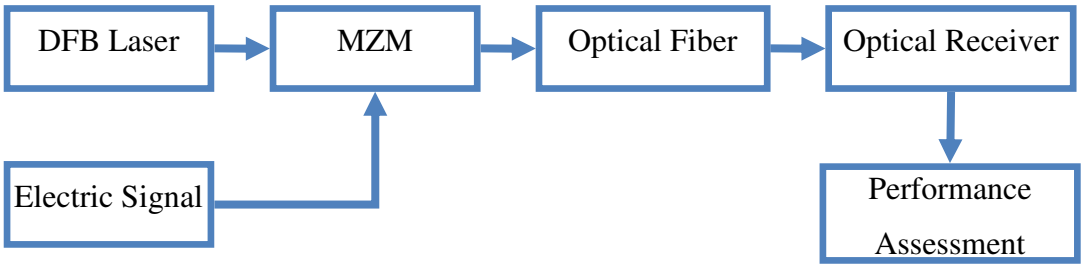

Figure 4.1 - Network schematic overview.

An optical amplifier might be used after the MZM to compensate for the MZM insertion loss and the fiber attenuation in order to keep the optical power level at the receiver constant. The optical signal is then transmitted over a standard single mode fiber (SSMF) link, with 0.2 dB/km attenuation and 17 ps/(nm.km), dispersion coefficient. Optical power at the input of fiber was always considered to be below 0 dBm. When optical amplifiers are used an optical filter is employed to reduce the amplified spontaneous emission (ASE) power. The optical signal is then converted to the electric domain using a positive-intrinsic-negative (PIN) photodetector with an ideal responsitivity. The photodetected signal is down converted by mixing with the appropriate RF carrier and the down converted signal filtered by a 100% roll over square root raised cosine filter in order to the data to be recovered. The performance of the system is assessed though the quantification of the Bit Error Rate (BER), using BER assessment tools provided by VPItransmissionMaker™ suite with appropriate clock recovery.

In this section, the system the effect of system operating conditions such as the modulation depth of the MZM, are analyzed and optimized, through simulation, considering different digital modulation formats as well as different optical channel bandwidths.

4.1.2 Simulation environment

The simulator used was the VPItransmissionMaker™ suite. This software provides an integrated design environment specially tailored for simulation of optical systems. A common issue with the simulation of optical networks is huge bandwidth difference between the signals from different domains. For example the 1550 nm transmission window operates in the 193.4 THz band, the 12^{th} order of magnitude when compared with the baseband frequency unit, the Hertz. The electrical signals and data modulated usually range from the MHz the up to 60 GHz. There is a 6 order of magnitude difference between the operating frequency of the electrical signals when compared with the frequency of optical signals. Applying Nyquist criterion the sampling frequency should be at least twice the bandwidth of the signal of highest bandwidth signal, therefore sampling time should be less than $T_s < \frac{1}{2\times 193.4\times 10^{12}} \approx 2.6\times 10^{-15}$ s. To simulate 1000 bits at 1 Gbit/s approximately $4x10^8$ samples are needed, which is not possible using a normal computer. VPItransmissionMaker™ provides a wide range of signal representations to enable efficient simulation of a range of scales of problems, from device physics to system and network performance [4.3]. The simulator also provides a large collection of simulation blocks, such as lasers, couplers, photo detectors, modulators, electrical filters, data generators, etc. On top of the pre build modules, it also allows for co-simulation blocks, such as Matlab code, so that new device or system models can be added to the simulation.

4.2 Transmission limitations of OSSB modulation with data

In the previous chapter we have analyzed the performance of an unmodulated RF carrier using OSSB, and it was shown that these modulation schemes are robust to fiber dispersion. It was demonstrated that due to the inherent nonlinear characteristics of MZM, even when driven by low modulation depths OSSB modulation generates higher order harmonics. Upon photodetection the beating of any two optical harmonics or/and beating of any order optical harmonic with the optical carrier, generates mm-wave signals with frequencies corresponding to the beatings giving rise to received power fading effects. In this section, it is shown that, when data is present, besides the power fading effects other effects such as dispersion within the data bandwidth, and the optical carrier

intermodulation power within the optical carrier component also affect the system performance. Due to the nonlinear behavior of the MZM intermodulation terms fall within the optical carrier as shown in Figure 4.2.

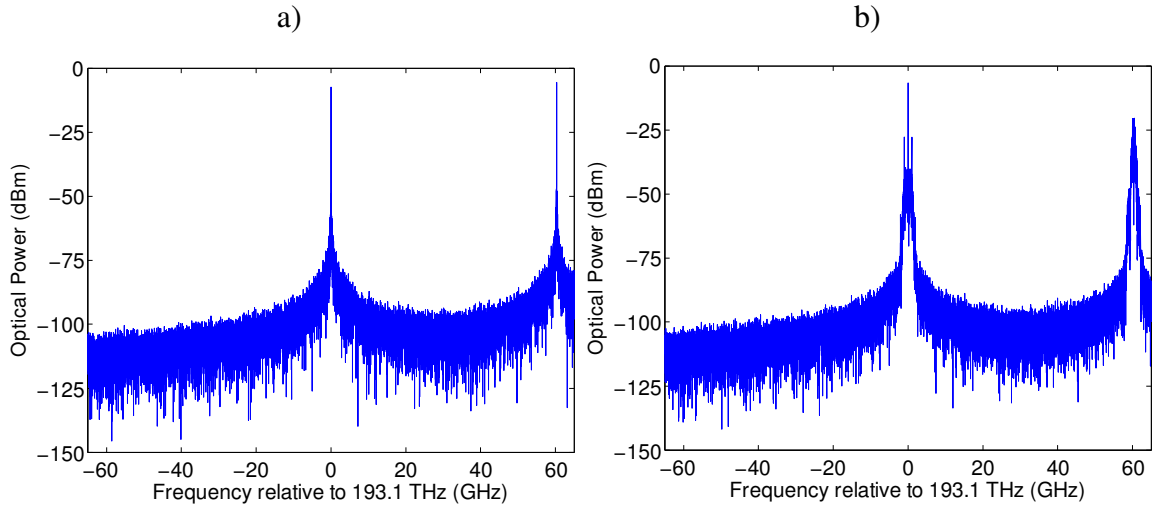

Figure 4.2 - OSSB spectrum for a 60 GHz RF signal a) without data b) with data

To explain the intermodulation at the output of the MZM, we refer to equation 3.6, written in the following form:

$$E_{OSSB}(t) = \frac{E_{in}(t)}{2} e^{-j\frac{\pi}{4}} \left(e^{j\pi x_c m(t)} + e^{j\left(x\pi_c \hat{m}(t) + \frac{\pi}{2}\right)} \right) \tag{4.1}$$

which can be expanded into a Taylor Series showing up to the third order:

$$E_{OSSB}(t) = \frac{E_{in}(t)}{2} e^{-j\frac{\pi}{4}} \left[\begin{array}{l} \left(\frac{1}{2} - \frac{1}{2}\pi x_c \hat{m}(t) - \frac{1}{4}(\pi x_c)^2 m^2(t) + \frac{1}{12}(\pi x_c)^3 \hat{m}^3(t) + \cdots \right) + \\ + j\left(\frac{1}{2} + \frac{1}{2}\pi x_c m(t) - \frac{1}{4}(\pi x_c)^2 \hat{m}^2(t) - \frac{1}{12}(\pi x_c)^3 m^3(t) + \cdots \right) \end{array} \right] \tag{4.2}$$

Considering $m(t)$ a BPSK signal $m(t) = d(t)\sin\omega_m t$, $d(t)$ the digital data, the optical spectrum consists of a single side band signal for the first harmonic corresponding to the terms $-\frac{1}{2}\pi x_c \hat{m}(t)$ and $+\frac{1}{2}\pi x_c m(t)$, while the second order terms $-\frac{1}{4}(\pi x_c)^2 m^2(t)$ and $-\frac{1}{4}(\pi x_c)^2 \hat{m}^2(t)$ give rise to a double side band spectrum spaced from the optical carrier by $2f_m$, and a term that is located in the optical

carrier frequency as illustrated in Figure 4.2b. In a first approach, this effect can be seen as an increase of the laser linewidth and therefore lead to an increase of the phase decorrelation [4.4-4.6] upon detection at the photodetector.

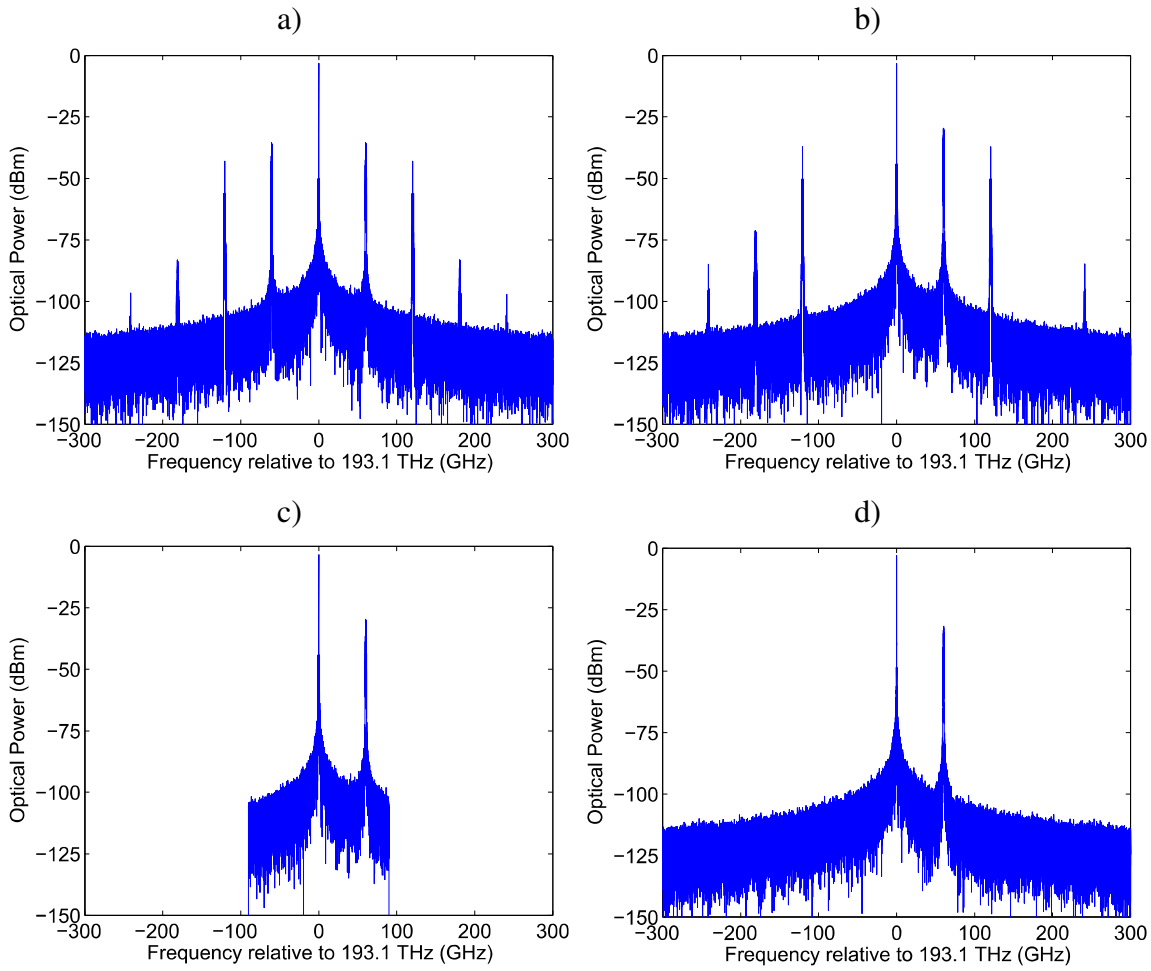

Figure 4.3 - Spectrum at output of optical modulator for a) ODSB; b) OSSB; c) F-OSSB; d) P-OSSB.

In order to quantify the different effects, besides the ODSB and OSSB modulation using MZMs with the configuration presented in the previous chapter, we consider two modified signals: F-OSSB and P-OSSB. F-OSSB has a rectangular optical filter with 199 dB attenuation in the reject band connected at the output of the MZM. The pass band is configured so that only the optical carrier and the first harmonic pass through. The results obtained with this configuration allow for the measurement of the impact of the unwanted harmonics when compared with the OSSB results. The last configuration, P-OSSB, is a bit more exoteric, the end result is an unmodulated optical carrier and the first optical harmonic. The optical carrier is split in two parts, one enters the modulator while the other is reused after modulation, being the modulated signal filtered in such a way that

only the first harmonic is present. This signal is than coupled with the optical carrier that did not pass through the MZM. Figure 4.3 illustrates the four signals under consideration.

4.2.1 BER versus modulation depth for 0 km

Figure 4.4 shows the BER versus the modulation depth, for the four modulation schemes, in a back to back configuration. For ODSB and OSSB, as clearly shown in Figure 4.5a, for a $x_c < 0.5$ the received electrical signal results mainly from the beating of the optical carrier and first optical harmonics, plus the beating of the first optical harmonic and the second optical harmonic. While for F-OSSB received electrical signal results only from the beating of the optical carrier and the first optical harmonics, and P-OSSB results from the beating of the optical carrier that is kept at its maximum value and the first harmonic, as illustrated in Figure 4.5b. Considering Figure 4.4, F-OSSB is the first to experience the high BER, because $J_0 * J_1$ beating loses power first, especially the J_0 component. OSSB can handle a higher modulation depth, because higher beatings, i.e. $J_1 * J_2$, compensate for the loss in the first beating, $J_0 * J_1$. P-OSSB is the best at handling higher modulation depths, simply because the only optical component dependent to the modulation depth is J_1, which has the best power factor in the $0.4 < x_c < 0.5$ range.

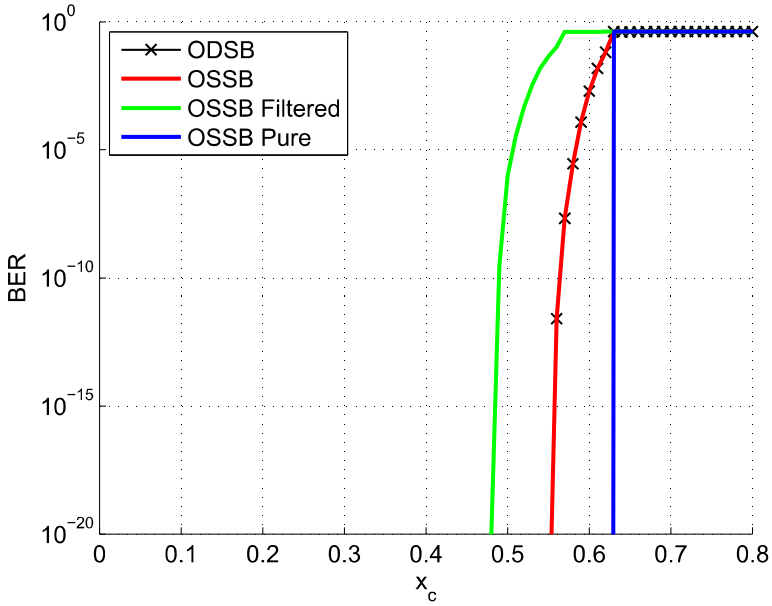

Figure 4.4 - BER versus modulation factor x_c for the 4 optical modulations with a single channel.

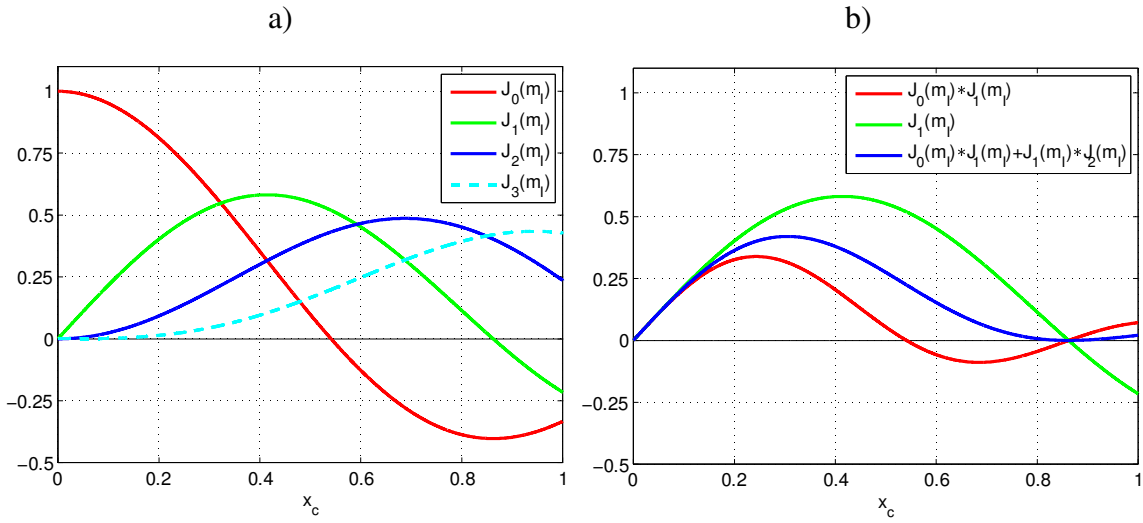

Figure 4.5 - First kind Bessel function a) for the first 4 orders b) considering some of the optical beatings at the receiver.

4.2.2 Impact of the modulation depth on BER for 0 km

In this section the back-to-back transmission is analyzed with six modulation depths being considered, from $x_c = 0.05$ to 0.5.

In Figure 4.6 the BER is presented in function of the received optical power for several modulation depths, in a back-to-back (B-t-B) configuration. To better analyze this results we should look back to the Bessel function behavior regarding the different modulation depths. When changing the x_c we are removing power from some harmonics in favor of others, and this will have different impacts, especially when applying filtering, e.g. F-OSSB scheme.

The first conclusion we can take from Figure 4.6 is that the ODSB and the OSSB signals have the same behavior for every x_c, from a BER standpoint. This is expected because we are using a system in a B-t-B configuration, so the effect of fiber dispersion is not present.

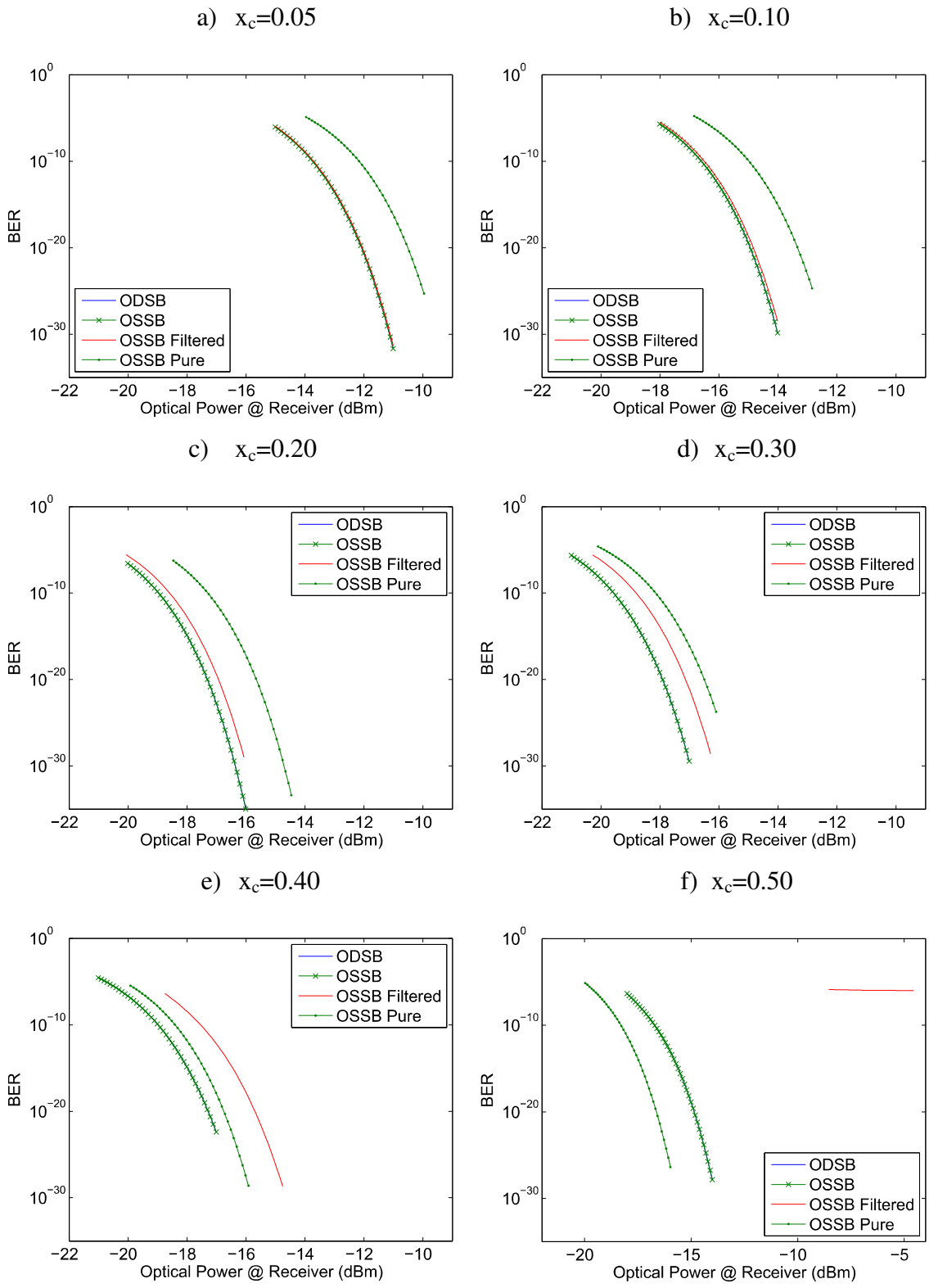

Figure 4.6 - BER in function of received optical power in a back-to-back configuration, for several x_c with a single channel.

In the first plots (lower x_c) the OSSB and F-OSSB have similar BER performance, with the first having the best results. This can be easily explained by Figure 4.5b and the

equation for the received optical power from the previous chapter. F-OSSB only has the contribution from J_0 and J_1, while the regular OSSB has the infinite J_n, but for small x_c, the impact of J_2 and higher is very small when compared with J_0 and J_1. It does exist, and is the source of the slight advantage of OSSB, because the beating of the higher harmonics, such as J_1 with J_2, and J_2 with J_3. As the x_c keeps increasing, so does the performance difference between the both schemes. It should be taken into consideration that the first two harmonics are common to both schemes, so the difference will occur in the higher harmonics. The last plot (f) is particularly interesting, as the F-OSSB presents a particularly bad performance with an almost flat behavior, due to low power on the optical carrier (J_0). While the OSSB keeps presenting a regular performance, although with worst results than x_c = 0.40, 0.30 or 0.20. OSSB with x_c = 0.50 benefits from the beating of the higher order harmonics, replacing the fundamental beating J_0 with J_1.

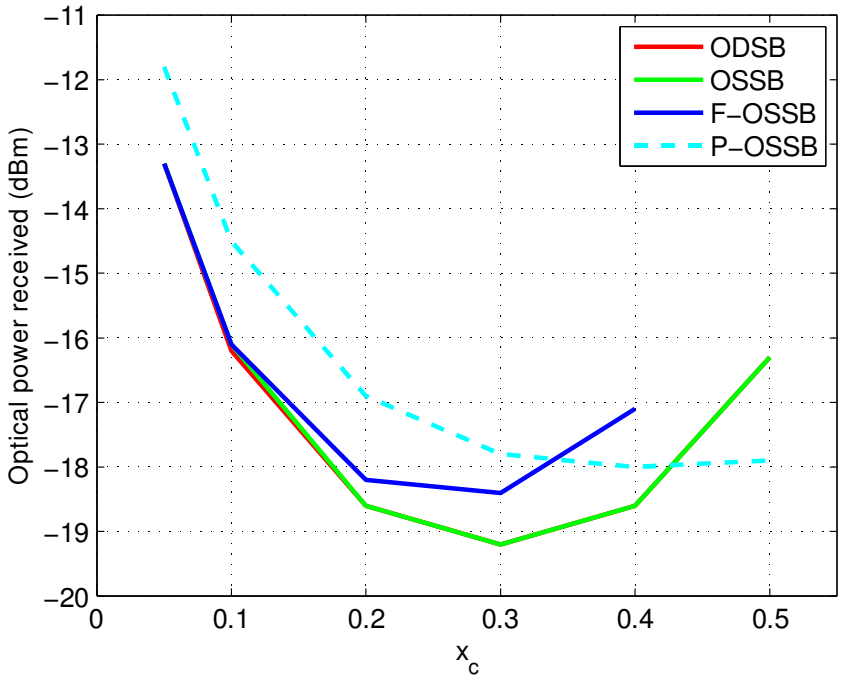

Figure 4.7 - System sensitivity for a fiber length of 0 km with a single channel.

At first look one might expect the P-OSSB to behave similarly to the F-OSSB, but as shown here, it does not. P-OSSB has about 1 to 2 dB penalty in a) and b) to OSSB and F-OSSB. The reason for this behavior is that J_0 will have some of the data signal modulated on it, while the P-OSSB has a pure optical carrier instead of J_0. As the x_c factor increases the difference between P-OSSB and F-OSSB decreases, because the power of J_0 harmonic decreases for F-OSSB. However, when the OSSB and P-OSSB performance is

compared, the positive effect of higher harmonics does not compensate the power reduction of J_0. This is true only up to a degree, for x_c = 0.40 the difference between the two schemes is almost zero, and with x_c= 0.50 P-OSSB is the scheme with the best performance, the beating of the higher harmonics in the OSSB keeps the system operational, but with higher BER.

The optical power needed at the receiver for a BER of 10^{-12} is shown Figure 4.7.

4.2.3 BER versus modulation depth for 14 km

Figure 4.8 shows the BER versus modulation depth, for the four modulation schemes, with 14 km of fiber. The fiber attenuation was set to be zero, therefore dispersion is the only effect under consideration. As expected, ODSB is highly affected by fiber dispersion.

OSSB scheme presents an acceptable performance for low values of x_c, where the high level harmonics (J_2 and higher have a low power level). But for x_c > 0.30 the beating of higher order optical harmonics will contribute to the received signal at 60 GHz. This contributions, unlike in the B-t-B scenario, will penalize the signal quality. Due to the dispersion effect each beating that generates a 60 GHz signal will have different phases. The final electrical signal will be the sum of this different signals, depending on the distance length, the effect could be more or less penalizing.

Looking into the F-OSSB we can see that while the x_c is not in the highest value (low J_0 contribution), it has better performance than the OSSB due to the lack of higher order harmonics. When x_c = 0.5, there is almost no contribution from J_0 thus the BER is much higher than the previous modulation depths.

P-OSSB behaves very similarly to the B-t-B configuration, as expected. This scheme only has two optical components, the unmodulated optical carrier (J_0) and the modulated signal (J_1) and therefore is not affected by dispersion. P-OSSB presents the best performance for high modulation depths scenarios ($x_c \geq 0.40$), due to its unmodulated optical carrier. However, P-OSSB continues to have a 2 dB penalty in lower modulation depth, where the baseband modulation improves the system sensibility for the remainder modulations.

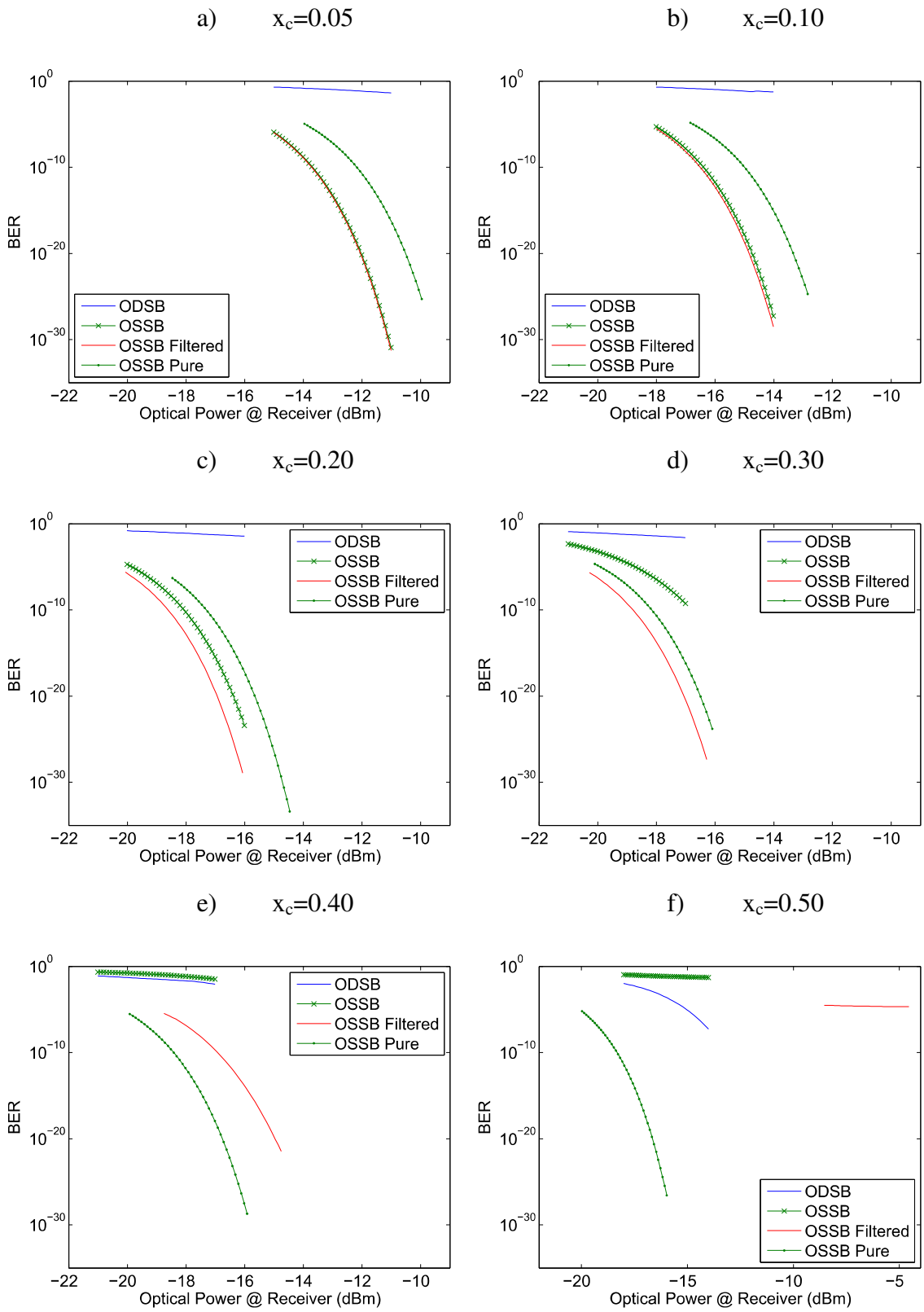

Figure 4.8 - BER in function of received optical power with 14 km of fiber, for several x_c values with a single channel.

The optical power needed at the receiver for a BER of 10^{-12} is shown in Figure 4.9.

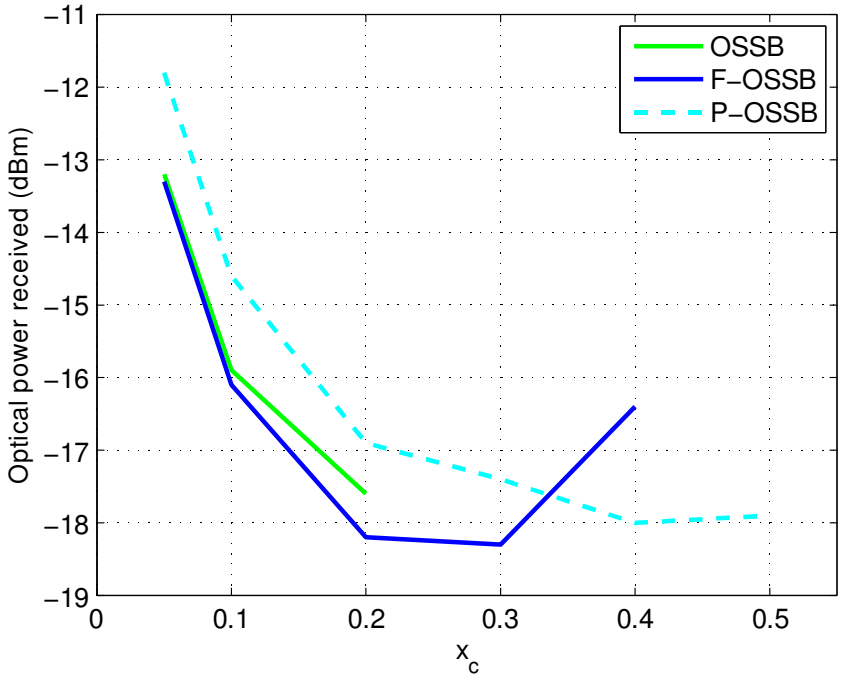

Figure 4.9 - System sensitivity for a fiber length of 14 km with a single channel.

4.2.4 BER versus optical fiber length

The objective of this section is to analyze the performance the four schemes under consideration as the signal propagates through optical fiber. Fiber attenuation is considered to be 0 therefore the only effect under consideration is fiber dispersion. Figure 4.10 shows the BER versus 50 km of optical fiber considering several modulation depths.

As expected, due to the optical received power fading, ODSB modulation is completely unreliable for the 60 GHz signal transmission for all modulation depth.

a) $x_c = 0.05$ b) $x_c = 0.10$

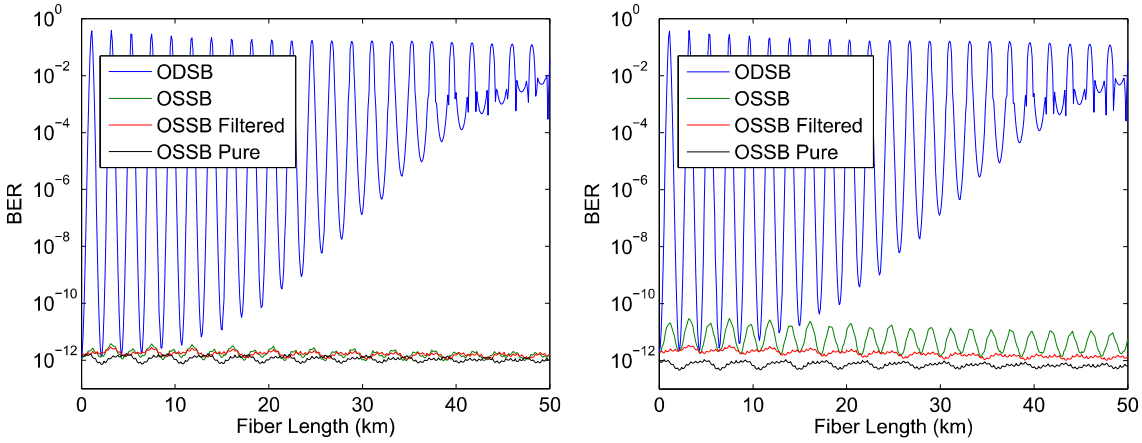

c) $x_c = 0.20$ d) $x_c = 0.30$

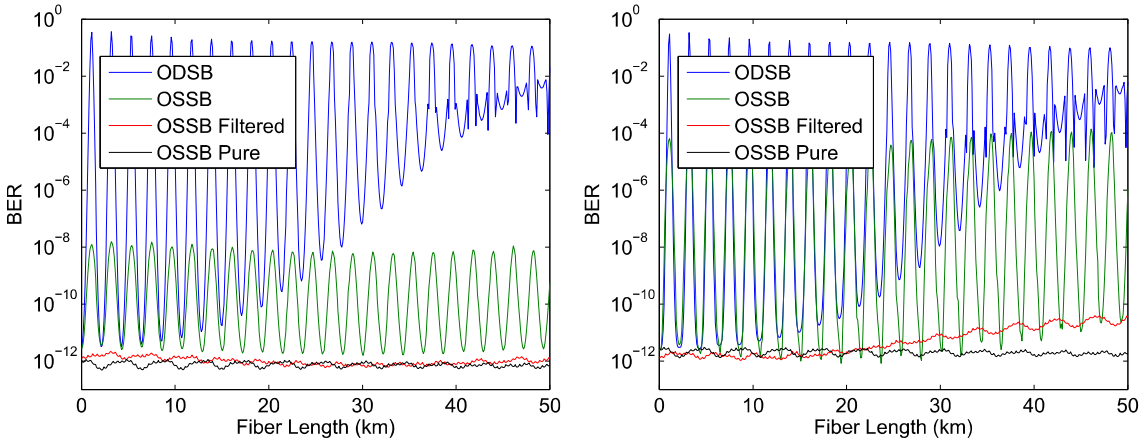

e) $x_c = 0.40$

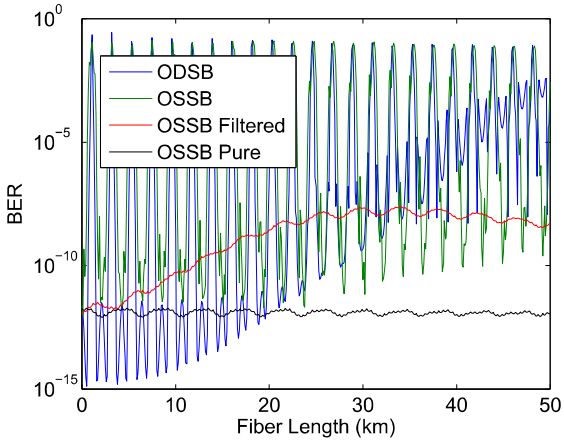

Figure 4.10 - BER in function of fiber length, for several x_c with a single channel.

OSSB, if only one band is present, can overcome the power fading problem. This can be seen in Figure 4.10a), when x_c=*0.05*, where very small BER swings are visible.

However, as the modulation depth increases, so do the BER oscillations. This happens because the OSSB modulator used is inherently nonlinear; there will always be higher order harmonics. The higher order harmonics spaced by 60 GHz, which are not single side band, upon photodetection will beat and generate a 60 GHz electrical signal. This will create the same power fading effect as experienced by ODSB modulation. Therefore, the robustness against dispersion of OSSB modulations schemes based on MZM, is limited to low modulation depths. Theoretically, if higher modulation depths are need, one can simply apply an optical filter centered at the optical carrier with almost 240 GHz bandwidth, ensuring that the 120 and -120 GHz harmonic are filtered out, such as the F-OSSB scheme. However, although F-OSSB, does not present higher order optical harmonics and therefore no optical power fading effects are presented, for higher modulation depths $x_c \geq 0.3$, the performance of the system degrades with the increase of the fiber length, whereas P-OSSB does not suffer from this effect. F-OSSB experiences bit walk-off [4.7] and therefore is still subject to a dispersion penalty. In F-OSSB the optical carrier is also modulated with data, particularly for higher modulation depths, due to chromatic dispersion, the optical carrier and its sidebands are transmitted along the fiber at different velocities, their coherent sum is constructive at some points and destructive at the other points, which are determined by their phase difference. P-OSSB copes with this effect, as is visible in Figure 4.10, since the optical carrier is not modulated, the information is imposed only onto the first optical harmonic walk-off effects are not presented.

4.3 Performance comparison between OSSB and OCS

Although, theoretically, under ideal conditions, both modulation schemes OSSB and OCS are not affected by RF power fading effects, as was discussed in chapter 3, this is not the case for the most common implementations that use MZM. MZM are highly nonlinear devices, even when small modulation depths are considered, they generate undesirable harmonics which leads to a non-ideal behavior of the system. It was demonstrated that the attainable transmission distance, when OCS is employed, is limited by the bit walk-off [4.7] introduced by fiber dispersion, while the attainable transmission when OSSB is employed is limited by the link power budget, and also by the phase decorrelation between the optical carrier and the single sideband [4.8]. Additionally, in section 4.2.4, it was demonstrated that OSSB modulation also suffers from bit walk-off

and therefore also limits the attainable transmission distance when data is present. In this section, conventional OSSB and OCS MZM presented in chapter 3 are employed.

4.3.1 Results and discussion

In this analysis 1 Gbit/s non return to zero (NRZ) data stream modulates the RF carrier, a DFB laser source with characteristics mentioned in section 4.2.1 is considered. An ideal optical amplifier was used after the MZM in order to keep the optical power at the fiber input at a constant level of 0 dBm. The fiber was assumed to be lossless so that by varying the fiber length, the impact of chromatic dispersion could be isolated and BER penalty could be deduced. The fiber dispersion coefficient considered was 17 *ps/(nm.km)* and fiber nonlinearities are not considered. At the receiver the signal is directly detected by an ideal high speed PIN photodetector amplified and down converted to recover the 1 Gbit/s data.

Figure 4.11 shows the BER versus modulation depth considering different fiber lengths for OSSB and OCS modulation. With OSSB, for a given fiber length there is a well defined optimum value for the modulation depth. This optimum results from a compromise, between the received power and the power fading introduced by the higher order harmonics. For OSSB, without optical fiber, the optimum modulation depth is 0.4. When the fiber length increases the optimum modulation depth decreases. For modulation depths around 0.2 it is interesting to note, that OSSB modulation is almost immune to dispersion transmission until 80 km, while the OCS modulation is immune to dispersion for modulation depths around 0.4, however the system robustness against dispersion only applies for the first 40 km. Since the operational optimum value of the modulation depth is higher for OCS this modulation strategy leads to improved system performance when compared with OSSB systems. For distances higher than 40 km, for OCS modulation, keeping the modulation depth fixed at 0.4, the system performance degrades sharply due to the walk-off effect.

Different design rules can be followed, for example if the objective is to optimize the system for distances shorter than 40 km, in terms of dispersion immunity and minimum BER, then the most appropriate modulation scheme is OCS using a modulation depth around 0.4, with the additional advantage of being a frequency doubler. However, if the objective is to have a robust system immune to dispersion for long distances OSSB modulation is the appropriate option, the modulation depth should be set according to the

required transmission distance, longer distances require smaller optimized modulation depth.

a) OSSB

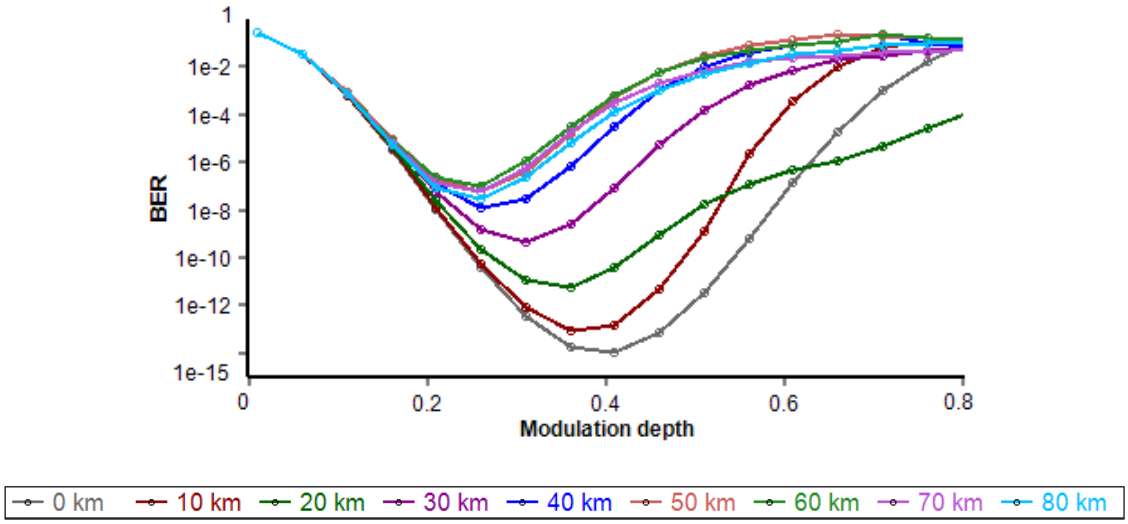

b) OCS

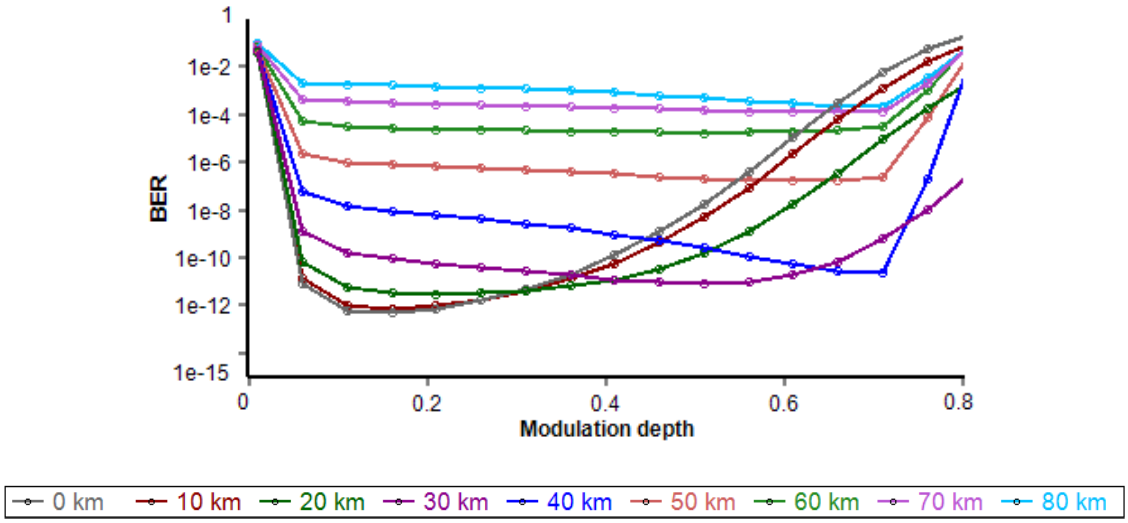

Figure 4.11 - BER versus modulation depth considering fiber lengths from 0 km to 80 km. a) OSSB. b) OCS.

4.4 The effect of the finite extinction ratio of MZMs

Owing to fabrication tolerances, practical lithium niobate ($LiNbO_3$) MZMs present imbalance power splitting ratios leading to finite extinction ratios [4.9]. The effect of the

imbalance power splitting ratio has been studied for OCS and OSSB modulation schemes considering an unmodulated RF carrier [4.10].

The output of the dual electrode MZM considering its imbalanced behavior can be expressed as:

$$E_{out}(t) = E_{in}(t)\left[r_{ps} \exp\left(j\pi \frac{d_1(t)}{V_\pi} \right) + (1 - r_{ps}) \exp\left(j\pi \frac{d_2(t)}{V_\pi} \right) \right] \qquad (4.3)$$

where $d_1(t)$ and $d_2(t)$ are the drive voltages applied to arms one and two, respectively, $E_{in}(t) = \sqrt{2P_o} \exp(j\omega_c t)$ is the optical field at the input of MZM with angular frequency ω_c and average power P_o, V_π is the switching voltage and r_{ps} denotes the power splitting ratio of the first Y splitter of the MZM. When $r_{ps}=0.5$ the MZM is balanced with a 50/50 splitting ratio, which is a condition difficult to achieve. In real MZM $r_{ps}\neq 0.5$ leading to finite extinction ratios a condition considered here. Assuming that the drive voltage is a pure carrier at angular frequency ω_m, plus a DC component, $d_{1,2}(t) = V_m sen(\omega_m t + \theta_{1,2}) + V_{DC1,2}$, $\theta_{1,2}$ and $V_{DC1,2}$ can be adjusted to generate different optical modulation r_{ps} formats as discussed in chapter 3. Being the modulation depth defined as $x_c = V_m / V_\pi$.

Figure 4.12 shows the optical spectra of OCS and OSSB signals considering different operating conditions. In both situations, the modulation depth considered is $x_c=0.2$. The dual-arm MZM is assumed to have a 6 dB insertion loss. Figure 4.12a and Figure 4.12b correspond to the OCS signal considering the power splitting ratio $r_{ps}=0.5$ and $r_{ps}=0.48$ respectively. For $r_{ps}=0.5$ an ideal OCS signal is generated without optical carrier and even harmonics. When the MZM has an imbalanced power splitting ratio, the optical spectrum presents a finite optical carrier suppression ratio impairing the performance of the system. For OSSB modulation the effect of the imbalance power splitting ratio is to generate odd higher order harmonic as is shown in Figure 4.12d. For both situations, OCS and OSSB, the imbalance leads to an optical spectrum that approaches an ODSB signal.

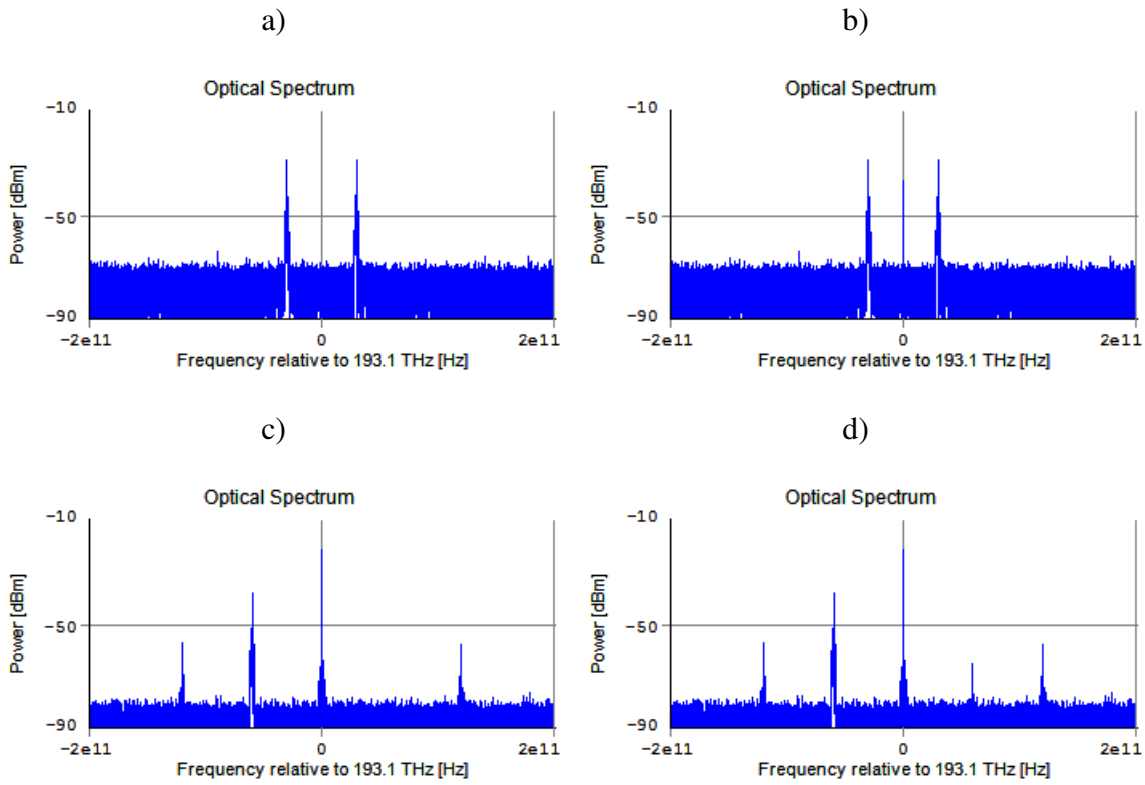

Figure 4.12 - Optical power spectra at the dual-arm MZM considering a modulation depth x_c=0.2, OCS and OSSB modulation are considered. a) OCS, r_{ps}=0.5; b) OCS, r_{ps}=0.48; c) OSSB, r_{ps}=0.5; d) OSSB, r_{ps}=0.48 .

4.4.1 Performance assessment in presence of data

The performance of both modulation schemes with digital data was compared by simulation. In this particular simulation, 2.5 Gbit/s NRZ data stream is filtered by a 100% roll over square root raised cosine filter and modulates the RF carrier using ASK modulation. A DFB laser with -5 dBm output power is considered. The fiber attenuation was set to 0.2 dB/km, dispersion coefficient was considered to be 17 *ps/(nm.km)* and no fiber nonlinearities were taken into account. At the receiver the signal is directly detected by an ideal high speed PIN photodetector amplified and down converted to recover the 2.5 Gbit/s data. The down-converted signal is then filtered by a 100% roll over square root raised cosine filter.

An optical amplifier was used after the MZM to compensate for the MZM insertion loss and the fiber attenuation in order to keep the optical power level at the receiver constant. A modulation depth $x_c = 0.2$ was considered. For OCS system the power level at

the receiver was kept at -25 dBm while for the OSSB system was kept at -20 dBm. These power levels insure approximate the same BER values for the two systems for a fiber length of 0 km. We note that although OCS based systems require less optical power in order to achieve the same level of performance they require the use of an optical amplifier with higher gain. We note that, for OCS the received optical power is mainly contained in the right and left first harmonics while for OSSB the received optical power corresponds mainly to the power of the fundamental harmonic and the first left harmonic. As it is noticeable in Figure 4.12, for $x_c=0.2$, the power of the first harmonics is similar for both modulations while the power of the optical carrier for OSSB is around 20 dB higher than the power of first harmonic. Therefore, when OCS modulation is employed an optical amplifier with higher gain is required.

Figure 4.13a and Figure 4.13b shows the BER versus fiber length of OCS and OSSB modulation respectively, for $x_c=0.2$ and considering the MZM power splitting ratios $r_{ps}=0.5$ and $r_{ps}=0.48$. An optical amplifier with a noise figure (NF) of 6 dB was used to compensate for insertion and fiber losses. Since data is transported in all harmonics, upon fiber transmission these harmonics are affected by different dispersion factors, in the time domain this means that the data transported into the different harmonics suffers different delays. Upon photo-detection data at frequency f_0 results from the beatings of all harmonics located f_0 apart, the combination of the strength of the harmonic combined with the dispersion effects can give rise to performance fading.

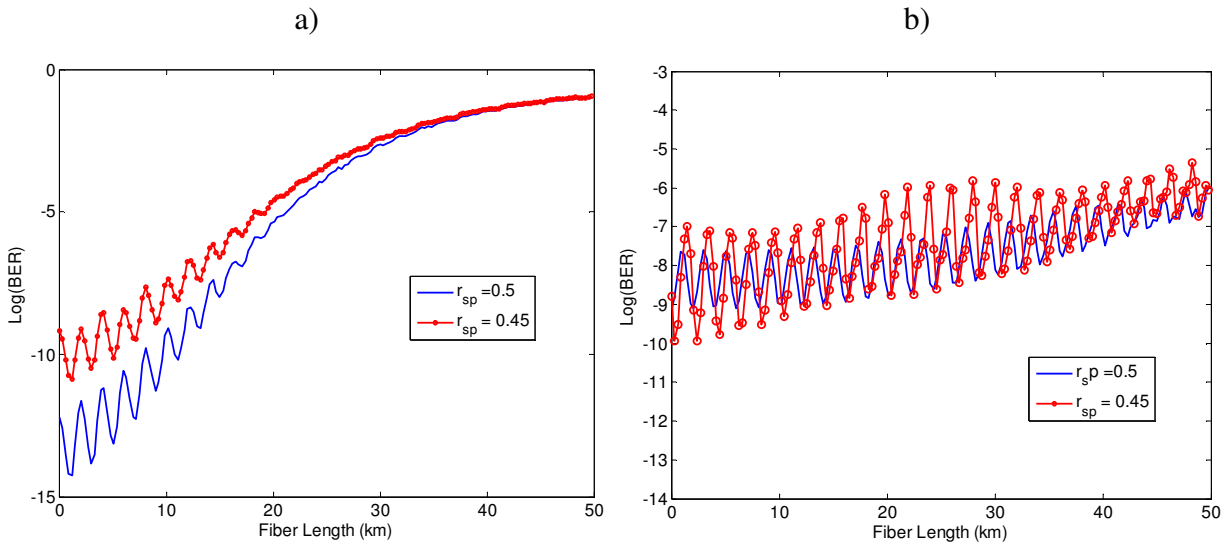

Figure 4.13 - BER versus fiber length with x_c = 0.2 for a) OCS modulation b) OSSB modulation.

For both modulation schemes the imbalance of the MZM increases the performance oscillations. However, while for OSSB modulation the average value of BER is not affected by r_{ps}, this does not apply for OCS. For OCS, although the power launched into the fiber is kept constant for $r_{ps}=0.5$ and $r_{ps}=0.48$, the received power at 60 GHz, resulting from the beating of the two first harmonics is smaller when $r_{ps}=0.48$ which leads to a BER increase. Another interesting feature of Figure 4.13a is the sharp system degradation due to walk-off phenomenon.

Figure 4.14 shows the BER versus modulation depths for several fiber lengths. For OCS, perfectly balanced MZM provide optimum performance, even small r_{ps} variations lead to high performance degradation. Contrarily, OSSB based systems are more robust against imperfect power splitting ratios. In fact as shown in Figure 4.14b, when fiber dispersion is taken into account MZM imbalance can even improve the system performance.

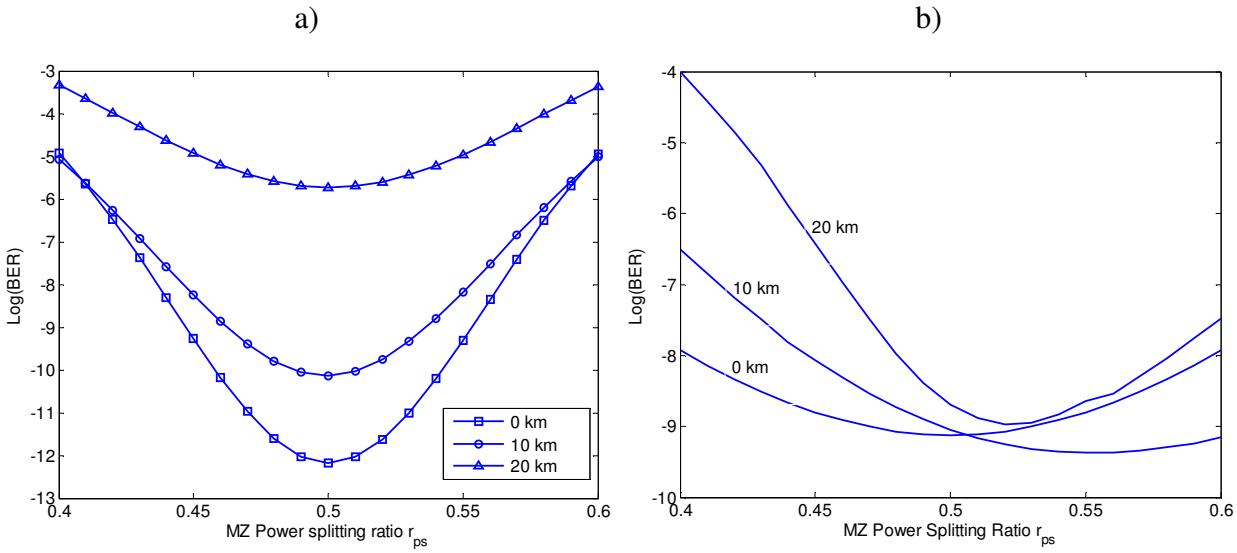

Figure 4.14 - BER versus power splitting ratio r_{ps} considering different fiber lengths for a) OCS modulation b) OSSB modulation.

4.4.2 The effect of the optical amplifier noise

Considering a back to back configuration, Figure 4.15a and Figure 4.15b shows the BER versus modulation depth. The optical level was adjusted in order to keep the same input power at the photodiode. For both OSSB and OCS there is a well defined optimum value for the modulation depth, for high values of modulation depth the system performance is limited by the power fading introduced by the higher order harmonics. For

small modulation depths, for OCS the system performance is limited by the noise introduced by the optical amplifier, as shown in Figure 4.15a with three different scenarios, no amplifier and amplifier with two noise levels. Considering OSSB, most of the optical power is concentrated on the optical carrier, and since the power at the output of the MZM is kept constant no optical amplifier is required. For OSSB the system performance is limited by low power of the first order harmonic and the other noise sources of the system, such as laser RIN and receiver noise. As shown is Figure 4.15b. the optimum modulation depth depends on the transmission distance.

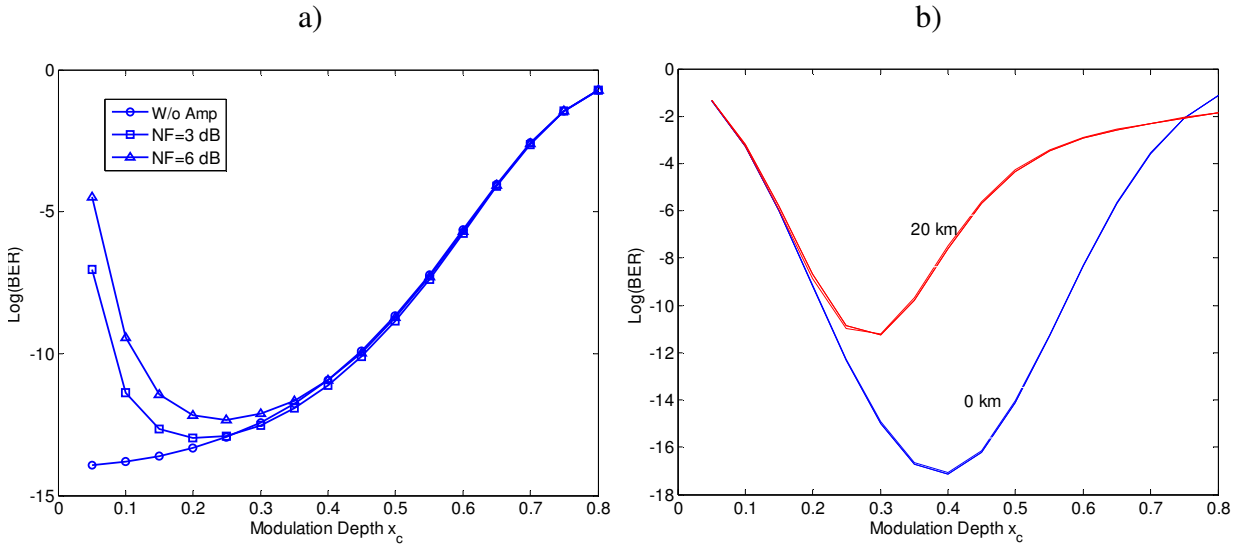

Figure 4.15 - a) BER versus modulation depth considering different amplifier noise figures for OCS modulation; b) BER versus modulation depth without amplifier and for two fiber lengths.

4.5 Subcarrier multiplexed channel transmission using OSSB

It has been demonstrated that optical single sideband when combined with subcarrier multiplexing techniques (named OSSB/SCM) can significantly improve the system immunity to chromatic dispersion, as well as being more spectrally efficient [4.11, 4.12]. As in conventional SCM systems, two major impairments on OSSB/SCM systems are the relative intensity noise (RIN) and the intermodulation distortion [4.13]. Intermodulation results from the use of nonlinear components, which will generate the unwanted products. The products can be represented as *m.carrier1*±*n.carrier2*, with *m* and *n* integers. The sum of *m* and *n* represents the intermodulation order. For an OSSB/SCM system, intermodulation distortion mainly arises from the nonlinear characteristics of the optical

modulator, the linear fiber dispersion and from the square law characteristics of the photodetection process. The focus here is on the intermodulation distortion arising from the nonlinear characteristics of the optical modulator.

4.5.1 The effect of intermodulation distortion

Considering *m(t)* the applied SCM electrical signal composed by *N RF* channels,

$$m(t) = A_m \sum_{i=1}^{N} s_i(t) \tag{4.4}$$

The optical field at the output of the OSSB modulator, $E_{OSSB}(t)$, can be expanded as a series of Bessel functions, for small channels modulation indexes [4.13] and can be rewritten as:

$$E_{OSSB}(t) = \sqrt{\frac{P_0}{2}} e^{\frac{-j\pi}{4}} \left\{ \prod_{i=1}^{N} \left[1 - j\frac{\sqrt{2}m_I}{2}(-s_i(t) - \hat{s}_i(t)) \right] + j \prod_{i=1}^{N} \left[1 - j\frac{\sqrt{2}m_I}{2}(s_i(t) - \hat{s}_i(t)) \right] \right\} e^{j\omega_c t} \tag{4.5}$$

with channel modulation index $m_I = \sqrt{2}x\pi A_m$, $\hat{s}_i(t)$ is the Hilbert transform of $s_i(t)$, all the other symbols have been defined previously.

The optical field at the output of a fiber link of length z is given by [4.13],

$$E_{out}(t) = \sqrt{\frac{P_0}{2}} e^{\frac{-j\pi}{4}} \left\{ \prod_{i=1}^{N} \left[1 - j\frac{\sqrt{2}m_I}{2}(-s_i(t) - \hat{s}_i(t)) e^{\frac{-j\beta_2}{2} i^2 w_1{}^2 z} \right] + j \prod_{i=1}^{N} \left[1 - j\frac{\sqrt{2}m_I}{2}(s_i(t) - \hat{s}_i(t)) e^{\frac{-j\beta_2}{2} i^2 w_1{}^2 z} \right] \right\} e^{j\omega_c t} \tag{4.6}$$

Furthermore, as the envelope of the optical field is detected by a photodetector with responsivity, R_λ, the detected photocurrent is proportional to the envelope of optical field at the fiber output. Considering the intermodulation products, the temporal expression of the detected current may be expressed as $i(t) \approx i_{DC} + i_{sig}(t) + i_{int}(t)$, where i_{DC} is the detected current DC term, $i_{sig}(t)$ is the SCM electrical signal, $i_{int}(t)$ accounts for the intermodulation products, which acts as noise.

In SCM/OSSB systems it is important to consider the intermodulation effects between the sub-carriers as well as between sub-carrier and higher harmonics when high modulation indexes are considered. Only 3rd order, intermodulation products will be assessed, since the frequency of the mm-wave carriers were selected in order to avoid 2nd order intermodulation. It is clear that the 3rd order intermodulation products can be an issue, because they fall within the neighbor carriers.

For small modulation indexes intermodulation can be calculated using equation 4.6, however, for high values of m_I system simulation is necessary. When using system simulation the bandwidth of each channel and not just the carrier are taken into account.

4.5.2 Results and discussion

In this section the transmission of four SCM channels with RF carriers corresponding to 58.1 GHz, 60.3 GHz, 62.5 GHz and 64.7 GHz is considered. The RF carriers are modulated with 1 Gbit/s data using BPSK. All the other system parameters were defined in section 4.2. The performance results presented correspond to the 60.3 GHz channel.

4.5.3 BER versus modulation depth

The modulation depth referred here and in subsequent sections is the overall modulation depth. To maintain the same overall modulation depth when compared with single channel transmission, the individual amplitude of each carrier was reduced by 1/4. Meaning that each channel will have less power available, so to attain the same BER higher optical power should be need at the photodetector.

In Figure 4.16 the BER behavior is shown for the four optical modulation schemes under consideration with several modulation depths per channel, in a configuration without any attenuation added. Comparing this figure with the one with only one channel, Figure 4.4, we can see that the behavior is similar, but the usable x_c range is smaller for all modulations schemes. Acceptable performance values is obtained for modulation depths ranging from 0.02 to 0.5, therefore this is the range of values that will be used in the following studies.

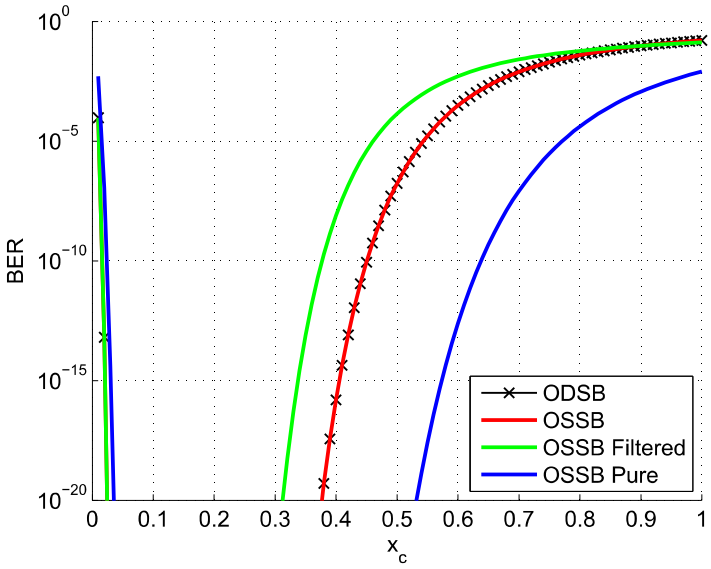

Figure 4.16 - BER versus modulation depth factor x_c for the 4 optical modulations schemes with four channels.

4.5.4 BER versus receiver sensitivity

Figure 4.17 shows the receiver sensitivity versus BER evaluated for the 60.3 GHz channel, for 0 km of fiber length.

If we compare Figure 4.17 with the equivalent configuration using a single channel Figure 4.6, we can see that for the lower three modulations depths the behavior is very similar, except for the higher power level required. This happens, since with these low modulation depths the effect of intermodulation is not relevant. However, it should be noted that although not visible in Figure 4.18, ODSB has exactly the same values as OSSB. In Figure 4.17d), F-OSSB starts to underperform, comparing with the other modulations, and just like for the single channel operation, F-OSSB does perform as well as OSSB for higher modulation depths. This can be explained by the power loss transported on the higher order optical harmonics. The small improvement, when compared with P-OSSB, at low modulation depths is not noticeable.

P-OSSB is once again the only modulation that can work consistently over all modulation depths, although with a power penalty in almost all scenarios. Using the results from Figure 4.17 and defining a BER objective of 10^{-12} we can calculate the power margin available for each configuration, as shown in Figure 4.18.

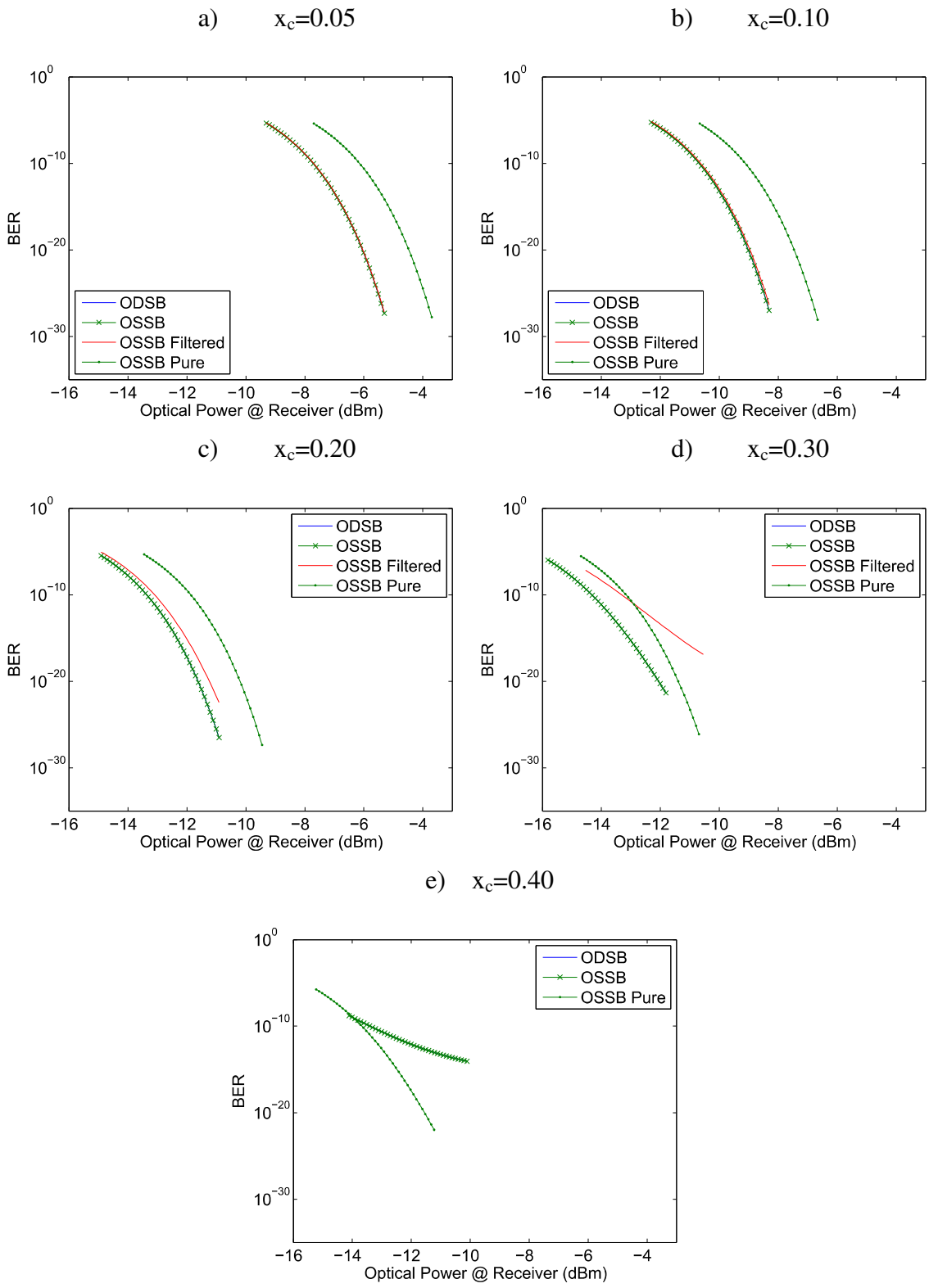

Figure 4.17 - BER in function of received optical power in a back-to-back configuration, for several x_c with a four channels.

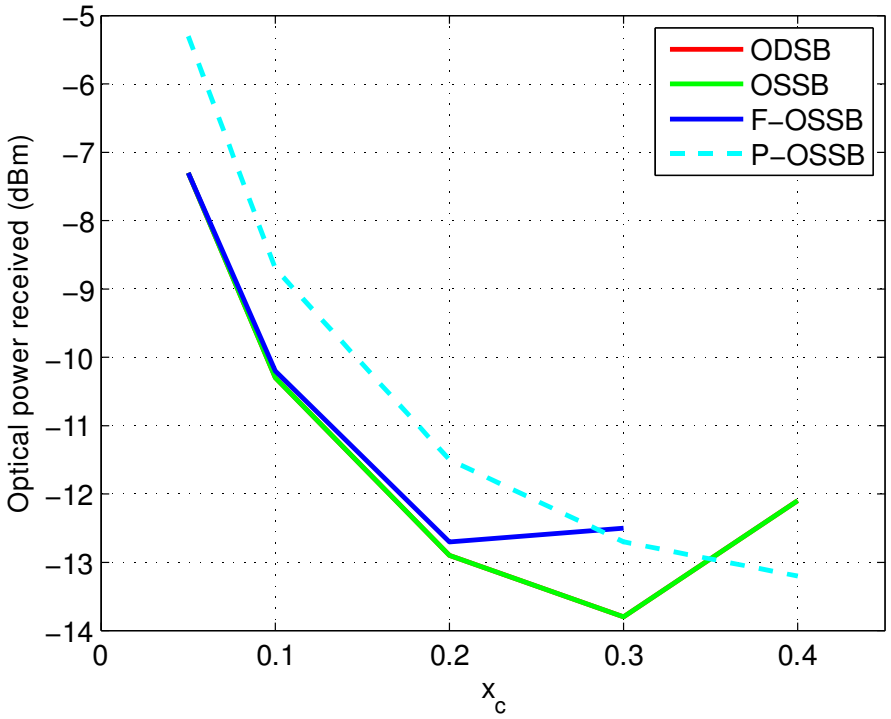

Figure 4.18 - System sensitivity for a fiber length of 0 km with four channels.

4.5.5 BER versus optical fiber length

The system was configured with the attenuation provided by Figure 4.7, which ensures BER=10^{-12} for all modulation depths when the fiber length considered is 0. In order to analyze the effect of fiber dispersion the fiber length was swept in steps of 100 m until 50 km. The results are presented in Figure 4.19.

The behavior of the SCM/ODSB system is very similar to the single channel ODSB system, the power fading characteristic of ODSB systems is the principal factor that dominates the performance of the system. As before P-OSSB is the most consistent scheme, without major oscillations in the BER. For the other modulations, their behavior is very similar for the lower x_c, however has the modulation depth increases OSSB starts to experience BER oscillations owing to the photodetection of the double side band higher harmonics. Focusing is F-OSSB we can see that the BER oscillations are not present, since the higher order harmonics have been filtered. But in both modulations, OSSB and F-OSSB, an interesting phenomena occurs, the BER improves as the fiber length increases, since P-OSSB does not present this behavior, this happens because the intermodulation products that fall near the optical carrier are 'washed way' by dispersion.

Therefore, such systems might be improved by the use of a dispersion compensation scheme.

a) $x_c = 0.05$ b) $x_c = 0.10$

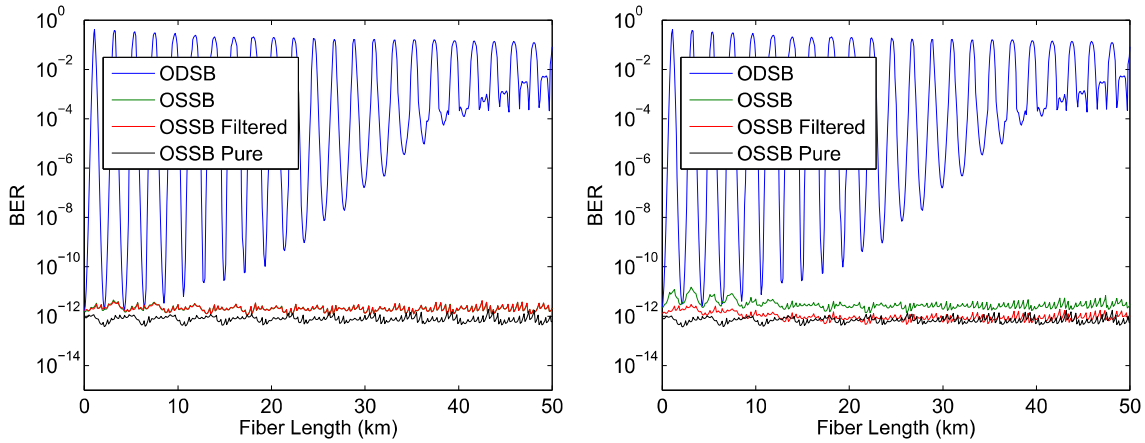

c) $x_c = 0.20$ d) $x_c = 0.30$

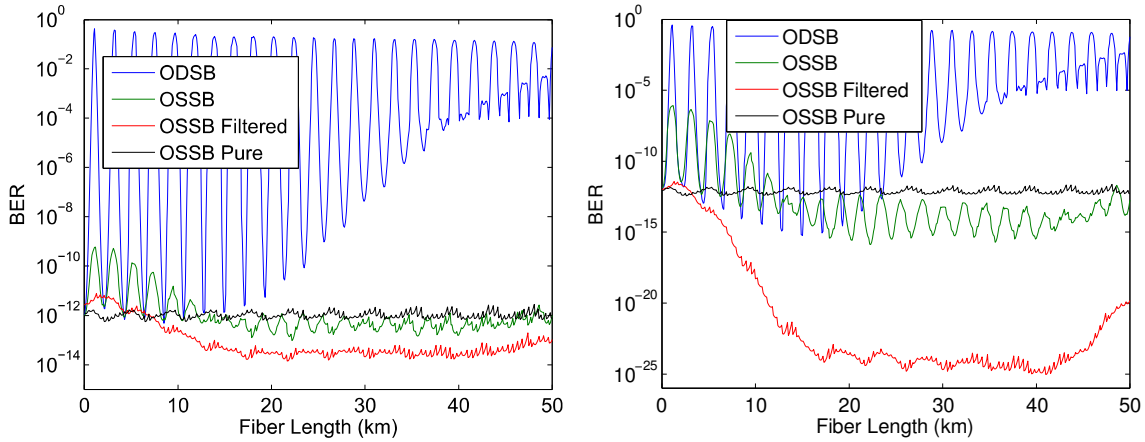

e) $x_c = 0.40$

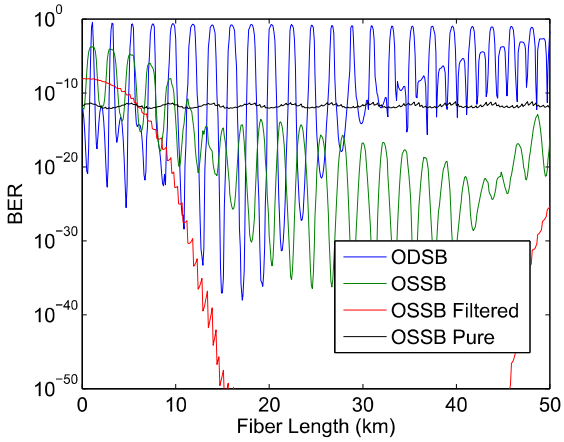

Figure 4.19 - BER in function of fiber length, for several x_c with four channels.

4.6 Summary

By using numerical simulation we have shown that the fiber chromatic dispersion combined with intermodulation distortion introduced by the optical modulator are key system parameters in single carrier and subcarrier multiplexed mm-wave radio over fiber system employing OSSB modulation. As expected ODSB is unviable for 60 GHz transmission for distances over 500 m.

The modulation depth employed is a key operational factor. For low modulation depth is system performance is dominated by the system noise, however, as the modulation depth increases higher order optical DSB harmonics become significant leading to power fading at the receiver. Additionally, by increasing the modulation depth the value of intermodulation products that fall near the optical carrier also increases, leading to system degradation. It was shown, that this last effect can be partially compensated, for SCM/OSSB system, by fiber dispersion.

F-OSSB and P-OSSB helped to identify the deficiencies of the OSSB generated using the MZM. F-OSSB identified the high order harmonics has a source of distortion when transmitting longer distances with higher modulation depths, but also shown that for shorter distances the higher harmonics actually help the system performance. Next in the pursuit for extra causes for distortion, P-OSSB was developed. This modulation scheme proved that the optical carrier is modulated, expected from the mathematical expressions, but it shown that MZM cannot work with high modulation depths if the primary optical components expected to use are the optical carrier and first harmonic.

The chapter also provides a comparative study between OSSB and OCS, considering the finite extinction ratio of MZMs and the optical amplifier noise. OCS proved to be a good option for distances up to 40 km, with the ability to double the modulated signal frequency. This is good feature for RF that are design with it in consideration. Pure transparent systems cannot use OCS modulation. For larger distances, the best option is to use OSSB instead. It was shown that 5% imbalance different can create a BER penalty of 10^3.

4.7 References

[4.1] L. Cimini, Jr., "Analysis and Simulation of a Digital Mobile Channel Using Orthogonal Frequency Division Multiplexing," *Communications, IEEE Transactions on,* vol. 33, pp. 665-675, 1985.

[4.2] A. Gusmao*, et al.*, "Comparison of two modulation choices for broadband wireless communications," in *Vehicular Technology Conference Proceedings, 2000. VTC 2000-Spring Tokyo. 2000 IEEE 51st*, 2000, pp. 1300-1305 vol.2.

[4.3] VPIsystems, "User's Manual," *VPItransmissionMaker(tm)/VPIcomponentMaker(tm),* 2011.

[4.4] U. Gliese*, et al.*, "Chromatic dispersion in fiber-optic microwave and millimeter-wave links," *Microwave Theory and Techniques, IEEE Transactions on,* vol. 44, pp. 1716-1724, 1996.

[4.5] R. Hofstetter*, et al.*, "Dispersion effects in optical millimeter-wave systems using self-heterodyne method for transport and generation," *Microwave Theory and Techniques, IEEE Transactions on,* vol. 43, pp. 2263-2269, 1995.

[4.6] C. Lim*, et al.*, "Mitigation strategy for transmission impairments in millimeter-wave radio-over-fiber networks [Invited]," *J. Opt. Netw.,* vol. 8, pp. 201-214, 2009.

[4.7] M. Jianxin*, et al.*, "Fiber Dispersion Influence on Transmission of the Optical Millimeter-Waves Generated Using LN-MZM Intensity Modulation," *Lightwave Technology, Journal of,* vol. 25, pp. 3244-3256, 2007.

[4.8] L. Christina*, et al.*, "Impact of chromatic dispersion on 60 GHz radio-over-fiber transmission," in *IEEE Lasers and Electro-Optics Society, 2008. LEOS 2008. 21st Annual Meeting of the*, 2008, pp. 89-90.

[4.9] L. Chun-Ting*, et al.*, "Impact of Nonlinear Transfer Function and Imperfect Splitting Ratio of MZM on Optical Up-Conversion Employing Double Sideband With Carrier Suppression Modulation," *Lightwave Technology, Journal of,* vol. 26, pp. 2449-2459, 2008.

[4.10] P. Laurencio*, et al.*, "Dispersion Robustness of Millimeter Waves Generated by Up-Conversion Strategies," *Fiber and Integrated Optics,* vol. 29, pp. 441-452, 2010.

[4.11] W. H. Chen and W. I. Way, "Multichannel single-sideband SCM/DWDM transmission systems," *Lightwave Technology, Journal of,* vol. 22, pp. 1679-1693, 2004.

[4.12] H. Rongqing*, et al.*, "Subcarrier multiplexing for high-speed optical transmission," *Lightwave Technology, Journal of,* vol. 20, pp. 417-427, 2002.

[4.13] P. Laurencio*, et al.*, "Impact of the Combined Effect of RIN and Intermodulation Distortion on OSSB/SCM Systems," *Lightwave Technology, Journal of,* vol. 24, pp. 4250-4262, 2006.

5

Wireless overlay backhauling over bidirectional colorless WDM-PONs

5.1 Introduction

Next generation wavelength division multiplexed passive optical networks (WDM-PONs), employing reflective semiconductor optical amplifiers (RSOAs) can provide a cost effective solution to jointly support both, classic PON services and transparent overlay wireless backhauling. In this approach, the wireless signals are transparently transmitted over the WDM-PON, thus creating a virtual dedicated network without incurring into additional network installation and maintenance costs. In this chapter, the performance of a WDM-PON operating at 1 Gbit/s and transmitting an overlay orthogonal frequency-division multiplexing (OFDM) wireless signal is assessed

analytically and experimentally, with the relevant system impairments being identified. The intermodulation due to the beating of the baseband signal and wireless signal at the receiver is quantified, and it is demonstrated that it can seriously impair the wireless channel. Performance degradation of the wireless channel, caused by the RSOA gain modulation due to the downstream baseband data is also assessed, and system design guidelines are provided.

This chapter continues by presenting the motivation for this work, followed by section 5.3 where an introduction to the IEEE 802.11 standard family is presented. Section 5.4 introduces the system architecture under consideration and the experimental setup. Detailed system performance results, discussion and explanation are presented from section 5.5 to section 5.9. The chapter ends with an overview of all the chapter results.

5.2 Motivation

One of the most promising implementation approaches for WDM-PON relies on the use of RSOAs as transmitters at the customer premises, allowing for colorless operation [5.1] and bidirectional transmission with a single fiber. In these networks the RSOA is seeded with either continuous wave (CW) light from the optical line terminal (OLT), or with the downstream signal [5.2]. Such wavelength reuse strategy improves both the cost-effectiveness and wavelength control functionalities of WDM-PONs. Although recent RSOA based systems, potentially providing 10 Gbit/s transmissions, have been reported [5.3, 5.4], in the work presented here we consider conventional commercially available RSOA devices with a 3 dB bandwidth around 1.3 GHz. Since the RSOA frequency transfer characteristics decreases smoothly, it is possible to use more than 1 GHz bandwidth beyond the device initial 1.3 GHz 3 dB bandwidth, with less than 20 dB attenuation.

Independently of the technology used, future access networks will need to converge towards a single platform for broadband fixed access and backhauling of wireless networks. This convergence is required to be a non-disruptive solution that minimizes the network operational expenditures (OPEX) and the capital expenditures (CAPEX). Converged wireless over WDM-PON architectures can follow different models [5.5]. The approach considered in this thesis is the overlay approach, where a wireless signal operating in the 1 to 3 GHz band is transmitted in combination with 1 Gbit/s baseband data. The objective is to create an architecture compatible with current technologies, i.e.

reusing wavelengths, but at the same time able to use dedicated wavelengths. When reusing wavelengths signal bandwidths must be taken in consideration, to avoid frequency overlapping. Ideally, the wireless signal should be transmitted without the use of intermediate frequency down conversion. Fortunately all major cellular technologies and wireless local area networks (WLANs) can operate beyond 1 GHz, e.g. global system for mobile communications (GSM) at 1.8 or 1.9 GHz, high speed packet access (HSPA) family at 1.7, 1.9 or 2.1 GHz, long term evolution (LTE) at 1.8 or 2.6 GHz and 802.11g/n at 2.4 GHz. In case of using dedicated wavelengths for wireless transmission the lower frequency versions can also be used, such as 700-900 MHz GSM, HSPA, and LTE. Additionally, integrating wireless system with WDM-PON optical network terminals (ONTs) simplifies the deployment of picocells, since the wireless system is locked to a determined WDM-PON network, a global positioning system (GPS) receiver is unnecessary to ensure the picocell only operates on a pre-determinate region.

In this thesis, to demonstrate the concept, experimental work is performed. The experimental setup uses an OFDM signal transmitted at 2.412 GHz compliant with the 802.11g standard, combined with 1 Gbit/s baseband data. Although, the 802.11g standard is aimed mainly to be used at local area networks, the frequency range of operation, the OFDM modulation format employed as well as the available performance assessment tools, allow for an experimental evaluation which conclusions can be easily be applied to other wireless and mobile communication standards.

5.3 IEEE 802.11

IEEE 802.11 standard [5.6] is part of the wider IEEE 802 family [5.7] which provides standards for several systems and subsystems. Some of the most used standards are presented in Table 5.1. 802.3 is used in fixed local area networks (LAN), also known as Ethernet, 802.15 is used in wireless personal area networks (WPAN), i.e. Bluetooth, 802.11 is used in WLAN, i.e. Wi-Fi, 802.16 in wireless metropolitan area networks (WMAN) and 802.2 which defines the logical link control behavior, thus not a physical network as previous standards.

The IEEE 802.11 standard has suffered several evolutions. The first version provides speeds up to 2 Mbit/s and three transmission modes. One transmitting mode uses infrared (IR) light and two use RF signals in the 2.4 GHz band. One radio frequency (RF)

modulation scheme uses frequency hopping spread spectrum (FHSS), while the other uses direct-sequence spread spectrum (DSSS) with fixed channels.

Number	Standard	Commercial Name
802.2	Logical link control (LLC)	
802.3	CSMA/CD	Ethernet (LAN)
802.11	WLANs	Wi-Fi
802.15	WPANs	Bluetooth, Zigbee
802.16	WMANs	WiMAX

Table 5.1 - Selected IEEE 802 standards.

The second version, 802.11b focused in upgrading the DSSS modulation, creating the high speed DSSS (HS/DSSS) with the 5.5 and 11 Mbit/s speed classes. The 802.11a version changed the RF frequency band to 5 GHz and the modulation from DSSS to OFDM. OFDM uses several orthogonal subcarriers, each subcarrier is modulated using binary phase shift keying (BPSK), quadrature phase shift keying (QPSK) or 64 quadrature amplitude modulation (QAM). Each modulation combined with different forward error correction (FEC) values creates several speed classes, 6, 9, 12, 18, 24, 36, 48 or 54 Mbit/s, for the same occupied spectrum, but different signal to noise ratio (SNR) requirements. This allows for dynamic data rates, which are adapted to the channel conditions. For example: 6 Mbit/s uses 1/2 FEC and BPSK modulation, while 54 Mbit/s uses ¾ FEC and 64 QAM.

802.11g was later released using the same functionally as 802.11a, but using the 2.4 GHz band with backward compatibility with 802.11b.

The latest version, 802.11n, updates the OFDM modulation scheme, uses more subcarriers for data, 56 of 64 instead 52 of 64, half the guard band and a new FEC algorithm, the low-density parity-check code (LDPC), which puts the maximum bandwidth up to 72.2 Mbit/s. But from the new features, the ones with the largest gains are channel bonding to 40MHz bandwidth, multiple input multiple output (MIMO) technology, allowing the transmission of several spatial streams and the new 5/6 coding rate. In the best case scenario the maximum available is 600 Mbit/s, when using four spatial streams with 64 QAM modulation, 5/6 coding rate, 40 MHz bandwidth and 400 ns guard band. 802.11n standard is also defined for the 5 GHz band, but it is not mandatory.

Thirteen channels are available in Europe and eleven in the US in the 2.4 GHz band. Each channel has only 5 MHz of unique bandwidth. 802.11b and g are modulated using 20 MHz bandwidth, but it is recommended to use 22 MHz bandwidth as a reference when channel planning, so only 3 channels are available without overlapping, as presented in Figure 5.1.

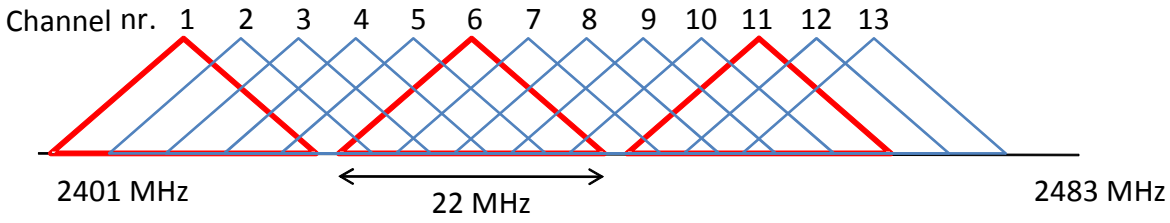

Figure 5.1 - 802.11 2.4 GHz channel map.

OSI Layers	IEEE 802 Layers
Data link layer	Logical link control (LLC)
	Media access control (MAC)
Physical layer	Physical medium

Table 5.2 - IEEE 802 lower OSI layers.

The LLC layer is common to all the IEEE 802 standards and its main function is to interface the network layer, and the lower layer, media access control (MAC). The MAC layer manages the access to the physical layer, and it is specific to each standard.

5.3.1 Medium access

RF transmission is a shared medium by nature, especially when using unlicensed spectrum, as is the case with the 2.4 and 5 GHz bands used by 802.11. A multiple access protocol must be applied to allow communication between several devices. The wired 802 standard (802.3) uses carrier sense multiple access with collision detection (CSMA/CD), but this protocol have several limitations when used in a wireless environment. While on wired transmission is fairly easy to assess if simultaneous transmissions occur, as all devices on the same network segment will receive the corrupt data, the same is not true in wireless transmissions.

IEEE 802.11 uses a difference technique, carrier sense multiple access with collision avoidance (CSMA/CA), it primarily tries to avoid collisions instead of detecting it and retransmitting. Before a station tries to send data, it waits a random amount of time, if no data is sensed during that period, it transmits.

Wireless transmissions can experience the hidden node problem. This problem occurs when one or several nodes cannot receive or sense transmission from other nodes. Hidden node problem usually occurs with the nodes at the network extremity.

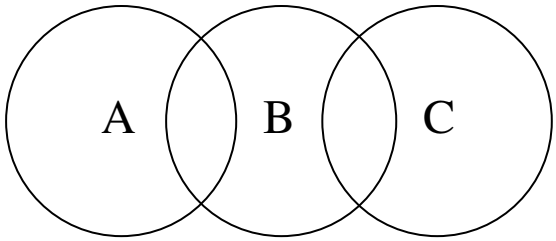

Figure 5.2 - Hidden node problem.

In Figure 5.2 we can see three wireless nodes (A, B and C), each node has the capability to receive and send information within a certain area, represented with a circle for each node. If basic CSMA/CA where to be used, node A or node C would not sense each other, so if A and C were to communicate with node B at the same time, collisions would occur.

Collisions can be minimized if request to send / clear to send (RTS / CTS), an optional scheme developed to work on top of CSMA/CA, is used. Instead of transmitting data right after the sensing period, station A will transmit a RTS packet informing that it wants to communicate with station B, then station B will respond with a CTS. This way, although station C will not receive the RTS packet, it will receive the CTS, thus becomes aware the medium will be occupied. If for some reason the CTS packet is not received by station A, it will wait a random amount of time before retransmitting the RTS packet.

These schemes to access the medium are highly reliant on timeouts. It should be noted that 802.11 protocols were intended to be used for LAN access, and if no major change is made, such as violating transmission power regulation or very high gain antennas, no problems related with protocol timing are expected.

We should take into account that the propagation speed in air is different from fiber. If we look at the propagation speed equation:

$$v = \frac{c}{n} \tag{5.1}$$

where *c* represents the electromagnetic radiation speed in vacuum and *n* the refractive index.

The refractive value for air is approximately 1.00 (rounded) and for fused silica at 1550 nm is around 1.44 to 1.46 [5.8, 5.9]. We can establish that a wireless radio frequency modulated in an optical fiber will travel 1.45 times slower than through air. This means that if the timing defined at MAC layer protocols enforces a timeout of 30 µs to receive a response from another station, the maximum distance between stations (ignoring processing delays) would be about 4.5 km, 15 µs to reach the destination plus another 15 µs to go back to the sender. But if the same signal travels by fiber, the maximum distance would be reduced to 3.1 km.

The impact of fiber propagation delay on 802.11 has been studied in [5.10-5.12].

5.4 System architecture and experimental setup

The system architecture, as evaluated in the laboratory, is presented in Figure 5.3. The architecture can be divided in three parts, the central office, the signal distribution system and the base station. In the central office a distributed feedback (DFB) laser is modulated with the wireless and band base (BB) signal, and sent through an optical circulator to the base station through the access fiber. There the optical signal is divided in two branches, one is connected to a photodetector (PD) where the signal is recovered to the electrical domain, the other branch is connected to the RSOA where the optical signal is amplified and modulated with the uplink BB and wireless uplink signal. The uplink signal travels in the same optical fiber and wavelength used for the downlink but in the central office direction, where it is converted to the electrical domain. The wireless signal is generated and received by the 802.11g commercially available access points (APs) Aironet 1200 from Cisco, the BB signals are generated by a random pulse generator and received by an oscilloscope were it is analyzed.

The optical receiver used at the central office (CO) has a 4 GHz bandwidth therefore the uplink bandwidth limitations are imposed solely by the 1.3 GHz bandwidth RSOA, SOA-RL-OEC-1550 from CIP Technologies. At the CO, the CW light wave was

generated by a DFB laser operating in the 1550 nm band. The CW is modulated by means of 10 GHz electro-absorption modulator (EAM). The optical receiver at the ONT has a bandwidth of 1.75 GHz, being therefore the bandwidth bottleneck of the downlink. To avoid interferences between the baseband and the wireless signals, low pass filters (LPFs) with cut-off frequency of 1.75 GHz were used to filter the baseband signal before modulating the optical carrier.

The optical circulator is used to ensure minimal power loses and optical isolation between the downlink and uplink signal. The optical attenuators next to the PD are used to keep the PD at the optimum received power level. The attenuator next to the laser is used to lower the input optical power while allowing the laser to operate with necessary minimum current. The optical isolators are used with the optical splitter to reduce reflections from the PD and from the unused port.

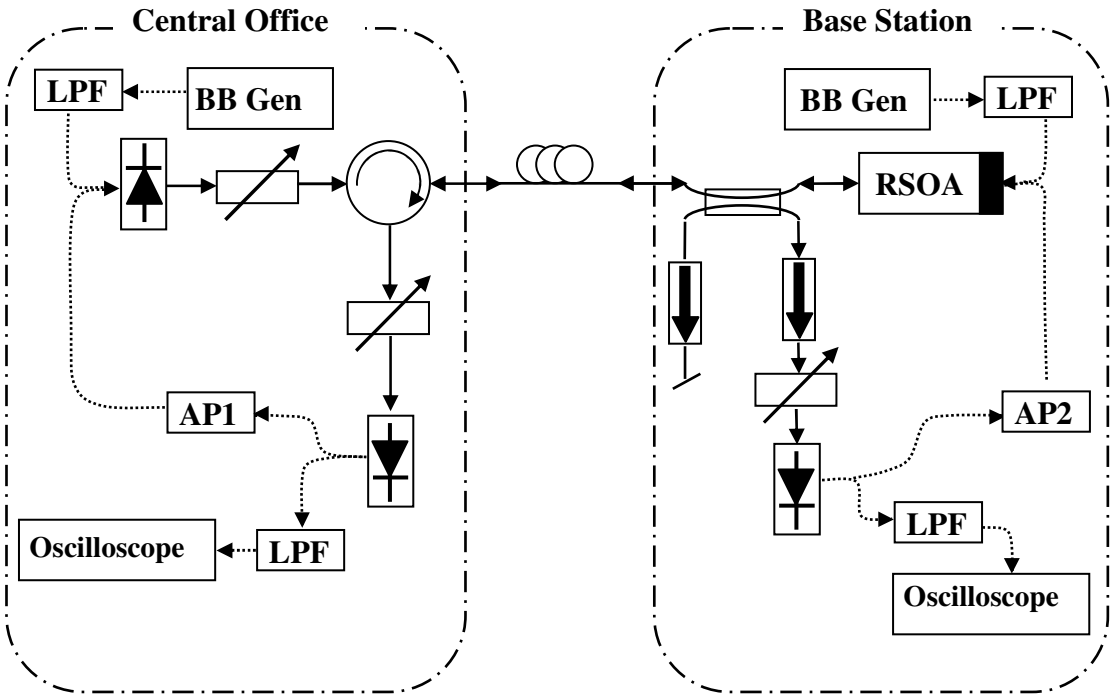

Figure 5.3 - Complete system schematic.

The full duplex system, downlink and uplink for the wireless signal and BB signal were not possible to assemble, because only one BB signal was available. We considerate to use the inverse output from the generator, but this is a correlated signal which might had unwanted effects in the results.

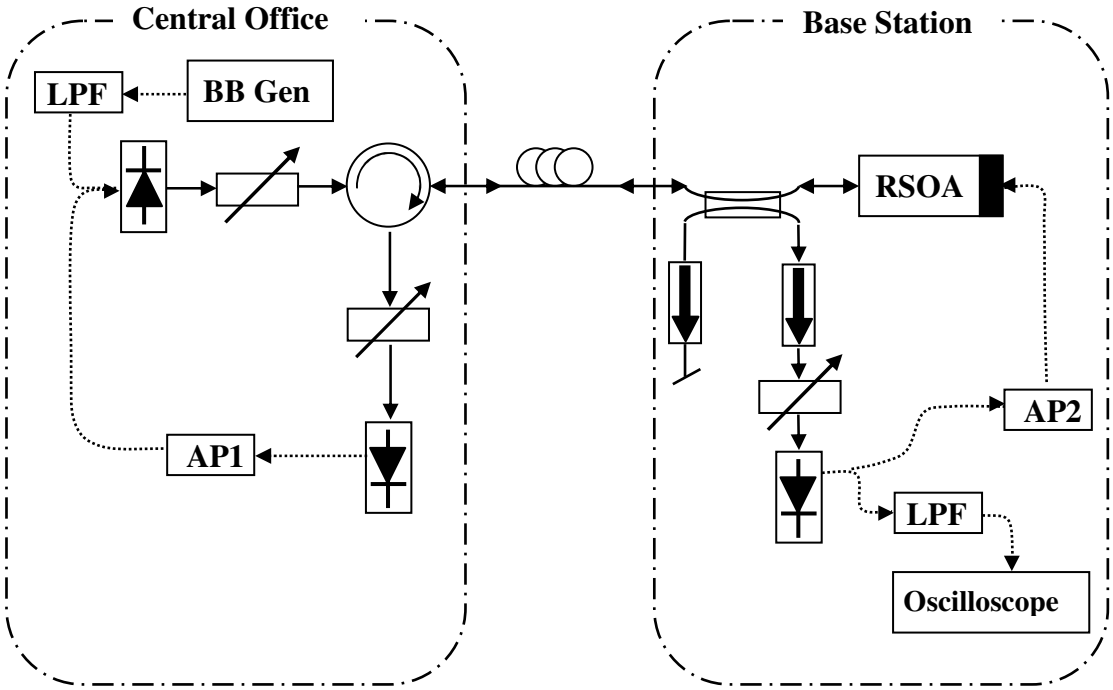

Figure 5.4 - Downlink schematic.

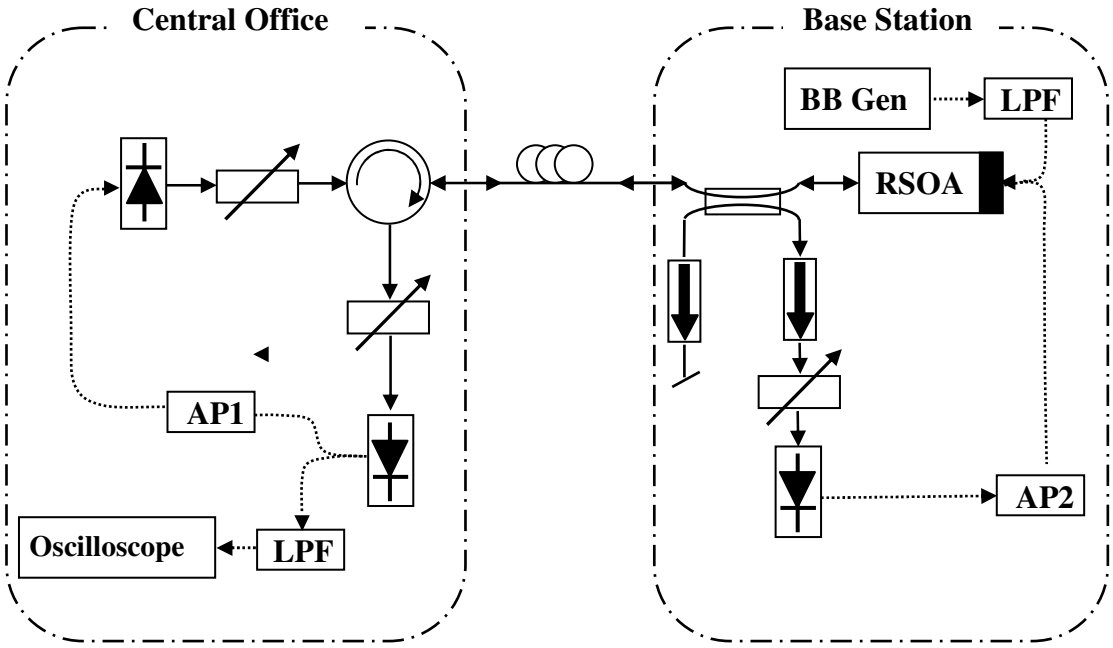

Figure 5.5 - Uplink schematic.

Two setups were used, one with the BB signal being transmitted from the CO to the base station (BS), called the downlink schematic as shown in Figure 5.4, and the second

setup with the BB signal being transmitted from the BS to the CO, the uplink schematic as shown in Figure 5.5. When comparing the two new schematic with the one in Figure 5.3, it can be seen that the optical network is the same. The main difference is the absence of the second BB generator, oscilloscope and two low pass electrical filters.

5.4.1 Methodology

It was assumed that the main system impairments would arrive from the wireless signal operating beyond the 3 dB bandwidth of the RSOA, as well as, the intermodulation between the BB signal and the wireless signal. Taking this into account, the system operating parameters, such as received optical power and input electrical power, were adjusted to the best results with only the wireless signal in the system. Later, the baseband signal was added and the system performance study started with the following measurements:

- Wireless data rate and BB bit error rate (BER) in function of BB peak to peak voltage
    - The impact of the 1 Gbit/s signal is assessed by increasing the signal amplitude from 0.0 to 2.0 V. With this study the best operating power for the BB signal is determined.
- Wireless data rate and BB BER in function of BB signal bit rate
    - The effect of bit rate speed on the wireless data rate is studied. This allows to test if it is trivial to increase the used BB bandwidth and if the system works better with lower bit rate signals.
- Wireless data rate and BB BER in function of RSOA bias
    - Assess the effect of the RSOA bias. In this study the best amplification value for the RSOA is determined. A trade-off should be expected between amplification and noise.
- Wireless data rate and Baseband BER in function of RSOA input optical power
    - Study the impact of the input optical power at the RSOA. So that the sensibility of the RSOA is determined. The optical signal is attenuated before exiting the CO and the attenuators associated to each photodetector are tuned to keep the same power level, when possible. Another possibility considered to make this measurement was to attenuate the signal at the BS

before reaching the RSOA, this would allow the same optical power at the BS PD, but would also attenuate the uplink signal, further penalizing it, thus it was abandoned.

5.4.2 Performance evaluation

By default the APs come configured to use 802.11b and 802.11g standards, so DSSS and OFDM signals can be generated. As the objective of this work is to study the OFDM performance, the 802.11b was disabled. There are several speed sub-classes in 802.11g, they differ in the modulation complexity of each subcarrier, from BPSK to 64QAM, and from the FEC ratio used. Usually the speed class is automatically chosen taking into account the signal quality, thus maximizing the network availability. In this work, the APs were configured to only use the 54 Mbit/s speed class. It was considerate to use all the OFDM classes, 6 Mbit/s up to 54 Mbit/s, but it was experienced that using all the OFDM data classes the maximum achievable data rate was slightly lower in some conditions than using only the 54 Mbit/s class. Using this approach we guaranty the best data rates are used when the system is in a good operation point. However, on the other hand when the system conditions degrade, it becomes easily unusable. This approach was followed, because the objective here was to determine the operating parameters, which lead to the best performance. The extra margin provided by lowering the wireless data rate should be used in the wireless (air) transmission and not by the optical system.

The baseband signal quality was measured by evaluating the eye diagram on a oscilloscope. The oscilloscope makes an automatic Q-factor measurement using the mean and standard deviation for the bit 1 value and for the bit 0. From the Q factor the BER was calculated considering noise to Gaussian random process.

Commercial wireless equipment was used, without access to the bit level or similar low level quality measurements. Instead bandwidth measurements were made with the freeware tool AIDA32, running on Microsoft Windows XP. This is a software suite that provides system information, diagnostics, and auditing program, but more importantly it also provides a plug-in for network benchmarking. This plug-in is designed to measure the performance of TCP/IP networks using the classic HTTP protocol in a master-slave architecture between 2 computers. The master-slave configuration in the two computers was configured as: master the computer in the CO and slave the computer in the BS when measuring the wireless downlink performance, and the reverse when measuring the

uplink performance. A screenshot of the program running is shown in Figure 5.6. The value used as the bandwidth available is the average field shown on the screenshot.

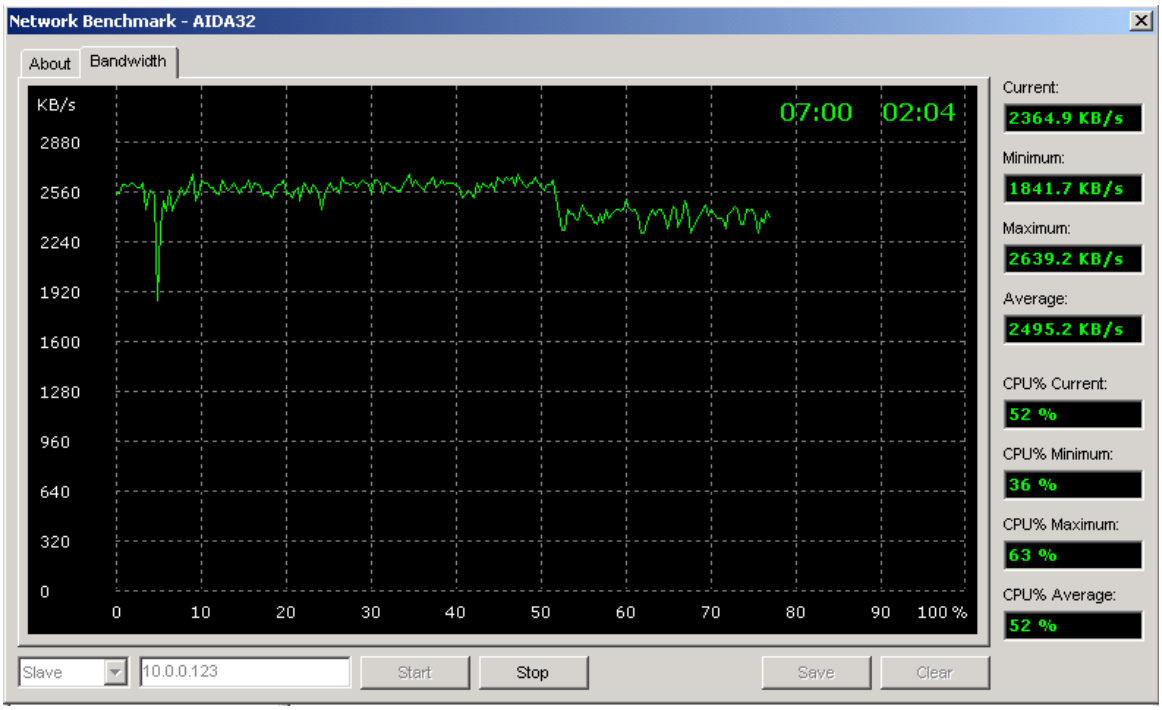

Figure 5.6 - AIDA32 network benchmark screenshot.

5.4.3 Reference values

Some reference measurements were considerate to assess the system performance. In the baseband a transmission was labeled as 'good' when the BER was lower than 10^{-9} error bits per bits transmitted.

These measurements are compared to the reference value for two specific scenarios. Scenario A, the two access points were configured with the provided antennas and positioned at close range, about 1 meter. Scenario B, the antennas were replaced with a coaxial cable and connected directly, attenuators were added to avoid the APs frontend saturation. The wireless downlink and uplink data rate were measured for the two scenarios, in terms of kibibyte per second (KiB/s).

The best scenario, as expected, is scenario B. The use of a coaxial cable ensures a near interference free environment. While scenario A has to deal with interference from other 2.4 GHz equipment. The experimental results that approach the values of scenario B are considered 'good', while results similar to scenario A are considered 'acceptable'.

Scenario	Downlink (KiB/s)	Uplink (KiB/s)
A -With antennas	2490	2144
B - With coaxial cable	2755	2410

Table 5.3 - Reference wireless data rates.

5.4.4 System transfer function and RSOA characteristics

The overall system transfer function was measured to better assess the feasibility of the proposed architecture. As we can see in Figure 5.7 it is not expected problems from the baseband signal, as the downlink performance is virtually flat, with only ~3dB difference from the lower frequencies to 1 GHz. In the uplink direction the useable bandwidth is lower than in the downlink. When comparing the two directions it can be seen that the power penalty at 1 GHz is similar, but the uplink starts with ~8 dB less attenuation than the downlink. This is expected because the system was tuned to optimize the transmission of the wireless signal, which is outside the RSOA operating range. By maximizing the operating range, the lower frequencies will experience less loss. Considering the 2.4 GHz region both directions are operating over the recommended frequencies. The downlink is being limited by the 1.75 GHz photoreceiver and the uplink by the 1.2 GHz RSOA.

The system bandwidth was adjusted by tuning the RSOA bias to 60 mA, and the optical power at the RSOA input to -10 dBm in order to maximize the usable bandwidth of the RSOA and to accommodate the 2.4 GHz wireless signal, which is outside the device 3 dB bandwidth. Under this conditions the RSOA is operating in the saturation regime as can be seen in Figure 5.8, which depicts the RSOA measured gain versus injected optical power for different bias current values. Additionally, the RSOA gain versus current, considering different input optical powers, P_{in} = -7 dBm, P_{in} = -10 dBm, P_{in} = -13, dBm, P_{in} = -15 dBm and P_{in} = -17 dBm is presented in Figure 5.9.

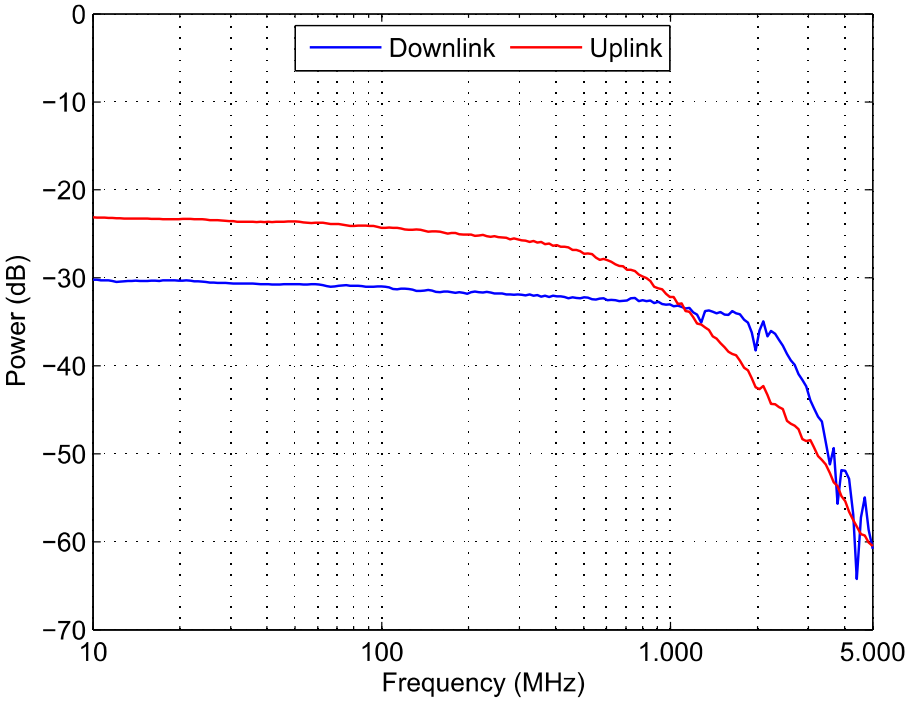

Figure 5.7 - System transfer function.

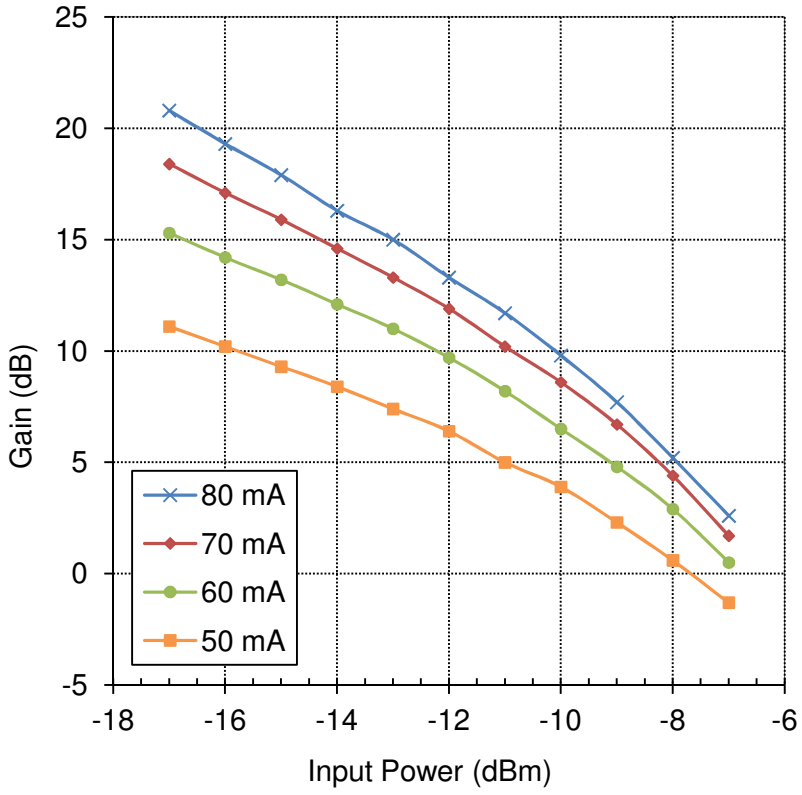

Figure 5.8 - RSOA gain versus input power for different bias currents.

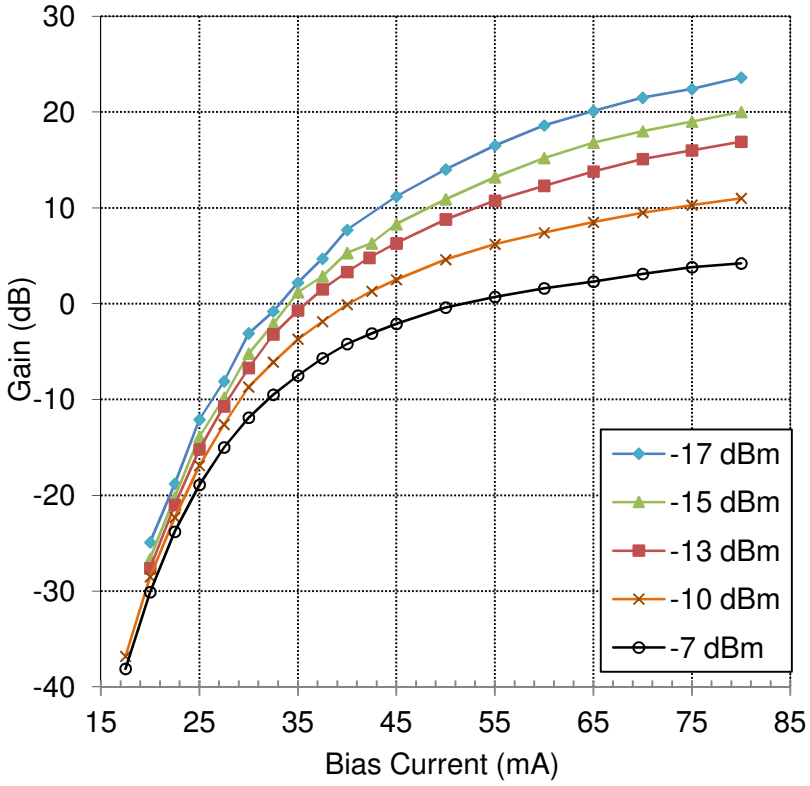

Figure 5.9 - RSOA gain versus current, considering different input optical powers, P_{in} = -7 dBm, P_{in} = -10 dBm, P_{in} = -13, dBm, P_{in} = -15 dBm and P_{in} = -17 dBm.

5.5 System performance versus baseband signal amplitude

This section analyses the impact of the BB signal amplitude on the system performance. The system performance is the overall performance i.e. wireless signal performance and baseband signal performance. Low BB signal amplitude levels should lead to higher BER of the BB signal than high amplitude levels; otherwise it might indicate operation under saturation. The two wireless channels should perform seamlessly for different BB amplitude levels, otherwise it might indicate the presence of saturation and consequently intermodulation.

5.5.1 BB on the downlink

In this scenario the downlink, the transmission from the CO to the BS, has a wireless channel, wireless downlink (DL), and a BB signal. While in the opposite direction, only the wireless channel is transmitted (wireless uplink (UL)).

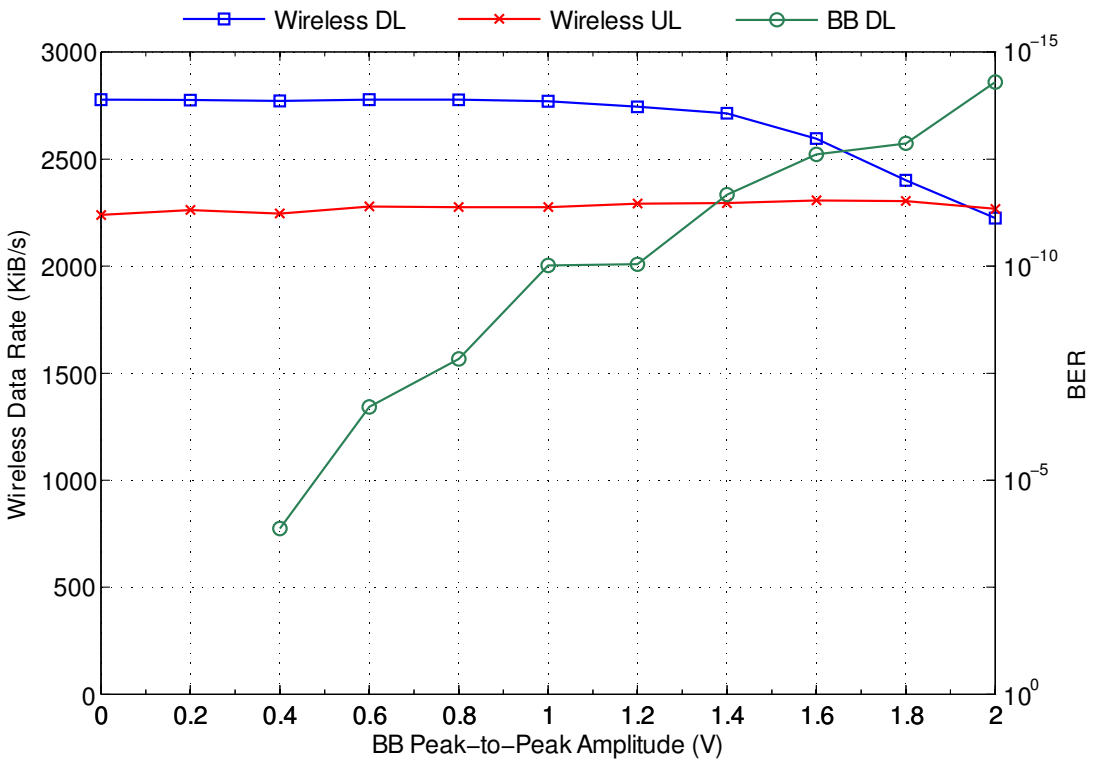

Figure 5.10 - System performance versus band base signal amplitude.

Figure 5.10 presents the wireless attainable data rate for the uplink and downlink as well as the BER for the 1 Gbit/s baseband signal for different BB amplitudes. As expected the 1 Gbit/s signal performs better when higher amplitude levels are used. As the signal amplitude increases so does the SNR, lowering the bit error rate. BERs of 10^{-9} or lower are experienced with signal amplitude higher than 1.0 V.

The effects on the wireless uplink signal are virtually inexistent. On the other hand, in the wireless downlink channel degradation is experienced with amplitudes higher than 1.2 V. This degradation is due to intermodulation between the BB and the wireless downlink channel. A test setup was developed to measure the third order intermodulation distortion (IMD_3) from the electric absorption modulator. The setup consists of two carriers at 2.0 GHz and 2.01 GHz respectively as well as the 1 Gbit/s BB signal. These three signals modulated the absorption modulator. The IMD_3 is measured for several RF carriers' power levels. A variable optical attenuator (VOA) after the electric absorption modulator insures a constant optical power at the receiver. Otherwise, the increase in the power of the RF carriers would also increase the average optical power as shown in Figure 5.11. The IMD_3 measured at 1.99 GHz becomes noticeable when the amplitude of the BB reaches 1.0 volts and increases for higher amplitudes, as shown in Figure 5.12.

The IMD_3 is simply the power difference between one of the fundamental signals and the third order product, as in [5.13], thus larger values represent smaller interference.

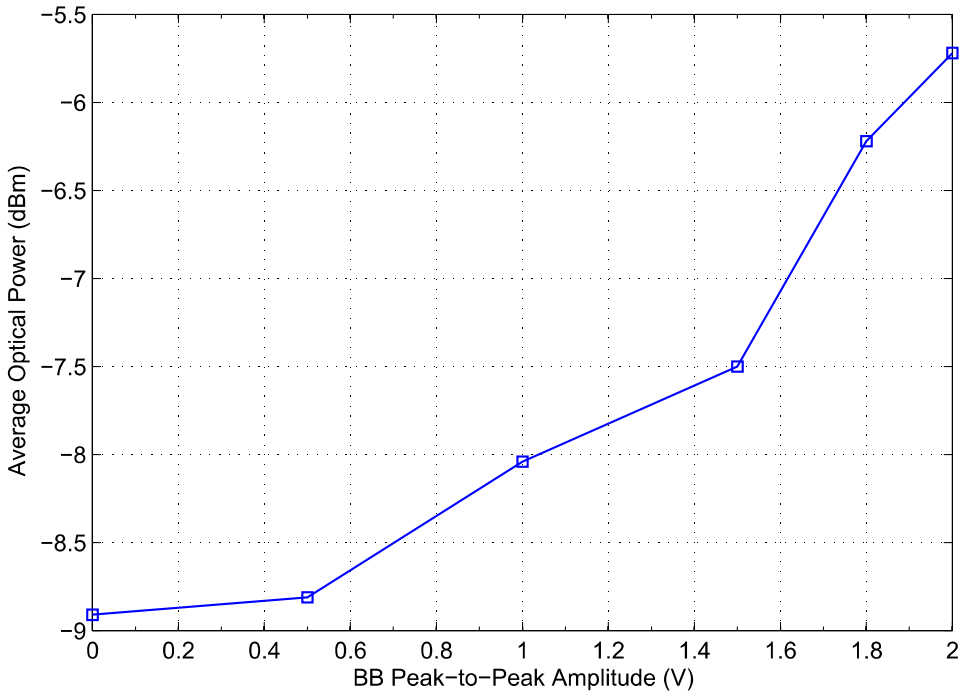

Figure 5.11 - Electric absorption modulator output power as function of band base signal amplitude.

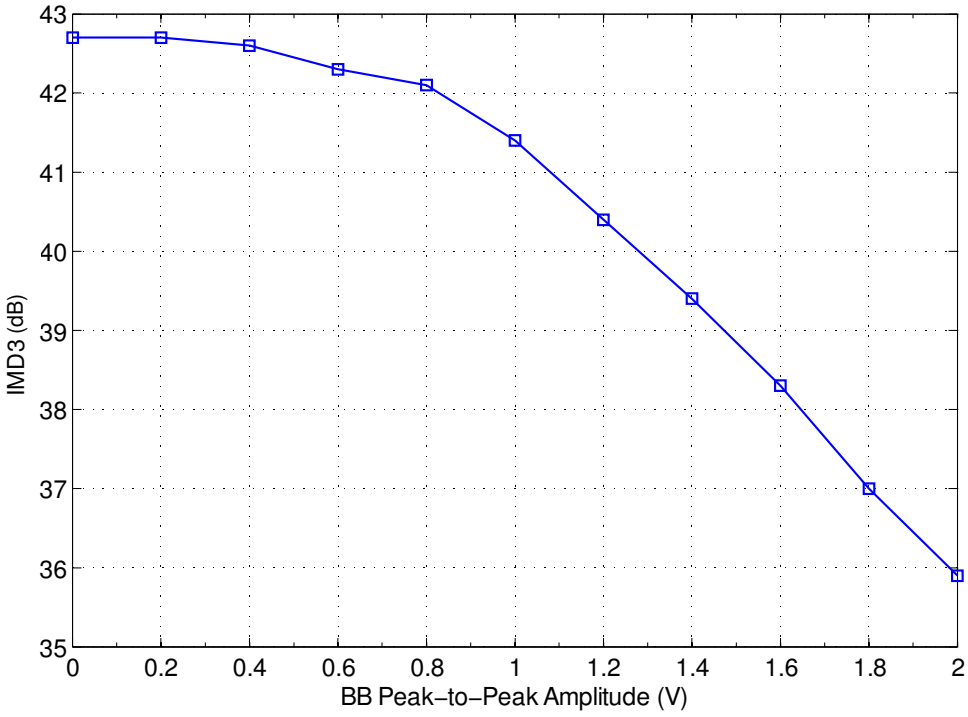

Figure 5.12 - Third order intermodulation distortion in function of band base signal amplitude, measured at 1.99 GHz.

The amplitude value for the baseband signal, when transmitted from the CO, was chosen to be 1.2 V for all the other scenarios, since this value provides a BER lower than 10^{-9}, a wireless downlink data rate of ~2750KB/s and ~2300KB/s uplink rate. These values are very close to the best scenario presented in Table 5.3.

5.5.2 BB on the uplink

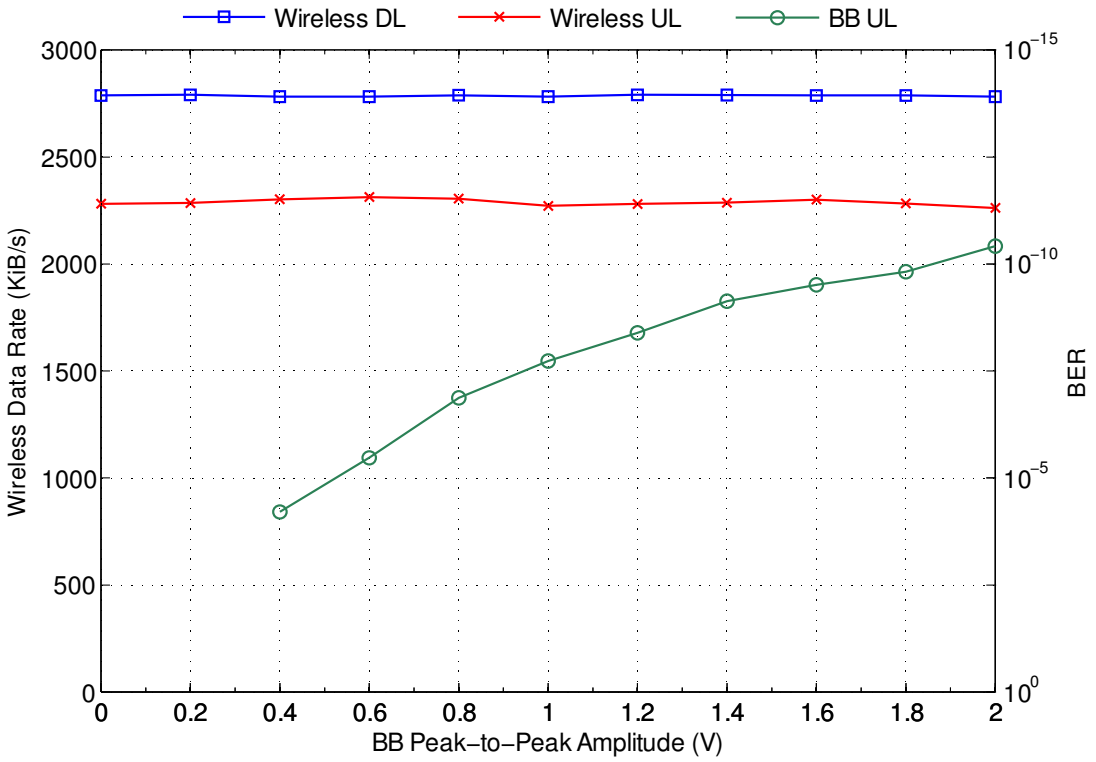

Figure 5.13 - System performance versus baseband signal voltage amplitude.

In Figure 5.13 it is shown that the wireless DL channel is virtually immune to changes in amplitude of the BB signal, only minor fluctuations on the data rates are experienced. The wireless UL has slightly higher fluctuations but without a high impact. As expected the UL BB signal is the most affected, since low signal amplitudes will have low SNR. To obtain a BER lower then 10^{-9}, a minimum amplitude of 1.6 V is necessary, higher values can be used with better results, however some degradation is expected on the wireless UL.

The chosen value for the BB signal in the BS to CO direction is 1.6 V, since it leads to at least 10^{-9} of BER, and it has the best download / upload rate relation. This value will be used in the following experiments of system performance versus baseband bit rate.

5.6 System performance versus baseband bit rate

5.6.1 BB on the downlink

As we can see in Figure 5.14, there is some correlation between the band base bit rate and the wireless performance. When no band base data is present, the wireless performs flawlessly, but as soon as the band signal is introduced at low bitrates, the wireless signal is severely impacted, stopping until the BB signals reaches around 200 Mbit/s. This behavior can be explained by the following analysis.

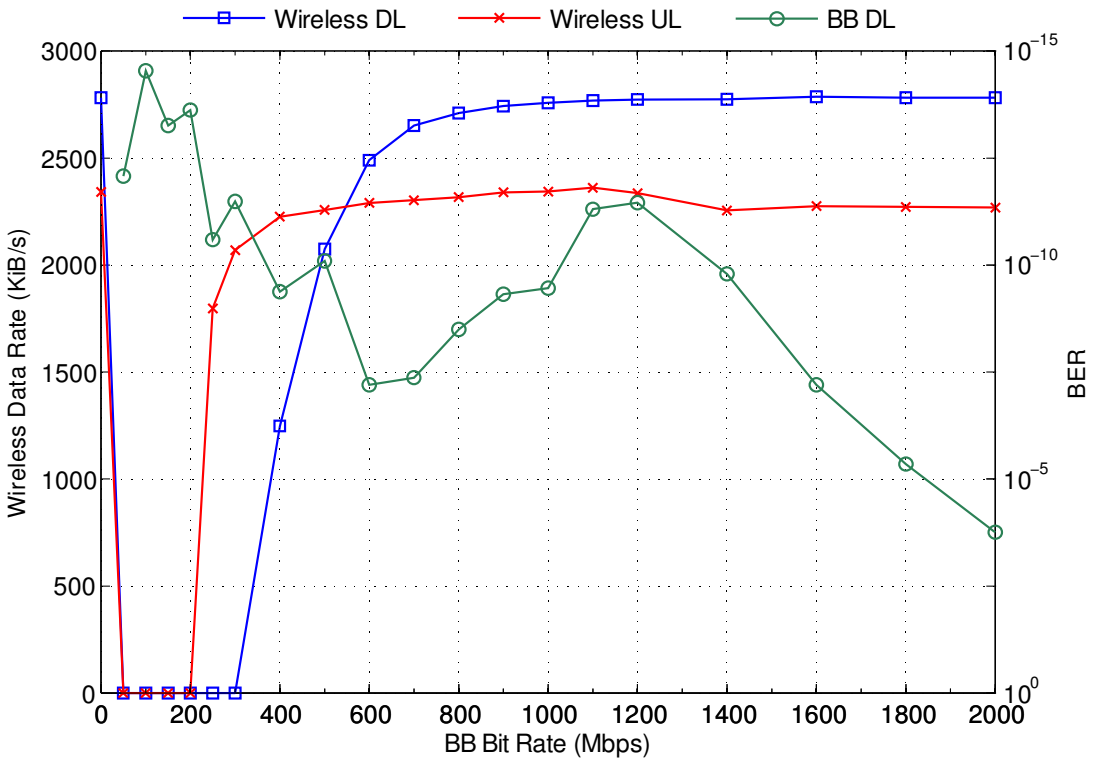

Figure 5.14 - System performance versus baseband bit rate.

5.6.2 Intermodulation analysis

Considering direct detection (DD) and intensity modulation (IM) of the optical carrier by the electro-absorption modulator at the CO and by the RSOA at the ONT/BS. The normalized optical field, *E(t)*, with optical angular frequency ω_c is modulated with baseband data, $x_b(t)$ and wireless OFDM signal $x_{OFDM}(t)$. A DC component, *A*, that includes both the average values of the OFDM signal and of the baseband signal is

considered separately, neglecting all the system noises, the normalized modulated optical field can written as [5.14]:

$$E(t) = \sqrt{A + x_b(t) + x_{OFDM}(t)}\, e^{j\omega_c t} \tag{5.2}$$

The corresponding photodetected current $y(t) = |E(t)|^2 = E(t)E(t)^*$, where * stands for complex conjugate, is obtained by considering only the first two terms of the Taylor series expansion on the square root term.

$$y(t) = \overbrace{A + x_b(t) + x_{OFDM}(t)}^{A} + \frac{\overbrace{x_b^2(t)}^{B}}{4A} + \underbrace{\frac{x_{OFDM}^2(t)}{4A}}_{C} + \underbrace{\frac{x_b(t)\,x_{OFDM}(t)}{2A}}_{D} \tag{5.3}$$

The term *A* corresponds to the DC current, the baseband and the wireless signals respectively, while the other terms correspond to intermodulation.

The OFDM signal, $x_{OFDM}(t)$, can be written as:

$$x_{OFDM}(t) = \mathrm{Re}\left[x(t)\exp^{j2\pi f_{RF} t}\right] \tag{5.4}$$

where f_{RF} is the center frequency of the passband OFDM wireless signal, which is assumed to be well above the bandwidth occupied by the baseband signal. *x(t)* is the baseband complex-valued OFDM signal, which can be written as:

$$x(t) = \left[\sum_{k=-K/2}^{K/2-1} x_k(t) e^{j2\pi f_k t}\right] \tag{5.5}$$

$x_k(t)$ represents the complex constellation symbols of the digital modulation corresponding to the data to be transmitted in subcarrier f_k, and *K* is the total number OFDM subcarriers. The OFDM subcarriers are orthogonal between themselves with $f_k = \frac{k}{T}$, being *T* the OFDM symbol duration. The baseband OFDM signal is assumed to occupy the bandwidth $-\frac{B_{OFDM}}{2}$ to $\frac{B_{OFDM}}{2}$.

Continuing with the equation 5.3 analysis; for illustrative purposes assuming the power spectral density of baseband data to be rectangular and occupying the bandwidth –

B_b to B_b, being $B_b >> B_s$, therefore the power spectral density of the *B* intermodulation term has a triangle shape and occupies the bandwidth $-2B_b$ to $2B_b$. The B intermodulation sum does not affect the wireless channel performance, if f_s is located above $2B_b+B_s/2$. The intermodulation term *C* corresponds to the quadratic term of the wireless signal which generates second order intermodulation terms falling within $-B_b$ and B_b bandwidth and at high frequencies that can easily be filtered. These two intermodulation terms, *B* and *C*, will degrade the performance of the baseband channel. Here, we focus on the performance of the wireless channel and therefore only the *D* term will be considered.

A simple analysis of this term can be developed considering the OFDM subcarriers to be unmodulated $x(t)=\left[\sum_{k=-K/2}^{K/2-1} e^{j2\pi f_k t}\right]$, therefore the unmodulated OFDM signal is given:

$$x_{OFDM}(t)=\mathrm{Re}\left[\sum_{k=-K/2}^{K/2-1}\exp^{j2\pi(f_{RF}+f_k)t}\right]=\frac{1}{2}\sum_{k=-K/2}^{K/2-1}\cos[2\pi(f_{RF}+f_k)t] \tag{5.6}$$

The power spectral density of term *(D)* is given by:

$$\begin{aligned} S_{(D)}(f) &= \frac{1}{16A}\sum_{k=-K/2}^{K/2-1}\left\{S_b(f)\otimes\left[\delta\left(f-\left(f_{RF}+f_k\right)\right)+\delta\left(f+\left(f_{RF}+f_k\right)\right)\right]\right\} \\ &= \frac{1}{16A}\sum_{k=-K/2}^{K/2-1}\left\{S_b\left(f-\left(f_{RF}+f_k\right)\right)+S_b\left(f+\left(f_{RF}+f_k\right)\right)\right\} \end{aligned} \tag{5.7}$$

$S_b(f)$, represents the power spectral density of $x_b(t)$, and $\otimes$ denotes convolution. The power spectral density of the intermodulation term *(D)* is located within the bandwidth of the OFDM signal bandwidth and is a summation of *K* shifted power spectral densities of the baseband signal, as schematically illustrated in Fig. 5.15. Since $B_b >> B_{OFDM}$, baseband signals with high power spectral density around DC will highly affect the performance of the wireless signals.

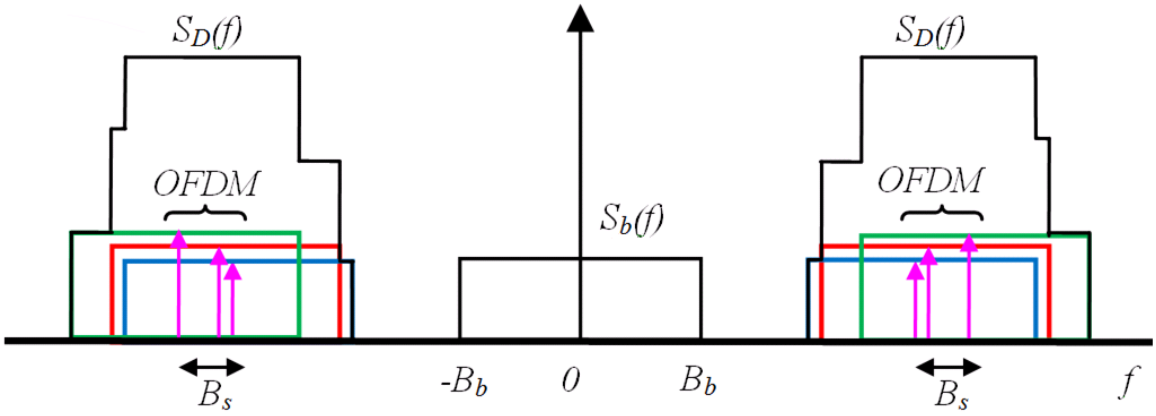

Figure 5.15 - Illustrative power spectral density resulting from the beating of the baseband and wireless signals.

The intermodulation effect due to the beating of the baseband signal and wireless signal was assessed by varying the bit rate of the baseband signal. For simplicity *b(t)* is assumed to be a train of NRZ rectangular pulses with normalized constant amplitude and transmitted at r_b bit/s. The power spectrum of *b(t)* being $S_b(f)=\frac{\mathrm{sinc}^2(f/r_b)}{4r_b}+\frac{\delta(f)}{4}$, with its maximum values inversely proportional to r_b. This can be seen in Figure 5.16 for two bit rates, 100 Mbit/s in the left and 2 Gbit/s in the right, because the two signals are transmitted with the same power, the 100 Mbit/s will have a higher power concentration in the 0-100 MHz band which will in turn create a higher interference with the wireless signal.

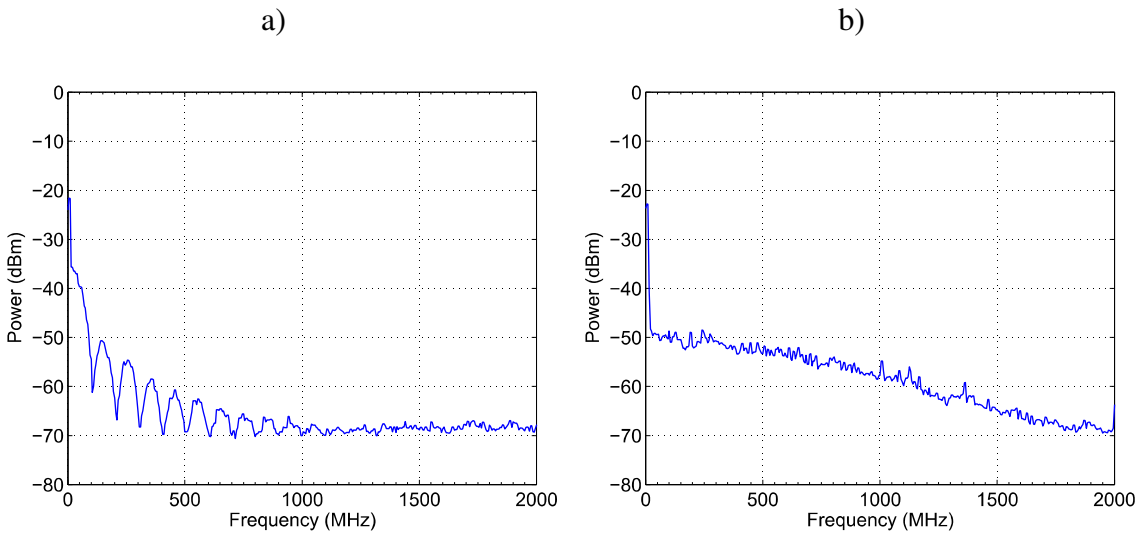

Figure 5.16 - Electrical spectrum at the base station photodetector for a) 100 Mbit/s baseband signal b) 2 Gbit/s baseband signal.

The interference impact on the wireless signal can be seen on Figure 5.17. In the right there is a perfectly define OFDM signal (2402 to 2442 MHz), this signal is being transmitted along the 2 Gbit/s baseband signal. While on the left we can see some subcarriers, with interference, in wireless channel band result of the protocol used for data transmission and some interference off band.

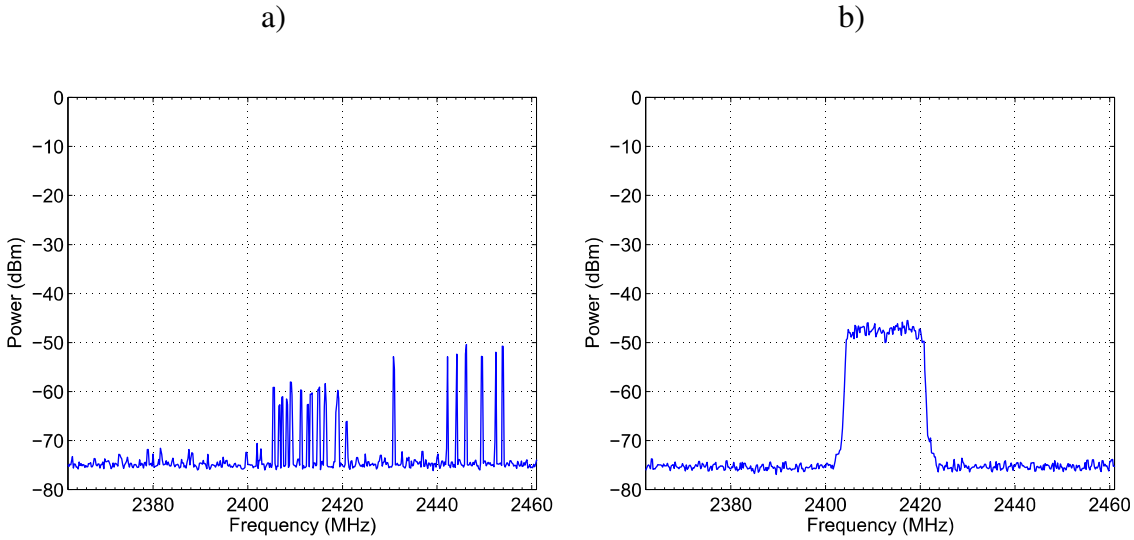

Figure 5.17 - Electrical spectrum at the base station photodetector in the wireless band for a) 100 Mbit/s baseband signal b) 2 Gbit/s baseband signal.

If we go back to Figure 5.14, we can see that when the baseband data rate decreases for values below 800 Mbit/s, the performance of the downlink wireless link starts to degrade rapidly, until is unable to transmit any data for bit rates below 300 Mbit/s. This behavior can be explained by the increase of the intermodulation term, resulting from the beating of the baseband upstream data and uplink wireless channel, as discussed previously and depicted in Figure 5.15. Since the wireless channel throughput is measured using a TCP benchmark software, bidirectional communication is needed. However, since the TCP acknowledge messages required for transmission use low bandwidth, the wireless link is not immediately affected by intermodulation, it only stops operating when the affected wireless link is severely degraded.

The baseband signal does have some unexpected behavior in the sub gigabit area. It was expected that lower bitrates would have better performance. But that is clearly not the case. EAMs are not the core focus of this work, thus no specific analysis was conducted, and also most of the BER values between 50 Mbit/s and 1 Gbit/s are in the 10^{-9} or better region. EAMs are not simple devices to characterize, however the author

feels the obligation to at least speculate on the cause of the problem. The impairment should be related to the use of a very high bias voltage on the modulator, actually higher then recommended by the manufacturer[4], this added with fact that all signals have the same overall power, regardless of the bit rate, thus lower bit rate signals will have the power concentrated in a smaller bandwidth.

The 1 Gbit/s bit rate was chosen to keep consistency with other laboratory experiences, but this architecture should perform similarly with bit rates from 900 Mbit/s up to 1.400 Gbit/s.

5.6.3 BB on the uplink

The overall system performance with the baseband signal is very similar with the BB in the downlink as presented in Figure 5.18. The exceptions are the BB behavior on the sub gigabit region and the uplink wireless failure instead of the downlink.

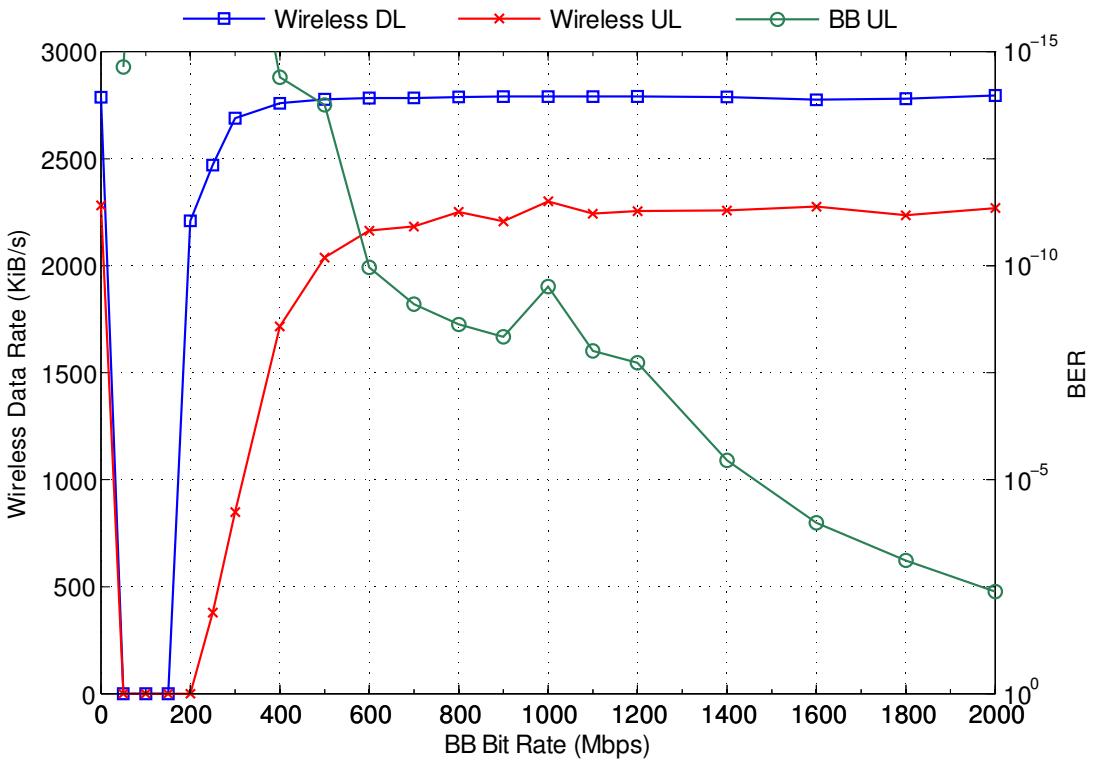

Figure 5.18 - System performance versus baseband bit rate.

[4] The maximum bias level recommended is -0.2 V, but for system assembly simplification 0.0 V (a short circuit) is much simpler. For the 1 Gbit/s bitrates there was no major difference in performance in this or the following experiments.

The wireless uplink signals is the cause of the poor performance below 600 Mbit/s due to the same reasons as the previous experiment, when BB signal in the same transmission direction creates intermodulation distortion in the lower bitrates due to the higher power density.

The intermodulation effect in the wireless signal is very noticeable when transmitting 100 Mbit/s baseband signals, as shown on the left of Figure 5.19. Notice the noise floor on the wireless channel surrounding frequencies (around -60 dBm) and how clearly is being corrupted by OFDM subcarrier, as well as how it compares to the right figure, which presents a clean noise floor at -70 dBm and a well define OFDM signal in the wireless channel.

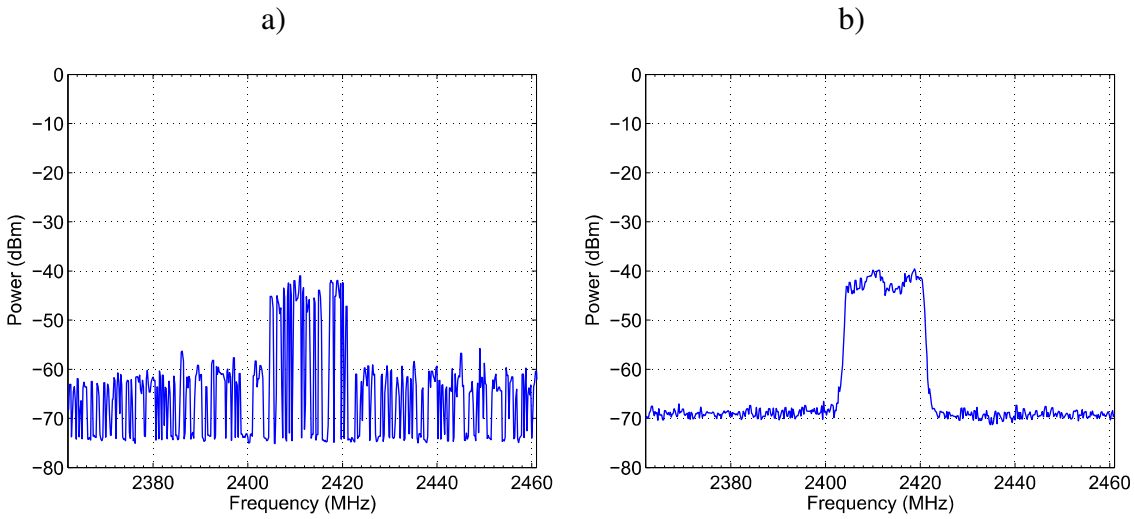

Figure 5.19 - Electrical spectrum at the central office photodetector in the wireless band for a) 100 Mbit/s baseband signal b) 2 Gbit/s baseband signal.

The proposed architecture has a good performance in the range of 600 Mbit/s to 1.1 Gbit/s. The lower limiting factor is the wireless signal, which performs poorly, or simply does not work for the lower BB bit rates, otherwise the system would perform well from 0 to 1.1 Gbit/s. The upper limiting factor is the BB BER itself.

The 1 Gbit/s bit rate was chosen because it is a local best value and to keep consistency with other laboratory experiences, but this architecture should perform similarly well with bit rates from 600 Mbit/s up to 1.1 Gbit/s.

5.7 System performance versus RSOA bias current

5.7.1 BB on the downlink

Figure 5.20 shows the impact of the RSOA bias current on the system performance. Taking into account the system architecture, the 1 Gbit/s BB downlink signal should not be affected by changes in the RSOA bias current. Additionally, if no major degradation is experienced in the wireless uplink, the wireless downlink should also be immune to the changes in the RSOA bias current. However, as can be seen in Figure 5.20 the RSOA bias current interferes with all the three channels. Surprisingly the BB signal is also affected, this happens because some of the amplified signal from the RSOA is detected at the BS photodetector. The reason is back scattering generated by fiber imperfections and most importantly fiber optics connectors. When the bias current increases, so does the optical power existing the RSOA, thus more power will reach the BS photodetector.

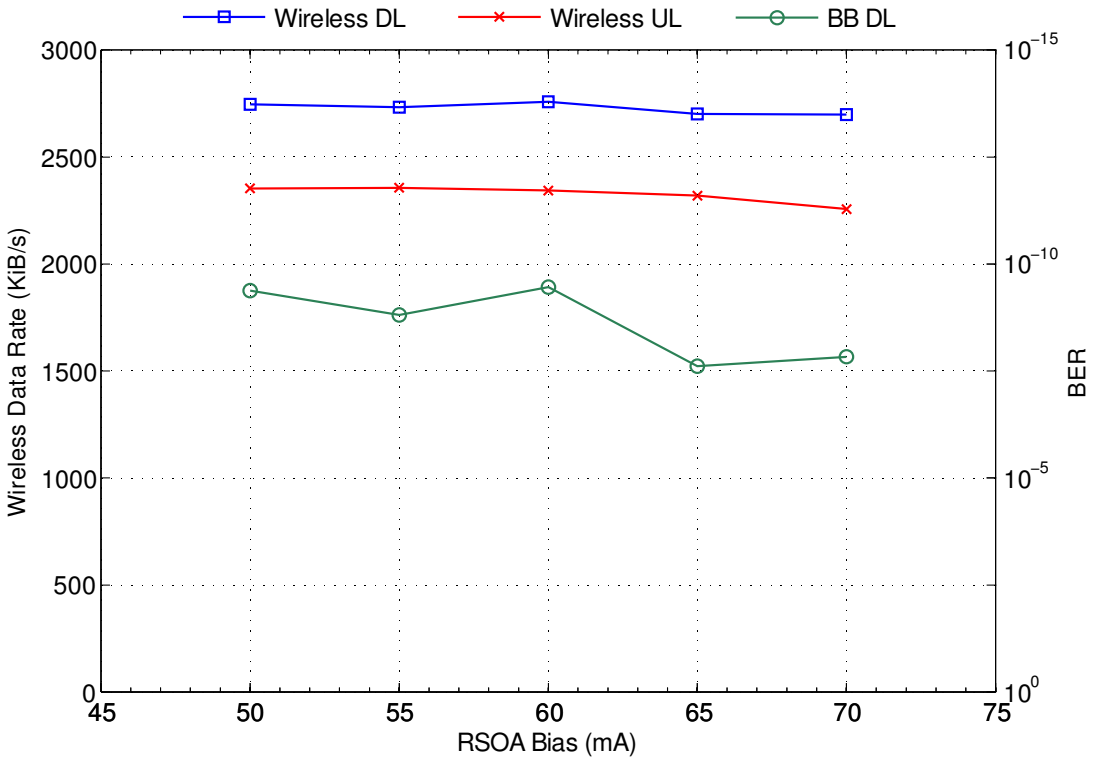

Figure 5.20 - System performance versus RSOA bias current.

The most sensible connections are the ones closer to the RSOA and photodetector, this translate to the connections with the optical coupler. In Figure 5.21 the 2:2 optical coupler is represented, port 1 is connected to the central office, port 2 is unused but has an optical isolator to avoid possible reflections, port 3 is connected to the RSOA and port 4

is connect to the photodetector. If reflections occur in ports 1 and 2, some power of the uplink signal will reach the BS photodetector. Port 3 reflections are also very problematic although they do not provide power to the BS photodetector, they will generate a positive feed loop, leading to distortion of the uplink signal increasing the optical power back reflected.

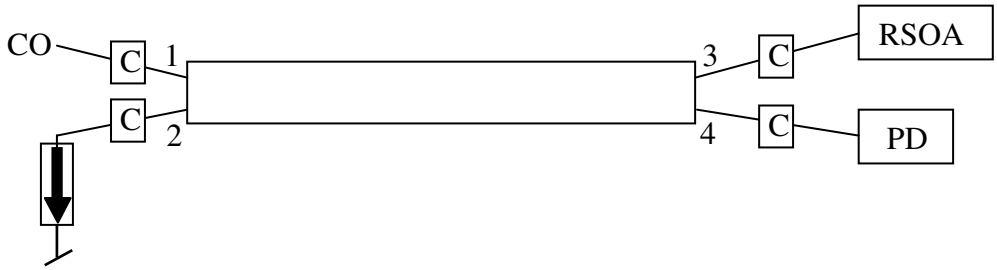

Figure 5.21 - Optical coupler connections diagram.

The wireless downlink signal also suffers from the same problem, but due to the protection schemes used, guard band and forward error correction, no major degradation is experienced from reflections. The very low performance loss experienced is due to loss in the wireless uplink channel.

In the data rate of the wireless uplink is affected by the RSOA bias current. But if the bias current is too high, the RSOA might be operating near saturation and optical modulated signal will experience a lower extinction ratio, lowering the SNR. In this case the performance loss of the wireless signal is not relevant due to the 802.11 protection schemes. The chosen value for the RSOA bias was 60mA, as it is the average best for the three channels.

5.7.2 BB on the uplink

Figure 5.22 shows the performance results versus the RSOA bias current with the baseband signal in the uplink direction.

Unsurprisingly the least affected is the wireless DL signal, it is immune to changes in the RSOA bias, except for the 50mA of bias current, but in this case the problem is in the inconsistent UL wireless speeds.

When the RSOA is biased at 50 mA, the attainable bit rate of the wireless UL is only about 1500 KiB/s. This happen due to the low average gain. The previous scenario, with only the WL connected to the RSOA, this did not happen, because the RSOA had time to

recover. When the BB signal is added, the bias will swing between values lower and higher than 50 mA, when it goes below 50 mA the RSOA will increase the gain recovery time. Increasing the bias to 55 mA is enough to overcome this problem. The slight drop in performance with bias current higher than 60 mA can be explained by the saturation of the RSOA. As in the previous subsection the wireless signals performance is only slightly affected when the bias current of the RSOA increases.

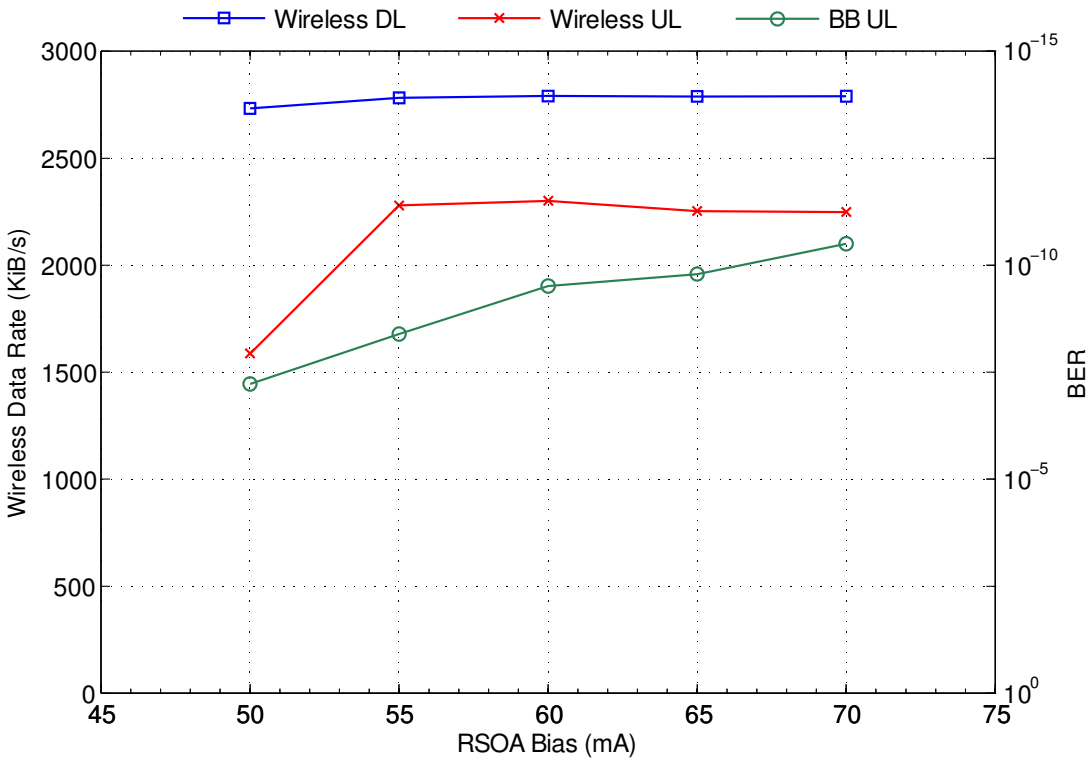

Figure 5.22 - System performance versus RSOA bias current.

The RSOA bias in this particular RSOA should be set to 60 mA. It guaranties that the modulated signals do not saturate the device, and ensures adequate gain recovery time.

5.8 System performance versus optical power at the input of the RSOA

5.8.1 BB on the downlink

In order to analyze the baseband downstream data effect on the wireless uplink performance, we start by considering a system transmitting only the baseband downstream data. At the CO the data is filtered by a low pass filter and an optical

attenuator is placed after the optical transmitter to control the average optical power that reaches the RSOA. The portion of the downstream modulated optical signal that enters the RSOA is amplified and re-transmitted back to the CO. The re-transmitted optical signal, depending on its power, can be highly distorted due to the RSOA gain saturation dynamics, according to equation (B.1) in Appendix B.

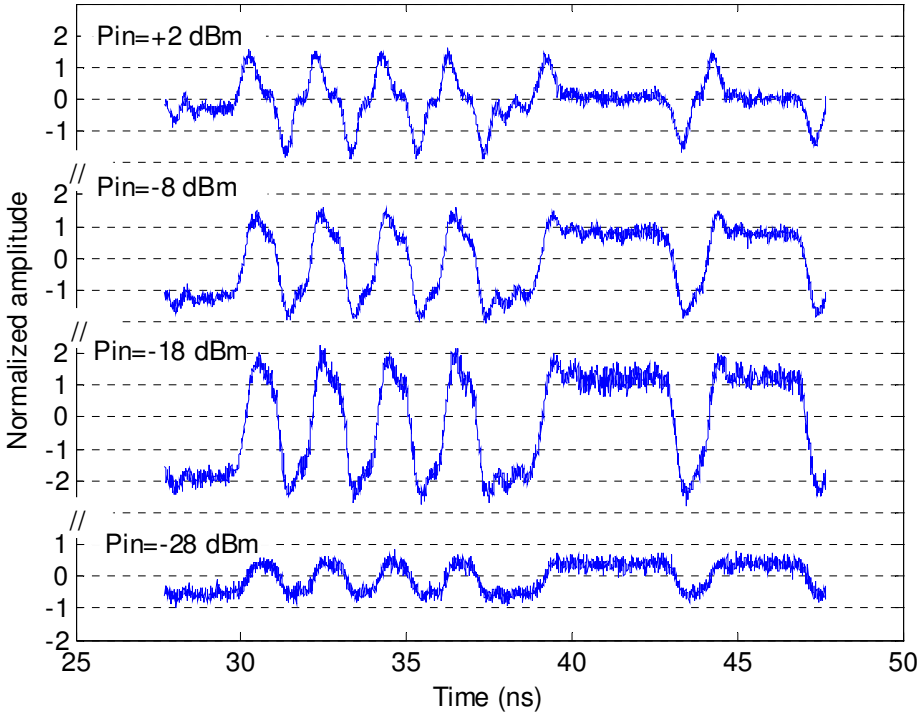

Figure 5.23 - Measured back reflected signal at the CO, considering different levels of optical power injected into the RSOA.

Figure 5.23 shows the measured signal received at the CO, in the time domain, originated by the back transmitted downstream baseband signal, for an illustrative data sequence and for different average power levels, (*Pin*). For *Pin* =-28 dBm the RSOA is operating in the linear regime and the retransmitted (upstream) signal is an amplified replica of the downstream plus added spontaneous emission noise. However, as the input pulse power increases, the leading edge of the pulse sharpens considerably leading to a highly distorted pulse. When the pulse enters the RSOA it is exposed to a high RSOA gain factor, however the leading edge of the pulse depletes the gain and the rest of the pulse experiences a lower gain. Therefore the distortion of the amplified pulse retransmitted to the CO occurs simply because different points of the pulse profile experience different gain factors. As expected the pulse distortion increases with the *Pin*.

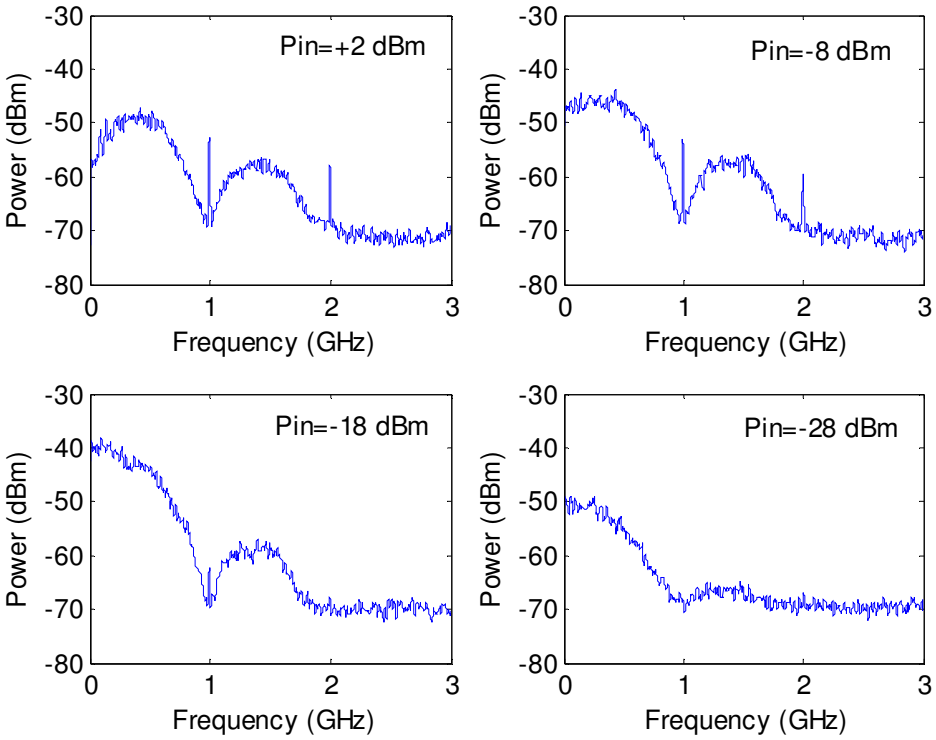

Figure 5.24 - RF spectra corresponding to the signals depicted in Figure 5.23.

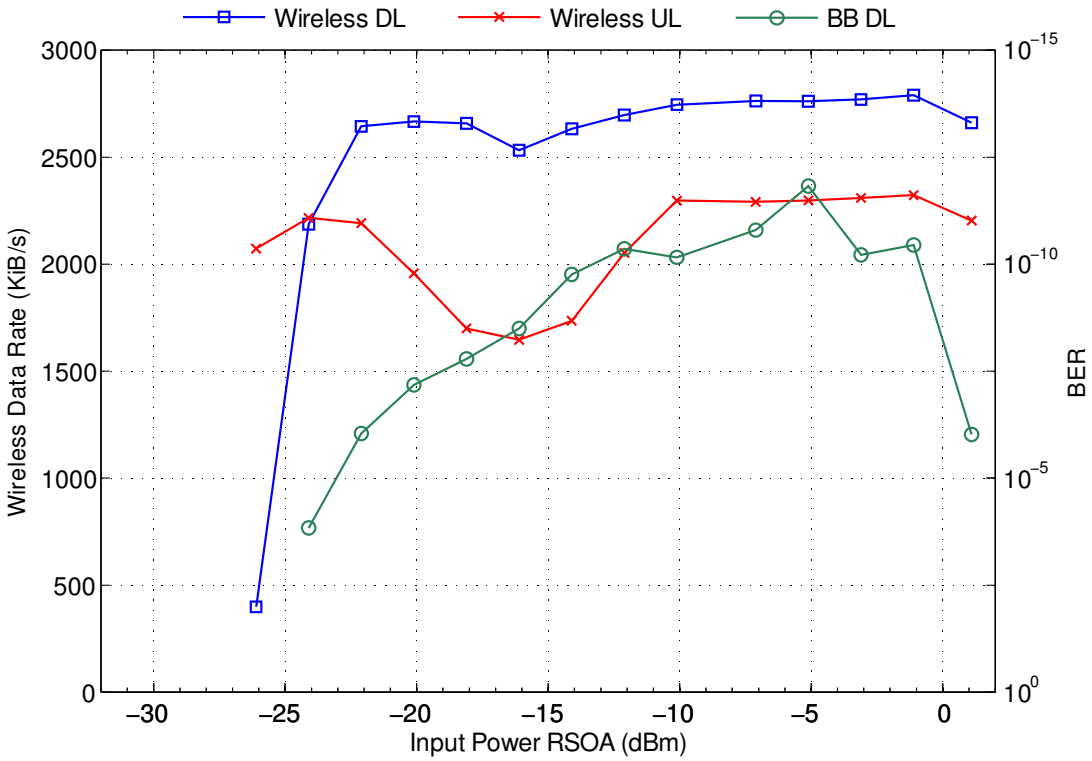

Figure 5.25 - System performance versus RSOA input power, baseband on the downlink.

The gain modulation also leads to self phase modulation of the pulse [5.15]. The combination of self phase and self gain modulation of the optical pulses leads to highly distorted power spectra as depicted in Figure 5.24. The main feature of this spectrum is that, when the RSOA is operating heavily under saturation with *Pin* =+2 dBm, the power spectral density of the distorted retransmitted signal that reaches the receiver at the CO presents a deep around DC, and the power spreads outside the bandwidth of the baseband signal. This is clearly benefic for bidirectional baseband as reported in [5.2] and also for the wireless channel since the intermodulation term identified as *D* in the previous section also decreases within the bandwidth of the wireless signal.

Figure 5.25 depicts the bidirectional link and baseband downlink performance versus the average optical power reaching the RSOA. Curves WL DL and WL UL in Figure 5.25 show the performance, in term of achievable data rate, of the wireless downlink and uplink respectively versus the average optical power reaching the RSOA when the system operates without baseband signal. Under these conditions, the degradation of the wireless link occurs for input optical powers smaller than -22 dBm. The relative intensity noise (RIN) of the RSOA, similarly to semiconductor optical amplifier is inversely proportional injected optical power [5.16]. When the injected optical power decreases the spontaneous emission noise increases, leading to the performance degradation of the wireless link. In Figure 5.25 we can identify 4 operating regions: (1) when the RSOA is highly saturated and the performance of the wireless link is not noticeably affected by the downstream back-reflected data (P_{in} > -10 dBm); (2) when the injection power into the RSOA decreases below -10 dBm, the suppression of the modulated downstream in the upstream transmission becomes less efficient, degrading the performance of the wireless channel; (3) eventually, when the downstream average power decreases for values below -16 dBm the level of the residual downstream component added to the upstream signal decreases and the wireless channel performance improves, (4) the performance of the wireless channel is dominated by the spontaneous emission noise from the RSOA.

5.8.2 BB on the uplink

The next step was to measure the system performance with different optical power levels at the BS. In Figure 5.26 the performance versus the input power at the RSOA is shown. The proposed system works well in the -10 dBm to 1 dBm range. The limiting factor is the UL 1 Gbit/s signal, very high BER are experienced with power levels lower

than -18 dBm, between -16 and -12 dBm the BER is very close to 10^{-9}, but only when the input power at the RSOA is higher than -10 dBm, the BER falls below the desired 10^{-9} number. It should be noted that below -18dBm and lower, the RSOA is working almost exclusively in spontaneous emission, thus the output signal is very affected by RIN.

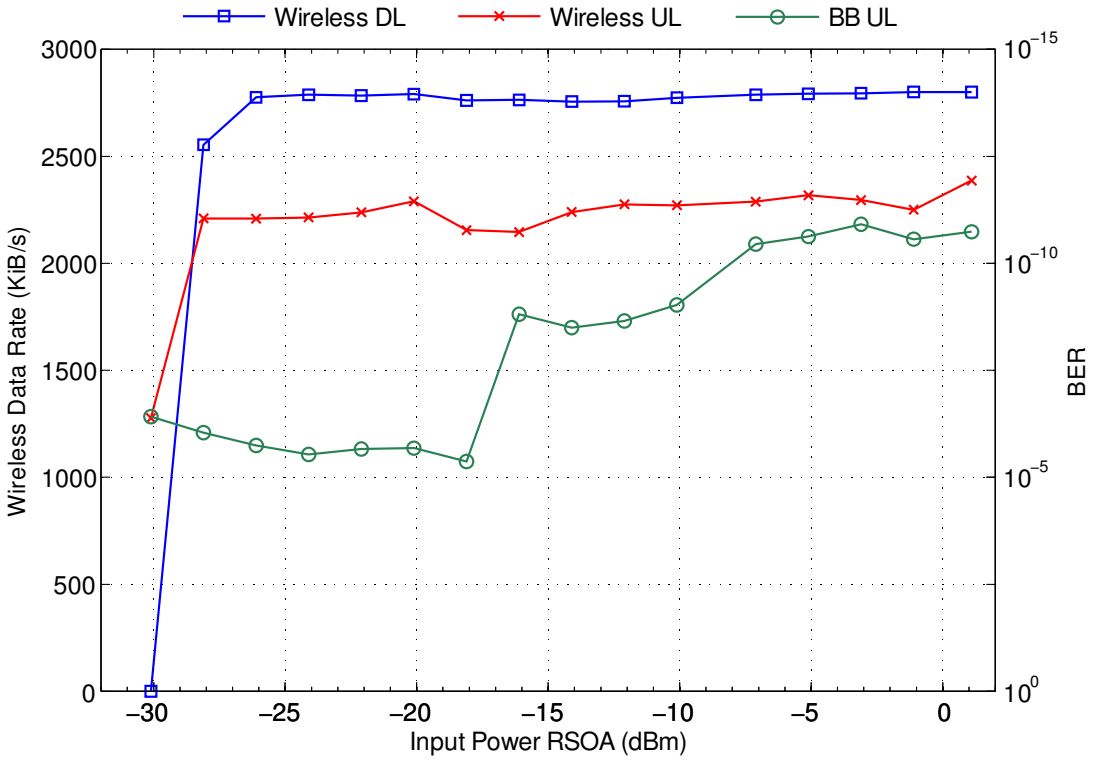

Figure 5.26 - System performance versus RSOA input power, baseband on the uplink.

The wireless DL works flawless through a 28 dBm margin, only experiencing degradation when the power of the wireless signal is below the receiver sensitivity. In the wireless UL there are not any major degradations, it only starts to fail when there is no DL channel to receive the acknowledgement packets. It is shown that the spontaneous emission of the RSOA is enough for the UL wireless signal. The wireless protection schemes are capable of overcoming the RIN.

Table 5.4 shows the optimized operational values for a wireless bi-directional communication with 1 Gbit/s baseband data, using the proposed architecture.

Parameter	Value	Unit
Laser optical power	-3	dBm
Laser bias	40	mA
Photodetector amplifier - central office	3.3	V
Photodetector bias - central office	20.0	V
Photodetector received power – central office	-13.3	dBm
RSOA bias	60	mA
RSOA input power	-7.13	dBm
Photodetector amplifier – base station	5.44	V
Photodetector bias – base station	15.0	V
Photodetector received power – base station	-14.6	dBm
Access point output power – central office	10	mW
Access point output attenuation – central office	10	dB
Wireless output power – central office	0	dBm
Access point input attenuation – central office	6	dB
Access point output power – base station	30	mW
Access point output attenuation – base station	10	dB
Wireless output power – base station	4.8	dBm
Access point input attenuation – base station	0	dB
Baseband bit rate	1	Gbit/s
Baseband signal amplitude – central office	1.2	V
Baseband signal amplitude – base station	1.6	V

Table 5.4 - Configuration parameters for bidirectional wireless and baseband communication.

5.9 Bidirectional wireless transmission performance versus fiber length

In this section the bidirectional transmission of the wireless channels is assessed without considering the transmission of the baseband signal. Two fiber lengths were used to connect the CO and BS, a B-t-B with around 4 m of fiber and 11 km of fiber. The two APs were configured in a bridge setup, each with a computer running the TCP benchmark software.

Figure 5.27 shows the system performance measured in terms of attainable data rate (KiB/s) versus RSOA average received optical power without baseband data. The average input RF power at the optical modulator and at the RSOA was optimized to be -6 dBm and -3 dBm respectively. The slight different data rate between downlink and uplink is due to the AP bridge configuration. The root AP is able to transmit at higher speeds than the non-root AP.

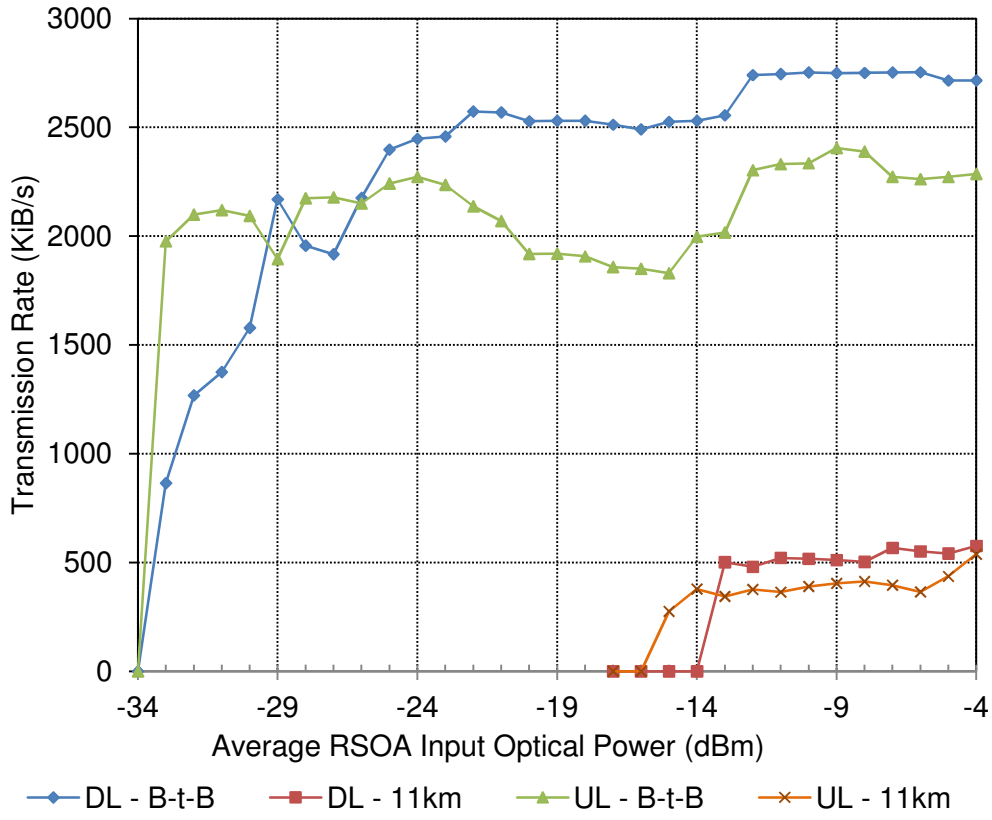

Figure 5.27 - Wireless data rate versus averaged power at the RSOA input for back-to-back and 11 km of fiber.

The B-t-B configuration is able to achieve the best possible results with at least 8 dB of optical margin, when comparing with the coaxial reference values. The optical margin can be increased by the use of optical fiber amplifiers and it can be used either to extend the link length and/or to compensate for extra network components.

As expected, when using the 11 km fiber, significant degradation is experienced owing to the inability of the 802.11 MAC protocol to cope with the propagation delay introduced by the 11 km fiber [5.17]. The APs used, Cisco Aironet 1200, allows for propagation delay compensation, however when 16 km of air propagation distance are selected corresponding to the 11 km of fiber propagation, the AP automatically decreases its transmission speed.

5.10 Summary

In this chapter, the performance limitations due to the intermodulation term resulting from the beating of the baseband signal and wireless overlay signal, transmitted over of colorless WDM-PONs, employing RSOA are assessed both analytically and experimentally. The intermodulation term is a sum of the baseband signal power spectral density multiplied by a factor and shifted to the wireless band. In order to minimize its effect, it is desirable to employ baseband modulation schemes that deplete the power spectral density of the baseband signal around DC with a frequency range larger than twice bandwidth of the wireless signal. Additionally we have analyzed the degradation of the wireless channel caused by the RSOA gain modulation owing to the downstream baseband data. The approach is valid for arbitrary OFDM wireless signals as long as they operate within the usable bandwidth of the RSOA and beyond the bandwidth occupied by the baseband data. Additionally, the bidirectional transmission performance of the wireless channel versus fiber length is assessed when the baseband is not considered.

The main contribution of this chapter is to provide optimum design guidelines and analysis tools to assess the performance limits of single fiber bidirectional WDM-PON, employing RSOAs supporting both baseband and wireless OFDM signals.

5.11 References

[5.1] P. Healey, *et al.*, "Spectral slicing WDM-PON using wavelength-seeded reflective SOAs," *Electronics Letters,* vol. 37, pp. 1181-1182, 2001.

[5.2] W. Lee, *et al.*, "Bidirectional WDM-PON based on gain-saturated reflective semiconductor optical amplifiers," *Ieee Photonics Technology Letters,* vol. 17, pp. 2460-2462, Nov 2005.

[5.3] M. Omella, *et al.*, "Full-Duplex Bidirectional Transmission at 10 Gbps in WDM PONs with RSOA-based ONU using Offset Optical Filtering and Electronic Equalization," *Ofc: 2009 Conference on Optical Fiber Communication, Vols 1-5,* pp. 1290-1292, 2009.

[5.4] S. C. Lin, *et al.*, "Simple approach for bidirectional performance enhancement on WDM-PONs with direct-modulation lasers and RSOAs," *Optics Express,* vol. 16, pp. 3636-3643, Mar 17 2008.

[5.5] G. X. Shen, *et al.*, "Fixed mobile convergence architectures for broadband access: Integration of EPON and WiMAX," *Ieee Communications Magazine,* vol. 45, pp. 44-50, Aug 2007.

[5.6] M. Gast, *802.11 Wireless Networks: The Definitive Guide*, 2 ed.: O'Reilly Media, 2005.

[5.7] C. Spurgeon, *Ethernet: The Definitive Guide*, 1 ed.: O'Reilly Media, 2000.

[5.8] I. H. Malitson, "Interspecimen Comparison of the Refractive Index of Fused Silica," *J. Opt. Soc. Am.,* vol. 55, pp. 1205-1208, 1965.

[5.9] M. Bass, *et al.*, *Handbook of Optics, Third Edition Volume IV: Optical Properties of Materials, Nonlinear Optics, Quantum Optics (set)*: McGraw-Hill, 2009.

[5.10] M. Mjeku, *et al.*, "TCP and UDP performance over fibre-fed IEEE 802.11 b networks," *12th Microcoll Conference, Budapest, Hungary,* 2007.

[5.11] B. Kalantari-Sabet, *et al.*, "Performance impairments in single-mode radio-over-fiber systems due to MAC constraints," *Journal of Lightwave Technology,* vol. 26, pp. 2540-2548, 2008.

[5.12] B. Kalantarisabet and J. Mitchell, "MAC constraints on the distribution of 802.11 using optical fibre," 2006, pp. 238-240.

[5.13] National Instruments, Two-Tone Third-Order Intermodulation Distortion Measurement - Developer Zone. *Tutorial,* Available: http://www.ni.com/white-paper/4384/en, retrieved on Feb 12, 2011.

[5.14] D. J. F. Barros and J. M. Kahn, "Comparison of Orthogonal Frequency-Division Multiplexing and On-Off Keying in Amplified Direct-Detection Single-Mode Fiber Systems," *Lightwave Technology, Journal of,* vol. 28, pp. 1811-1820, 2010.

[5.15] G. P. Agrawal and N. A. Olsson, "Self-Phase Modulation and Spectral Broadening of Optical Pulses in Semiconductor-Laser Amplifiers," *Ieee Journal of Quantum Electronics,* vol. 25, pp. 2297-2306, Nov 1989.

[5.16] W. Rideout, *et al.*, "Relative Intensity Noise in Semiconductor Optical Amplifiers," *Ieee Photonics Technology Letters,* vol. 1, pp. 438-440, Dec 1989.

[5.17] N. J. Gomes, *et al.*, "Radio-over-fiber transport for the support of wireless broadband services [Invited]," *Journal of Optical Networking,* vol. 8, pp. 156-178, Feb 1 2009.

6

Conclusions and future work

6.1 Summary and conclusions

In Telecommunications the quest for more bandwidth never ends. This is the telecommunication engineer mission, to provide bandwidth economically to end users and for the operators. The cost is even more important in the access networks, if it is too high the potential market size reduces considerably, leading to high cost per client, which may be not acceptable by clients and operators alike. A significant part of the access network cost, is supported by only one client, or a small number of clients. This is dramatically different from other network sections, such as core and transport networks, where operators have a large pool of customers supporting the investment.

To improve access networks profitability, it is of key importance the development of strategies to render cost effective high bandwidth access networks. This can be achieved

through the integration of wired and wireless network in a single infrastructure. This thesis was focused on identifying strategies and performance improvement approaches to help to reach such objective. The transmission of wireless signals directly and transparently on fiber, allows the setup of remote cells with a small footprint, as all the signal generation and logic hardware is offsite. Even main cell sites can be reduced and centralized in a small number of locations. Ultimately, one could expect that all users served by a PON network could have an enhanced optical network terminal (ONT), able to support a femtocell. This could have a massive effect on macro cell traffic, effectively offloading traffic. Currently some mobile operators provide free access to public Wi-Fi access points in an attempt to reduce cellular traffic, but it is the user option to enable or not Wi-Fi access. Using this approach it would be completely transparent to the user. Enabling the concept of always on, with the same quality of service, using any technology.

In chapter 2 we presented an overview on optical access networks. It was detailed the historic evolution of access networks to reach up to the point that optical access networks are unavoidable for a large number of operators. We reached the conclusion that the point-to-multi-point (P2MP) architecture is being favored by the operators in determent of point-to-point (P2P). The two P2MP standard families are detailed, presenting their evolution to the last version, as well as exploring what the future evolution can bring. In the future, the evolution is foreseen to be in the bandwidth increase, the reached distance and in the number of users within a single PON network. To achieve these goals the most promising solution is wavelength division multiplexed passive optical network (WDM-PON). Extra wavelengths bring extra bandwidth to single or smaller group of clients, the replacement of simple power splitters with arrayed waveguide gratings (AWG) optimizes the wavelength power distribution, potentially increasing reach. We introduced our solution for economically sustainable colorless ONT. The reflective semiconductor optical amplifier (RSOA) is a key component that is able to perform within a large optical spectral window, directly modulated by data and providing optical amplification.

One of the wireless frequency bands that is deserving much attention is the millimeter band region, specifically the 60 GHz band. On chapter 3 we presented the state of art of the proposed standards in the 60 GHz frequency, while explained the benefits, high bandwidth and high frequency reuse, as well as the challenges in the signal generation and its use on local networks. It was shown how relevant is the optical modulation scheme employed in such high frequency systems. We focused on the downlink

transmission study, using Mach-Zehnder modulator (MZM). We detailed several optical modulation techniques using MZM. 60 GHz signals if modulated as an optical double side band (ODSB) signal have a very limited reach due to chromatic dispersion. This is due to different propagation speeds of each signal lobe, and due to the large frequency used. The speed difference will generate phase shifts that will destroy the signal upon photodetection in some periodical predetermined fiber lengths. As a possible solution the optical single side band (OSSB) and optical carrier suppression (OCS) modulation can be employed. The OSSB technique removes the most significant side band, useful if not high modulation factors are applied. OCS is a very particular modulation, it eliminates the optical carrier, effectively doubling the signal frequency upon photodetection. If the wireless system is expecting the frequency to double, it is a low cost solution, however it cannot be used in a pure transparent system.

In chapter 4 we studied in more detail the OSSB and OCS modulation when the RF carrier is modulated with data. Its impact on the system performance was compared with the classical ODSB. It was also created OSSB modulation variations to help to identify some OSSB shortcomings. It was identified that for high modulation depths, the high order harmonics generated by the MZM will interfere with the signal quality. In some cases the system will perform just as badly as the ODSB modulation. This conclusion was reached using the filtered OSSB (F-OSSB) signal, which removes the entire optical signal above and below 60/-60 GHz, thus removing all the high order harmonics. However, we verified that the system performance was still not as expected from an ideal OSSB modulation scheme. Using the pure OSSB (P-OSSB) we were able to identify the residual optical carrier modulation by data. Due to the nature of the detection, the optical carrier quality is very important. When multiple RF channels are transmitted together by using SCM, a performance degradation is experienced by the system, mainly due to intermodulation.

In chapter 5 we changed our focus from the optical line terminal (OLT), to the optical network terminal (ONT). The performance limitations due to the intermodulation term resulting from the beating of the baseband signal, and wireless overlay signal transmitted over of colorless WDM-PONs employing RSOA were assessed both analytically and experimentally. Since the intermodulation term is a sum of the baseband signal power spectral density multiplied by a factor and shifted to the wireless band, in order to minimize its effect, it is desirable to employ baseband modulation schemes that deplete the power spectral density of the baseband signal around DC with a frequency range

larger than twice bandwidth of the wireless signal. Additionally we have analyzed the degradation of the wireless channel caused by the RSOA gain modulation owing to the downstream baseband data. The approach is valid for arbitrary OFDM wireless signals as long as they operate within the usable bandwidth of the RSOA and beyond the bandwidth occupied by the baseband data. Although, in the experimental work 802.11g standard compliant signal was used, the frequency range of operation, the OFDM modulation format employed as well as the available performance assessment tools, allowed for an experimental evaluation which conclusions can be easily be applied to other wireless and mobile communication standards. The main contribution of this chapter was to provide optimum design guidelines and analysis tools to assess the performance limits of single fiber bidirectional WDM-PON, employing RSOAs supporting both baseband and wireless OFDM signals.

6.2 Future work

The integration of wired and wireless network is a research topic that is far from being totally explored, there are many application scenarios and issues that still need to be addressed.

The topic of RF best appropriate modulation formats is foreseen to be a very relevant topic. OFDM is a good choice for wireless transmission with their limited bandwidth, however the OFDM over fiber systems have stringent requirement of orthogonality between the RF sub carriers. Since when operating in the 60 GHz region there is around 7 GHz of available spectrum, the traditional frequency division multiplexing can be used in the optical-wireless system to reduce the complexity of signal processing, increase the tolerance towards the frequency drift and therefore reduce cost. A detailed performance/cost analysis is required.

The media access control (MAC) is a promising direction for future research. Although the analog nature of RoF links offers transparency for the transmission of the wireless protocol stack, the additional propagation delay introduced by the optical fiber in the end-to-end logical link connection limits the maximum reachable distance.

Another problem related to distance is the different fiber lengths to each ONT. If one radio signal is to be shared by all clients in a PON network, it will generate interference in the transmitted and received wireless signal. If a wireless device is close enough to at least two enhanced ONTs, the signal received would be affected as it is when reflections

occur with physical structures. If the delay between signals is small and the modulation applied is OFDM, no major issues should occur. But if multiple PONs are in the vicinity, there would be multiple uncorrelated signals operating in the same frequency band.

The last scenario is very likely to occur in case the technology proves to be economically interesting to the operators. If current technologies serve as example, i.e. Wi-Fi in the 2.4 GHz band, it is included on virtually all the equipment provided by the Internet operators. This creates problems in some dense populated areas, where there are some serious interference problems between all the devices operating in the same frequency band. Operators cannot face the risk of disturbing their currently working cellular networks. Protocols must be developed to ensure that interferences are reduced to a minimal. These protocols should not be dependent in changes on the wireless standards. All enhanced ONT should sense the wireless spectrum and report to the central office, which should use that information to coordinate, at least, the output power levels. If one ONT goes offline, i.e. costumer disconnects power supply, another one in the vicinity should take over.

Increasing the optical source modulation bandwidth at the ONT must keep being persuaded. Electrical equalization in conjunction with RSOAs have proved to increase the modulated bandwidth to 10 GHz, EAM integrated with RSOAs (REAM) are also able to achieve the same bandwidth. Cost / benefit analysis should be conducted with these, as well as others possible solutions, to guarantee that uplink speeds do not stagnate, particularly when Internet applications are becoming more and more dependent on user generated content.

Appendix A – System architecture

Complete setup

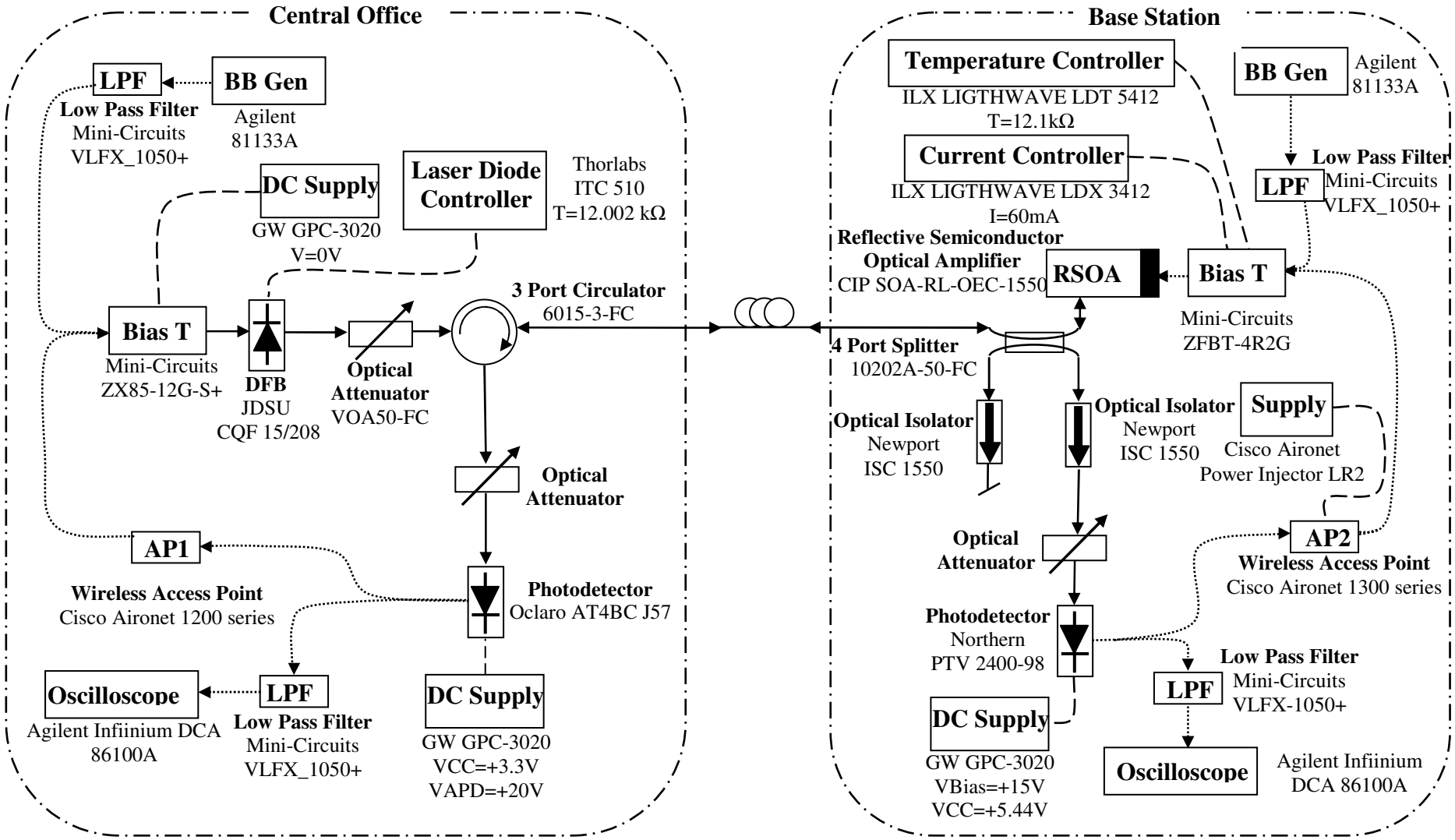

Bidirectional wireless and baseband signal in the downlink direction

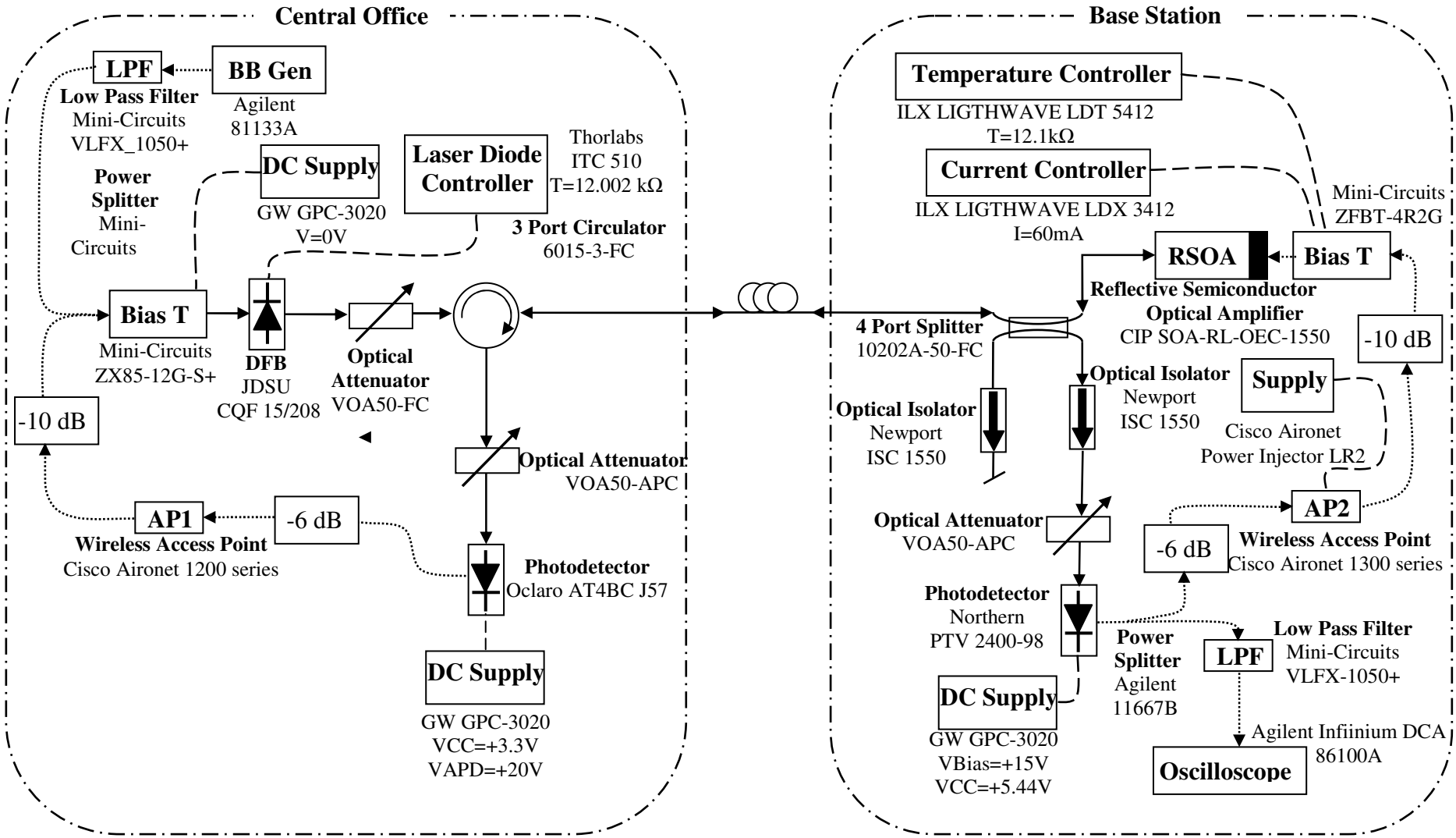

Bidirectional wireless and baseband signal in the downlink direction

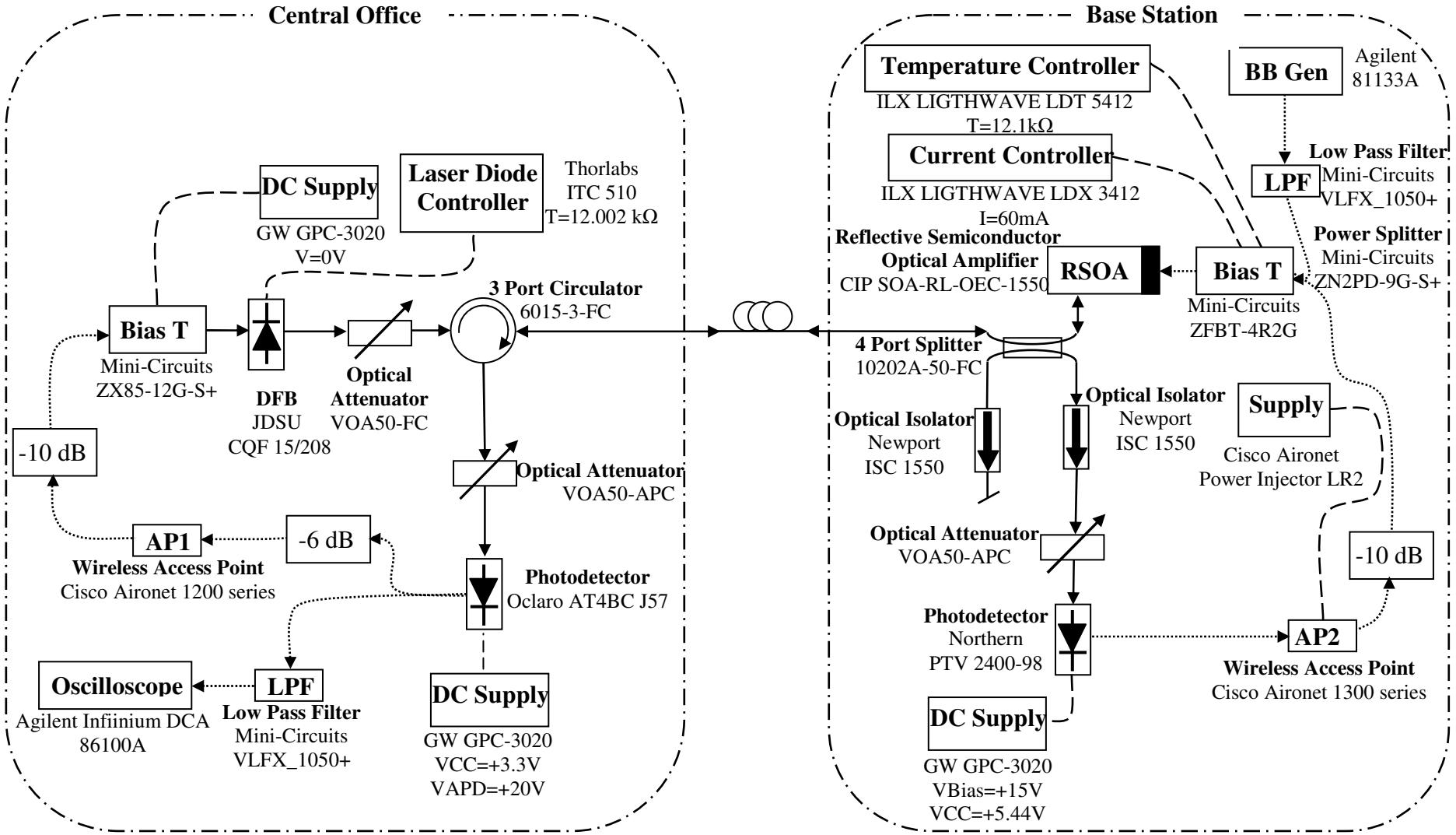

Appendix B – RSOA gain dynamics

Neglecting the intra band carrier processes and internal loss in the active layer of a semiconductor optical amplifier, the optical gain dynamic equation considering the optical field propagating in the positive and negative directions, is [B.1],

$$\frac{dg(z,t)}{dt} = \frac{g_0(t) - g(z,t)}{\tau_s} - \frac{g(t)\left(\left|A^+(z,t)\right|^2 + \left|A^-(z,t)\right|^2\right)}{P_{sat}\tau_s} \tag{B.1}$$

where τ_c is the carrier lifetime, P_{sat} the saturation power and $g_0(t) = \Gamma a N_0\left(\frac{I(t)}{I_0} - 1\right)$. $I(t)$ is the applied current, I_0 is the injection current required for transparency, N_0 the carrier density. $A^{\pm}(z,t)$ is the slow-varying envelope associated with the optical field, propagating in the forward direction (+) and backward direction (-). $A^{\pm}(z,t)$ can be written in terms of power, $P^{\pm}(z,t)$ and phase $\theta^{\pm}(z,t)$, $A^{\pm}(z,t) = \sqrt{P^{\pm}(z,t)}e^{\theta^{\pm}(z,t)}$. The propagation equations considering a reference frame moving with the pulse, neglecting internal loss and considering the effective linewidth factor α,

$$\begin{aligned} \frac{dP^{\pm}(z,t)}{dz} &= \pm g(z,t)P^{\pm}(z,t) \\ \frac{d\theta^{\pm}(z,t)}{dz} &= \mp\alpha\frac{g(z,t)}{2} \end{aligned} \tag{B.2}$$

In case of an ideal RSOA with reflection coefficients *0* and *1* at the input (*z=0*) and far end extremity (*z=L*) respectively, being *L* the length of the active region. The boundary conditions are,

$$\begin{aligned} A^+(0,t) &= A_{in}(t) \\ A^-(L,t) &= A^+(L,t) \\ A_r(t) &= A^-(0,t) \end{aligned} \tag{B.3}$$

The optical power, $P_r(t)$, and $\theta_r(t)$ at the output of the RSOA, are related with the optical power, $P_{in}(t)$, and phase $\theta_{in}(t)$ of the optical field at the input of the RSOA by:

$$\begin{aligned} P_r(t) &= P_{in}(t)e^{2\int_0^L g(z,t)dz} = P_{in}(t)e^{2h(t)} \\ \theta_r(t) &= \theta_{in}(t) - \alpha h(t) \end{aligned} \tag{B.4}$$

here $h(t) = \int_0^L g(z,t)dz$ represents the integrated gain at time *t*. We obtain an equation for $h(t)$ by integrating the A.1 over the RSOA length:

$$\frac{dh(z,t)}{dt} = \frac{g_0(t)L - h(z,t)}{\tau_s} - P_{in}(t)\frac{e^{2h(t)} - 1}{P_{sat}\tau_s} \tag{B.5}$$

The optical gain of the RSOA is then defined as:

$$G_{RSOA}(t) = \frac{P_r(t)}{P_{in}(t)} = e^{2h(t)} \tag{B.6}$$

References

[B.1] G. P. Agrawal and N. A. Olsson, "Self-Phase Modulation and Spectral Broadening of Optical Pulses in Semiconductor-Laser Amplifiers," *Ieee Journal of Quantum Electronics,* vol. 25, pp. 2297-2306, Nov 1989.